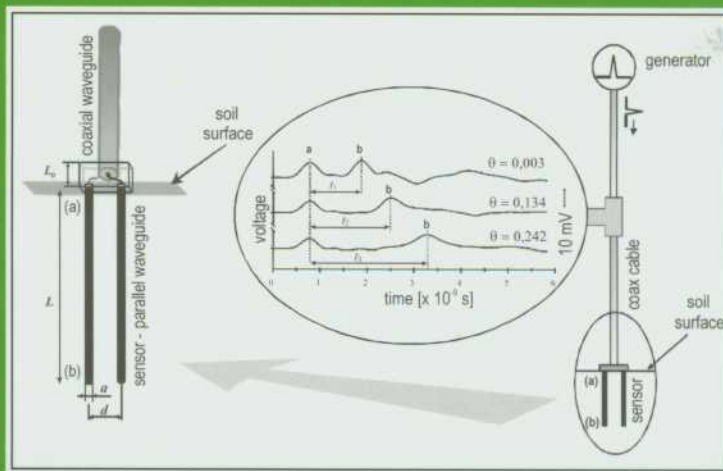


# TDR METHOD FOR THE MEASUREMENT OF WATER CONTENT AND SALINITY OF POROUS MEDIA

Wojciech Skierucha, Marek A. Malicki

EDITED BY

WOJCIECH SKIERUCHA, RYSZARD T. WALCZAK



Centre of Excellence for  
Applied Physics in Sustainable  
Agriculture AGROPHYSICS



Institute of Agrophysics Polish  
Academy of Sciences



EU 5<sup>th</sup> Framework Program  
QLAM-2001-00428

**TDR METHOD FOR THE MEASUREMENT OF WATER CONTENT  
AND SALINITY OF POROUS MEDIA**

*Wojciech Skierucha, Marek A. Malicki*

EDITORS:  
Wojciech Skierucha  
Ryszard Walczak

Lublin 2004



EC Centre of Excellence AGROPHYSICS  
Centre of Excellence for Applied Physics  
in Sustainable Agriculture  
QLAM-2001-00428

Reviewed by: Prof. Dr hab. Jan Gliński

ISBN

© Institute of Agrophysics PAS, Lublin 2004

Edition: 180 copies

Project of cover: Wojciech Skierucha

---

Printed by: ALF-GRAF, ul. Kościuszki 4, 20-006 Lublin, Poland

## PREFACE

The importance of water for human needs, material technologies and for the ecosystem is well known. Water is present in most areas of nature and technology and influences a variety of product properties, industrial systems and natural processes. However water is useful only, if it is present in the appropriate quantity, at the right place and time.

The material water content is an important quality criterion in many industrial processes, and has great influence on the production process. Soil water content determination is an important issue in tillage, irrigation, application of fertilizers and harvesting. Water content of agricultural goods is essential concerning harvest, trading, transportation and storage. The determination of water content of many raw materials, foods and agricultural products will help to improve the quality and reduce losses during manufacturing and storage. Adequate and accurate techniques and methods for water content determination are rare although they are commonly needed and required by ISO standards. Water content controlled manufacturing processes will help save energy for example in drying, and will thus reduce pollution of the environment and improve quality of life.

Trading of most natural goods is based on weight, which is mainly influenced by water content. Adequate water content measurement methods will help to fix the true value of the product to reflect this in its price. Natural hazards such as landslides, avalanches, mud streams and flooding depend on water content significantly, especially in mountainous regions or close to rivers.

The interaction of water with porous substances like soil needs interdisciplinary approach. It is necessary to know details about the presence of water in the various substances and its interactions with the material matrix. Physicists, hydrologists, soil scientists, agronomists, material scientists, civil and electronic engineers and food chemists are representative selections of the professionals that are confronted with water related problems day by day.

Electronic in-line determinations in production processes or fast continuous monitoring methods based on radio- or microwave frequency techniques are especially underdeveloped. Increased application and accuracy of such methods is of great importance.

The present reference method, the oven-drying is destructive, time and energy consuming technique that is unsuitable for continuous monitoring. This method also does not reflect all the water present in the material (bound water). It is also desirable to replace certain water content measurement methods such as obsolete

gamma radiation or neutron probe methods with advanced measurement techniques.

Time Domain Reflectometry (TDR) method for the determination of dielectric permittivity is widely accepted, especially for soil water content determination, for its advantages: simplicity of operation, accuracy and fast response, usually does not need calibration, is non-destructive, portable systems are available, is able to automatize and multiplex probes. Now many companies offer soil water content measurement devices based on TDR technique but they are still too expensive for common use. Moreover, the molecular behaviour in electromagnetic field needs much modelling research for describing dielectric physical processes and finding better calibrations for materials with variable densities and textures.

The presented monograph is based on the experience in developing TDR soil water content and salinity meters, both in the instrumentation and modelling fields. It presents basic theory, modelling approaches, construction and trends in development of TDR measurement technique for application in water content and salinity measurements of porous media. It is not intended to be the complete work on the TDR technique application in soil science but rather the sum of experience collected in the Institute of Agrophysics Polish Academy of Sciences in Lublin, Poland during the last several years of TDR development.

Wojciech Skierucha  
Marek A. Malicki

## CONTENTS

1.	Status of water as an significant issue of Agrophysics .....	8
1.1.	Water status monitoring .....	8
1.1.1.	Minimal number of variables describing the water status.....	9
2.	Requirements and means of soil water status monitoring.....	10
2.1.	Selectivity of the method.....	10
2.1.1.	Electrical measurement of soil water content.....	11
2.1.2.	Electrical measurement of soil salinity .....	11
3.	Electrical measurements methods of porous material properties, especially of soils .....	13
3.1.	Basics of TDR technique.....	14
3.1.1.	General idea of the TDR measurements.....	16
3.1.2.	Calibration of TDR soil water content measurement.....	17
3.2.	Calibration of TDR water content measurement of selected plant materials .....	19
3.3.	TDR soil salinity measurement .....	21
3.3.1.	Theory .....	22
3.3.2.	Experimental verification of the soil electrical conductivity measurement.....	22
3.3.3.	Summary .....	25
3.4.	Choice of frequency of the electric field in dielectric measurement of soil water content in saline soils .....	25
3.4.1.	Frequency dispersion of the electrolyte dielectric permittivity.....	26
3.4.2.	Summary .....	29
4.	The influence of soil electrical conductivity on the soil water content values measured by TDR method .....	30
4.1.	Material and method.....	30
4.2.	Results and discussion.....	31
5.	Evaluation of dielectric mixing models of mineral soils.....	33
5.1.	Material and methods .....	35
5.2.	Results and discussion.....	37
5.3.	Conclusions .....	41
6.	Temperature effect on soil dielectric permittivity- description of laboratory setup and applied software.....	43
6.1.	Description of the laboratory setup .....	44
6.2.	Summary .....	51
7.	Temperature properties of soil dielectric permittivity.....	52

7.1.	Introduction .....	52
7.2.	Temperature effect of dielectric permittivity of soil free water .....	55
7.3.	Materials and methods.....	56
7.4.	Results and discussion.....	58
7.5.	Temperature effect of soil bound water.....	63
7.6.	Soil conductivity influence on temperature effect of soil dielectric constant.....	66
8.	The accuracy of soil water content measurement by TDR technique.....	69
8.1.	Material and method.....	70
8.2.	Results and discussion.....	71
8.3.	Conclusions .....	82
9.	Comparison of Open-Ended Coax and TDR sensors for the measurement soil dielectric permittivity in microwave frequencies.....	83
9.1.	Hardware features of Time Domain Reflectometry method .....	85
9.2.	Open-Ended Coaxial Probe method .....	87
9.3.	Materials and methods.....	90
9.4.	Results and discussion.....	92
9.5.	Summary .....	94
10.	Microwave switches used in automatic reflectometric systems for soil water content and salinity measurements.....	96
10.1.	Introduction .....	96
10.2.	Electromechanical microwave switches.....	99
10.3.	Semiconductor microwave switches .....	100
10.4.	Materials and methods - prototype switches .....	101
10.4.1.	SP16T switches .....	101
10.4.2.	SP8T fully integrated switch .....	102
10.5.	Performance of the developed RF switches in TDR applications ....	103
10.6.	Summary .....	107
11.	TDR soil water content, salinity and temperature monitoring system – description of the prototype .....	108
11.1.	Functional description .....	110
11.2.	SLAVE module .....	112
11.3.	MASTER module.....	114
11.4.	MIDL system handling.....	115
11.5.	Configuration of basic parameters of the MIDL system .....	116
11.6.	System files .....	116
11.7.	Executable script files .....	116
12.	Soil water status monitoring devices.....	119
12.1.	FOM/mts - Field Operated Meter for determination of moisture, temperature and salinity of soils.....	121

12.2.	New prototype version of FOM/mts soil water content, salinity and temperature measurements .....	122
12.3.	TDR Data LOGger for soil water content, temperature and salinity measurements .....	124
12.4.	FP/m, FP/mts - Field Probe for soil moisture, temperature and salinity measurement.....	127
12.5.	LOM/mpts - Laboratory Operated Meter for recording soil moisture, matrix potential, temperature and salinity .....	130
12.6.	LP/ms - Laboratory miniProbe for soil water content and salinity measurement.....	133
12.7.	LP/t - Laboratory Probe for soil temperature .....	135
12.8.	LP/p - Laboratory miniProbe for soil water capillary pressure .....	136
13.	References.....	138
14.	Index of figures .....	144
15.	Index of Tables .....	150

## 1. STATUS OF WATER AS AN SIGNIFICANT ISSUE OF AGROPHYSICS

Agrophysics is a branch of science created from the need to insight into the physical elements of biological plant environment deciding about the process of photosynthesis (light, heat, water), and indirectly the yield. Implementation of the appropriate physical tools and methods of interpretation makes agrophysics an original and interdisciplinary science (like geophysics, biophysics and others, dealing with physical aspects of problems of appropriate scientific fields). The subjects of research are physical processes in the soil-plant-atmosphere continuum and techniques to control them.

The practical application of agrophysics is the prediction of the consequences of the physical processes and the control of factors deciding about them having in mind the optimisation of agricultural production. The production of biomass is evaluated on the base of its quantity and quality and it depends on the physical factors that cannot be fully controlled yet. Therefore, there is the need to enlarge the traditional area of agrophysical subjects on the physical processes involved in the formation of agricultural material properties (Gliński [34], Walczak and Sławiński [98]).

The key subject of agrophysics is the status of water because each analysed phenomenon depends on it (*ie* water quantity, potential, salinity, oxygenation and temperature).

The interaction of processes in the soil-plant-atmosphere continuum and their influence on the plant production efficiency form the criteria of research subjects' selection. The mathematical interpretation of research results, that is adequate for physics, enable to come to formalized conclusions, necessary for mathematical modelling and therefore the prediction of discussed processes and their consequences.

### 1.1. Water status monitoring

Water status monitoring defined as the spatial and temporal registration of the water properties that decide about the processes under consideration, is the basic instrument in natural research (in industrial processes, too). It is especially important in agrophysics because each process in the agrophysical research area depends on water properties present in the analysed system.

Increasing demands of water management result in the continuous development of its tools. One of the most important, beside the simulation models of water balance (Walczak and Sławiński [97]), is monitoring of water status in porous materials defined as a space-temporal recording of the water properties

that stimulate the phenomena and processes observed in the soil-plant-atmosphere system.

Monitoring of water status is accomplished using digital systems. The digital data acquisition systems react only on electric signals and the applied sensors must convert the measured value into the proportional electric signal.

Water status of soil, as a porous material should be expressed by minimum five variables: amount of water in the soil (*ie* soil water content), soil potential, salinity, oxygenation and temperature (Malicki and Bieganowski [55]).

The most difficult are the electric measurement of soil water potential and soil water content (soil water content), therefore they are the subject of permanent research. It is assumed here, that the method successfully verified for soils will be also applicable for other porous agricultural materials because their structure is not so complex as soil.

#### *1.1.1. Minimal number of variables describing the water status*

The number of variables for water status description in the porous material depends on the specificity of the analysed problem and, up till now, is arbitrary chosen. In majority of practical cases the status of water is described by one variable: water content of the material. One variable - water content – is enough for wood as building material. Two variables are practically enough to describe the status of water in grain: water content and temperature. Soil is a material in which water status should be describes by minimum five variables: amount of water (soil water content), its potential, salinity, oxygenation and temperature.

Soil is the most difficult biological material for water status monitoring because soil is diverse and its properties are not stable in time and space. Soil water content is the most challenging soil water status parameter for determination because the measurement results must be in the form of electric signal, while the current flow though the soil depends not only on its water content.

Assuming that:

- the methods effective for soil water content measurements are also effective for water content measurements of other biological materials characterized by simpler construction, and
- sensors, methods and instrumentation requirements in soil water content monitoring are not stronger than in water content monitoring of other biological materials

we can concentrate further discussion on soil water content measurement and monitoring.

## 2. REQUIREMENTS AND MEANS OF SOIL WATER STATUS MONITORING

Monitoring of soil water status, *ie* temporal and spatial registration of its water content, potential, salinity, oxygenation and temperature, is the necessary condition for modelling of processes in soil-plant-atmosphere continuum, prediction of their consequences and control.

The implementation of soil water status monitoring needs the application of automatic systems based on digital technique. The digital acquisition systems read only electrical signals; therefore the applied sensors must convert the measured quantity on the respective electrical signal. The sensors, methods and instrumentation requirements used for “electrical” monitoring of soil water status are:

- automatic and continuous registration of data *in situ* ensuring non invasive actions affecting soil and the observed processes,
- selectivity (the measurement method should not be sensitive on factors other than the selected one),
- security and simplicity (application of inoffensive medium and minimum specialized knowledge of the operator)

The actual means of agrophysical metrology gives diverse possibilities of soil water monitoring of the individual parameters:

- electrical measurement of temperature is easy because electrical temperature sensors are commercially available,
- electrical measurement of potential is possible for its matrix element in the range of 0-950 mbar with the application of electrical tensiometric converter , and above 950 mbar up to the value relating to the plant wilting point (about  $1.5 \times 10^4$  mbar) with the use of capillary-porous blocs (Campbell and Gee [13]) and thermoelectric tensiometers (Mullins [69]),
- oxygenation can be measured electrically or evaluated on the base of soil aeration, that is closely correlated with its water content,
- the electrical method of soil water content (moisture) and salinity measurement and is the subject of continuous research.

### 2.1. Selectivity of the method

The key feature of the applied method is the selectivity of the measurement, *ie* the lack of sensitivity of the conversion function (calibration) on the influence from the factors other than the measured one. Proper selectivity liberates the user from frequent, specific for each soil, *in situ* calibration measurements.

The solution to the problem of electric measurement of the physical quantity in selective way is to find such an electric property of the medium conditioning it, which is specific to the considered medium. For example, the specific property of molecular oxygen in electrolyte (“soil water”) is small activation energy of electrode reaction of its reduction. It can be concluded that electric measurement of oxygenation may be based on the amperometric measurement of the current of electrode reaction of oxygen molecules reduction (Malicki and Bieganowski [55]).

Similarly, concerning the issue of electric measurement of soil salinity, the media conditioning salinity are salts present in soils and the specific property is their ionic form. The ability to transport electric charge by the ions in “soil water” allows the soil to conduct electric current. Therefore the electric measurement of soil salinity should be based on the measurement of its electric conductivity.

#### *2.1.1. Electrical measurement of soil water content*

Concerning the problem of electric soil water content measurement, the medium conditioning water content is water and its specific property is the polar structure of water molecules (a water molecule has a permanent dipole moment of 1.87 D). Polarity of water molecules is the reason that dielectric permittivity (dielectric constant) of water is much higher than permittivity of soil solid phase (the relative dielectric constant of water in the electric field of frequency below 10 GHz and 18 °C temperature is 81, while the relative dielectric constant of solid phase is 4 ÷ 5 at the same conditions). The dielectric constant of soil strongly depends on its water content, therefore it may be concluded that electric measurement of soil water content should be based on the measurement of its dielectric constant.

The medium conditioning its water content is water and its unique property is the polar structure of water molecules. The real part of water dielectric permittivity (dielectric constant) is much higher than dielectric constant of soil solid phase therefore it can be concluded that electrical measurement of soil water content should be based on the measurement of its dielectric constant.

The efforts to measure soil water content indirectly, on the base of the resistance or electrical capacitance between the electrodes inserted into the soil, has been continuously undertaken since the end of nineteen age (Whitney *et al.* [102]).

#### *2.1.2. Electrical measurement of soil salinity*

Similarly, referring to the problem of electrical measurement of soil salinity, the medium conditioning its salinity is salt present in the soil and the unique

property is their ionic nature. The ability to conduct electrical charge by ions present in the soil water is the reason that the soil conducts current. Therefore, the electrical measurement of soil salinity should be based on the measurement of its electrical conductivity.

Soil salinity is expressed by a total concentration of salts in the soil, and practically their ions in the “soil water”. Due to technical reasons connected with the determination of such a defined salinity, its measure by indirect quantity – electrical conductivity of the soil extract, named as a soil electrolyte, which is taken from the soil after its saturation by distilled water (Marshall and Holmes [63]). This procedure proposed by US Salinity Laboratory [94], has been recognized as standard. However this method cannot be used in *in situ* measurements and also in automatic monitoring systems of soil salinity.

The *in situ* and non-destructive alternative is the measurement of the soil apparent electrical conductivity,  $EC_a$ , as the basis for determination of the electrical conductivity of the soil electrolyte,  $EC_w$  (Rhoades *et al.* [76], Nadler [70]). For this purpose a four-electrode method is often used (Kirkham and Taylor [46]; Gupta and Hanks [35]). It consists in the measurement of the voltage drop along the current, which is forced by other, in relation to measured, pair of supply electrodes. Such a solution enables to avoid disturbances caused by electrochemical polarization of at the interface electrode-electrolyte. However the  $EC_a$  depends also on soil water content,  $\theta$ , and to determine  $EC_w$  it is necessary to measure  $EC_a$  and  $\theta$ , simultaneously. Rhoades *et al.* [76] presented a model relating  $EC_a$ ,  $EC_w$  and  $\theta$  as follows:

$$ekG = ekE\theta(a_0\theta + a_1) + ekS \quad (1)$$

where:  $a_0$  and  $a_1$  are empirical indexes different for various soils and profile layers of the given soil,  $EC_s$ , is the electrical conductivity of the soil solid phase dependent on the concentration of cations adsorbed on the surface of clay minerals and the presence of ferrite minerals.

### 3. ELECTRICAL MEASUREMENTS METHODS OF POROUS MATERIAL PROPERTIES, ESPECIALLY OF SOILS

Agrophysics as a branch of science created from the need to get insight into physical properties and phenomena happening in biological environment of plants conditioning the process of photosynthesis (light, heat, water, nutrients), and therefore the yield. The application of research and interpretation tools characteristic to physics makes Agrophysics original, interdisciplinary branch of science.

The key problem in Agrophysics is water status in soil-plant-atmosphere system, because every phenomenon examined in its scope of interest relates somehow on the water status. The number of variables necessary to describe the water status in porous materials depends on the examined problem and is practically arbitrary. In majority of practical situations the status of water is described only by one variable – water content. Soil is the material where water status should be described by minimum five variables: water content (moisture), water potential, salinity, oxygenation and temperature. The most demanding biological material for monitoring the status of water contained in it is soil, because the soil structure is complex and its properties are not stable. Also, soil water content seems to be the most difficult water status variable to determine because the response of available soil water content sensors is not dependent only on soil water content. It may depend on soil salinity, temperature and texture. Therefore there has been much effort put down on the soil water content metrology. If there is a method of soil water content measurement it could be applicable to other biological materials with less differentiated structure.

There are three international standards for soil water content measurement. Two of them relate to the thermogravimetric methods: ISO11461 – for water content on volume basis, ISO11465 for water content on the mass basis and the norm describing neutron scattering method for soil water content determination in unsaturated zone – ISO10573. Thermogravimetric methods enable to determine the amount of water in the soil sample on the mass or volume basis in the direct way and they are the most popular. These methods are very laborious, time consuming and require the laboratory equipment. In the indirect neutron scattering method the value of soil water content is correlated with the energy loss of neutrons emitted by neutron probe, located in the access tube inserted vertically into the soil, bumping into the hydrogen nuclei having similar mass. Neutron scattering method is fast and precise but is becoming less popular because of radiation hazard.

The soil conductivity measurement method is described by the international standard ISO 11265. After drying the soil sample according to ISO 11464 standard, it is mixed with water in proportion 1 (by mass, *ex* 1g of soil) : 5 (by volume, *ex* 1 ml of deionized water) and then the filtered extract conductivity is measured by liquid conductometer. This method is time consuming, laborious and its application *in situ* is limited.

The reflectometric method for soil water content and electrical conductivity has become popular since the publication of Topp *et al.* [90]. This paper started research in TDR application in soil metrology and now recognized distributors of soil metrology offer the TDR meters for soil water content and electrical conductivity measurement. Time Domain Reflectometry technique was known even earlier; it was successfully applied by Fellner-Feldegg [30] for the determination of dielectric properties of liquids. The researchers from the Institute of Agrophysics took part in the development of this technique (Malicki and Skierucha[59]) as well as in the construction of TDR meters which are being produced on the license of IAPAS [29]. The main advantages of TDR over other soil water content measurement methods are:

- superior accuracy to within 1 or 2% volumetric water content;
- calibration requirements are minimal - in many cases soil-specific calibration is not needed;
- lack of radiation hazard associated with neutron probe technique;
- TDR has excellent spatial and temporal resolution; and
- measurements are simple to obtain, and the method is capable of providing continuous measurements through automation and multiplexing.

The common use of TDR method and above mentioned advantages place it as a possible standard of porous material, including soil, water content measurement method.

### **3.1. Basics of TDR technique**

Time Domain Reflectometry (TDR) method for the measurement of water content of isotropic and homogenous media becomes popular for the simplicity of operation, accuracy and the non-destructive, as compared to other methods, way of measurement (Malicki [52], O'Connor and Dowding [71]). This measurement technique takes advantage of four physical phenomena characteristic to the soil:

- (i) in the frequency range of 1 GHz the complex dielectric constant of the medium can be approximated by its real value and the electromagnetic wave propagation velocity,  $v$ , in the medium can be calculated from Eq. (2):

$$v = \frac{c}{\sqrt{\varepsilon(\theta)}} = \frac{1}{n} = \frac{2L}{\Delta t} \quad (2)$$

where:  $c$  is a velocity of light in free space,  $\varepsilon(\theta)$  is a real part of the complex dielectric constant dependent on its water content,  $\theta$ ;  $n = \sqrt{\varepsilon(\theta)}$  is the medium refractive index;  $L$  is the length of TDR probe rods inserted into the soil;  $\Delta t$  is the time distance between the reflections of TDR pulse from the beginning and the end of the probe rods, inserted into the medium (Skierucha [78]),

- (ii) the dielectric constant of the medium liquid phase has much higher value than the other medium phases, *ie* about 80 against 2÷4 for the solid and 1 for the gas phase,
- (iii) the relation between the water content of the medium and its dielectric constant is highly correlated for the majority of the porous media [22,59,78],
- (iv) the attenuation of the amplitude of electromagnetic wave traveling along the parallel transmission line inserted into the medium depends on its apparent electrical conductivity,  $EC$  (Dalton *et al.* [19]):

$$EC [\text{Sm}^{-1}] = \frac{\sqrt{\varepsilon}}{120\pi L} \ln\left(\frac{U_{in}}{U_{out}}\right) \quad (3)$$

where:  $U_{in}$  and  $U_{out}$  are the amplitude of the pulse before and after attenuation caused by the pulse travel twice a distance of the probe length,  $L$ .

Therefore water content in the soil, which is assumed to be an isotropic and homogenous medium, is the main reason determining its bulk dielectric constant.

The basic formula (2) is derived from more general one:

$$v = \frac{c}{\sqrt{\frac{\varepsilon'}{2} \left(1 + \sqrt{1 + \text{tg}^2 \delta}\right)}} \quad (4)$$

where:  $c$  is the light velocity of propagation in free space,  $\varepsilon'$  is the real value of the complex dielectric permittivity of the medium,  $\text{tg}\delta$  is the dielectric loss defined as (Chełkowski [14]):

$$\operatorname{tg} \delta = \frac{\varepsilon'' + \frac{\sigma}{2\pi f \varepsilon_0}}{\varepsilon'} \quad (5)$$

The complex dielectric permittivity of the medium,  $\varepsilon$ , is:

$$\varepsilon = \varepsilon' - j \left( \varepsilon'' + \frac{EC}{2\pi f \varepsilon_0} \right) \quad (6)$$

where:  $\varepsilon''$  represents dielectric loss connected with the dielectric polarization of soil particles,  $EC$  is the medium electrical conductivity,  $f$  is the frequency of the electromagnetic field,  $\varepsilon_0$  is dielectric permittivity of free space,  $j$  just equal to  $\sqrt{-1}$ .

### 3.1.1. General idea of the TDR measurements

The idea of simultaneous measurement soil water content and electrical conductivity is presented in **Fig. 1**.

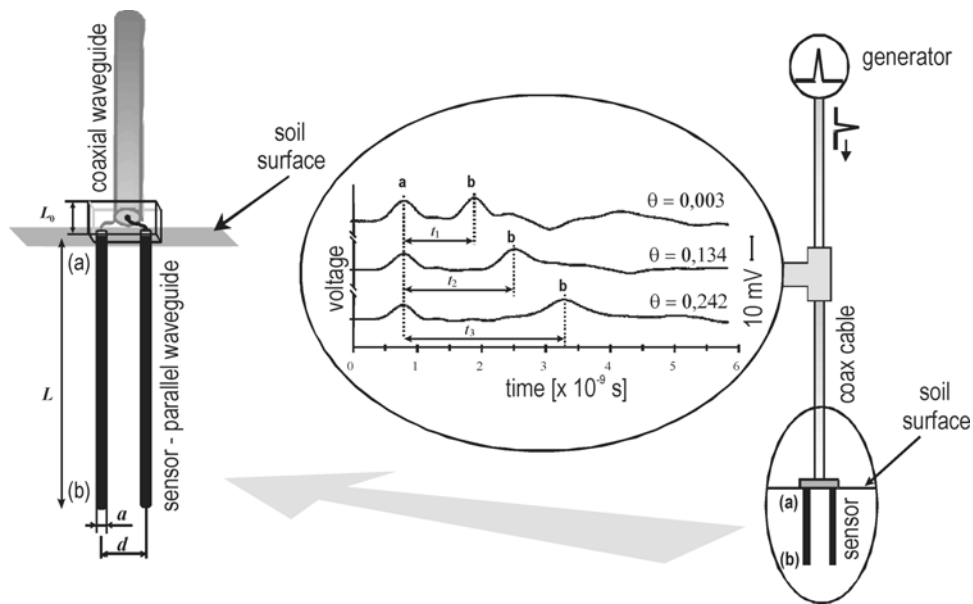


**Fig. 1.** Hardware setup for simultaneous measurement of soil water content and electrical conductivity using Time Domain Reflectometry method

The TDR probe consists of two waveguides connected together: a coaxial one, called the feeder, and a parallel one, called the sensor, made of two parallel metal rods inserted into the measured medium. The initial needle pulse travels from the generator by the feeder towards the sensor. The recorder registers this pulse as it passes T-connector. In the connector, between the feeder and the sensor, there is a rapid change in geometry of the electromagnetic wave travel path. At this point some energy of the pulse is reflected back to the generator, like in radar, and the remaining is traveled along the parallel waveguide to be reflected completely from the rods ending. The successive reflections are recorded for calculation the time distance between the two reflections (a) and (b). Three reflectograms (voltage as a function of time at the chosen point in the feeder) are presented in **Fig. 1**. They represent cases when the sensor was placed in dry, wet and water saturated soil. The time distance,  $\Delta t$ , necessary for the pulse to cover the distance equal to the double length of metal rods in the soil increases with the soil dielectric constant, thus water content. The reason for that is the change of electromagnetic propagation velocity in media of different dielectric constants, according to Eq. (2).

Also, the amplitude of the pulse at the point (b) decreases with the increase of soil electrical conductivity, according to Eq. (3).

### 3.1.2. Calibration of TDR soil water content measurement

There are two approaches that allow calculating the soil water content from the TDR measurements: empirical and theoretical - using dielectric mixing models.

The results of TDR measurements of mineral, organic soils as well as mineral/organic mixtures are presented in **Fig. 2**. The coefficients of linear regression equations fitted to empirical data points differ slightly showing that mineral composition of the soil significantly influences the TDR calibration curve:  $n(\theta_{grav}) = a_0 + a_1\theta_{grav}$ , where  $\theta_{grav}$  is the soil water content determined by standard thermogravimetric method ISO 11461. Reconfiguration of the calibration curve allows the calculation of  $\theta$  when TDR meter measures  $n$ . The accuracy of the TDR soil water content measurement is about  $\pm 2\%$  of the true thermogravimetrically determined value, Eq. (7).

$$\theta = 0.13\sqrt{\varepsilon} - 0.18 \quad (7)$$

The most popular calibration curve for TDR soil (mineral soils) water content measurement was given by Topp *et al.* [90] and is presented below:

$$\theta = -5.3 \cdot 10^{-2} + 2.92 \cdot 10^{-2} \cdot \varepsilon - 5.5 \cdot 10^{-4} \cdot \varepsilon^2 + 4.3 \cdot 10^{-6} \cdot \varepsilon^3 \quad (8)$$

The introduction in the Eq. (7) the correction on soil bulk density,  $\rho$ , that accounts for the influence of soil solid phase in the TDR readout decreases the measurement error to about  $\pm 1\%$  giving a new calibration curve presented by Eq. (9).

$$\theta = \frac{\sqrt{\varepsilon} - 0.57 - 0.58\rho}{7.75 + 0.92\rho} \quad (9)$$

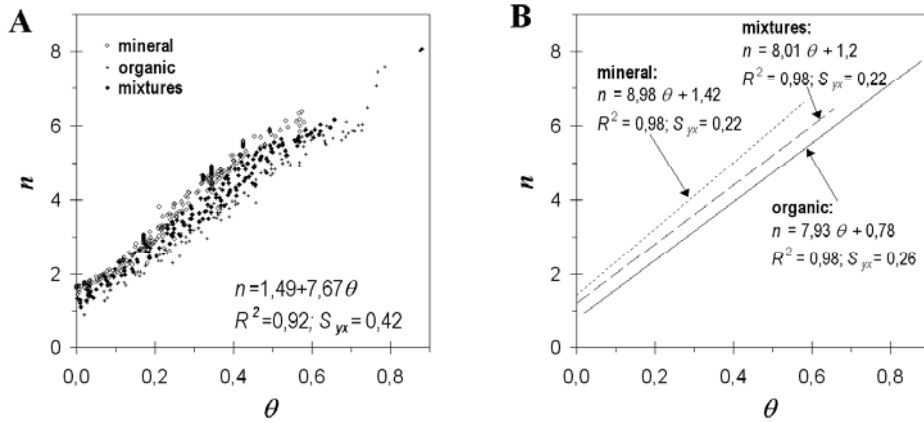


**Fig. 2.** Relation between the soil refractive index,  $n$ , and its water content,  $\theta$ , for mineral and organic soil samples as well as their mixtures. A - experimental data, B - regression  $n(\theta)$ .

Applying theoretical approach the soil is usually treated as a three phase mixture, and its dielectric constant of soil,  $\varepsilon$ , can be presented as:

$$\varepsilon^\alpha = \theta \cdot \varepsilon_w^\alpha + (1 - \phi) \cdot \varepsilon_s^\alpha + (\phi - \theta) \cdot \varepsilon_a^\alpha \quad (10)$$

where:  $\varepsilon$ ,  $\varepsilon_w$ ,  $\varepsilon_s$  and  $\varepsilon_a$  are the dielectric constants of soil as a whole, soil water, soil solids, and air,  $\alpha$  is a constant interpreted as a measure of the soil particles geometry. On the base of the measured data collected on various soils, it has been found by Roth *et al.* [77] that for the three phases dielectric model of the soil the average value of  $\alpha$  constant is 0.5. For typical values of  $\alpha=0.5$ ,  $\varepsilon_w=81$ ,  $\varepsilon_s=4$ ,

$\varepsilon_a=1$  and  $\phi=0.5$  the Eq. (10) has the form of Eq. (11) with coefficients values close to the ones from Eq. (7).

$$\theta = 0.125 \cdot \sqrt{\varepsilon} - 0.19 \quad (11)$$

TDR method of simultaneous measurement of soil water content and electrical conductivity (salinity) becomes more popular because of its advantages: simplicity of operation, accurate and rapid readout, usually does not need calibration, non-destructive operation, availability of portable systems, availability to multiplex probes make automatic measurements. Although it has also disadvantages because it requires excellent probe to soil contact, probe installation may disturb soil, and TDR meters are still expensive, it may become the standard of water content measurement applied not only for soil but also other porous materials like food products and building materials.

### **3.2. Calibration of TDR water content measurement of selected plant materials**

Soil is one of the most complex living system because of spatial and temporal diversity of the processes in the interfaces among soil-plant-atmosphere elements, its biological activity and the physical scale of the objects under consideration (from molecules to large area monitoring and predictions). Therefore it seems that the solutions effective for soil moisture measurement will be also effective in the water content measurement in other biological materials having less complex structure than the soil, *ex plant material*. Below there is the verification of time domain reflectometry water content measurement method in the application to grain (Malicki and Kotliński [56]) and wood (Malicki and Kotliński [57]).

Construction of the applied probes for the measurement of dielectric constant of cereal grain and wood are given in Malicki [54]. The cereal grain probe consists in a cylinder with a metal rod in the center forming a waveguide. The tested cereal grain fills the free space of the cylinder acting as a dielectric. The termination of such a waveguide is connected to a  $50 \Omega$  coaxial cable leading to the TDR measurement unit. The observed reflections in time scale are the markers for calculation of velocity of propagation of the electromagnetic wave in the tested material.

The relation between dielectric permittivity of cereal grain of wheat, rape, vetch, barley, triticale, maize and water content was tested. The characteristics of the tested cereal grain are in **Table 1**

**Table 1.** Selected properties of the investigated grain

type	pH	$EC_w$ (5:1)		porosity of the sample $\phi$		density of the sample $\rho$ [gcm <sup>-3</sup> ]	
		[dSm <sup>-1</sup> ]					
wheat	4.84	1.15	$\phi = 0.500 + 0.283\theta$	R = 0.8046	$\rho = 0.678 - 1.45\theta$	R = 0.9933	
rape	5.45	0.19	$\phi = 0.545 + 0.306\theta$	R = 0.5563	$\rho = 0.726 - 1.60\theta$	R = 0.9977	
vetch	5.41	1.21	$\phi = 0.550 + 0.222\theta$	R = 0.6870	$\rho = 0.666 - 1.36\theta$	R = 0.9934	
barley	5.95	2.42	$\phi = 0.419 + 0.270\theta$	R = 0.8680	$\rho = 0.835 - 1.53\theta$	R = 0.9947	
triticale	5.94	1.09	$\phi = 0.386 + 0.492\theta$	R = 0.9055	$\rho = 0.665 - 1.27\theta$	R = 0.9956	
maize	5.01	1.18	$\phi = 0.486 + 0.586\theta$	R = 0.9592	$\rho = 0.752 - 2.01\theta$	R = 0.9871	

The porosity,  $\phi$ , and gensity,  $\rho$ , of the samples change linearly with water content,  $\theta$ , the table contains the related regression equations. The grain samples of various water contents and homogenous wetting were obtained by mixing grains with water and leaving in  $20 \pm 3$  °C for 48 hours.

The relations between the refractive index,  $n = \sqrt{\epsilon}$ , and volumetric water content,  $\theta$ , and related regression lines are presented in **Fig. 3**.

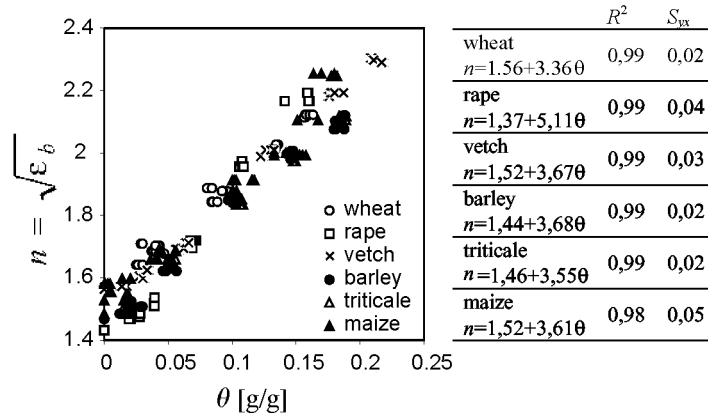


**Fig. 3.** Relations between the refractive index,  $n = \sqrt{\epsilon}$ , and volumetric water content,  $\theta$ , and related regression lines

The relation between the dielectric permittivity of pine, beech and oak wood of selected characteristics are presented in **Table 2**.

**Table 2.** Chosen properties of the investigated woods and parameters of  $n(\theta)$  relation

type	porosity		density of solid phase	pH	conductivity of water extract [dSm <sup>-1</sup> ]
	$\phi$	density $\rho$			
pine	0.681	0.398	1.250	5.60	0.10
beech	0.659	0.757	2.220	5.69	0.27
oak	0.197	0.653	0.813	3.94	0.15

The experiment description is given in [54] and its results are presented in **Fig. 4**.

The relations presented in **Fig. 3** and **Fig. 4** are calibrations of the TDR method for water content determination for individual materials.

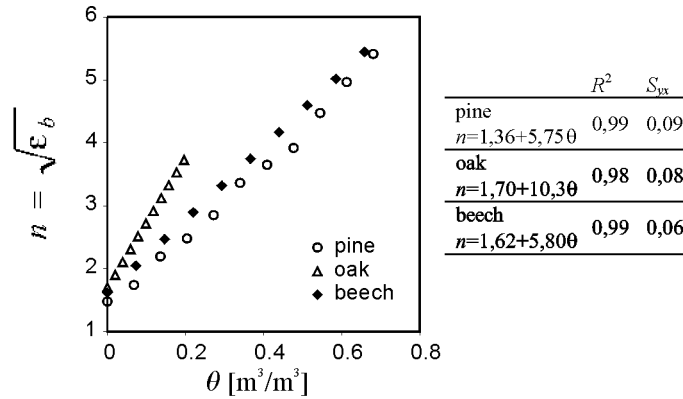


**Fig. 4.** Relative refractive index,  $n = \sqrt{\epsilon}$ , as the function of water content for selected wood types

Generally all selected materials have different calibrations, although when the highest accuracy is not required there might be one calibration applied for a group of materials, as it is presented for soil. The experiments performed on cereal grain and wood prove the applicability of Time Domain Reflectometry method for water content determination in other materials than soil. Generally the TDR could be applied for porous bodies in many branches of food industry, civil engineering, *ie* where the porous bodied water content is of special interest.

### 3.3. TDR soil salinity measurement

To determine soil salinity, as expressed in terms of electrical conductivity of soil water,  $EC_w$ , the apparent electrical conductivity,  $EC_a$ , and the relative dielectric permittivity (dielectric constant),  $\epsilon$ , of the soil have to be known (Malicki *et al.* [62]). The two parameters can be obtained using time domain reflectometry (TDR), which provides nondestructive simultaneous measurements of  $\epsilon$  and  $EC_a$  from the same sensor, over the same sampling volume [19,20,21,53,91].

### 3.3.1. Theory

TDR - time domain reflectometry - was primarily applied to determine soil water content (Davis and Chudobiak [23], Topp *et al.* [90]) as correlated to the soil relative dielectric permittivity,  $\varepsilon$ , according to the following formula derived from Eq. (2):

$$\sqrt{\varepsilon} = \frac{c}{2L}t \quad (12)$$

where:  $c = 3 \cdot 10^8$  [ $\text{ms}^{-1}$ ] - velocity of propagation of electromagnetic waves in free space,  $L$  [m] - distance the pulse covers in the soil, equal to the length of the rods of the TDR sensor,  $t$  [s] - time necessary for the pulse to cover the distance  $L$ . The necessary instrumentation setup is presented in **Fig. 1**.

From (12) it can be seen that in order to calculate the dielectric permittivity,  $\varepsilon$ , of the soil, knowledge of time the pulse covers a certain, fixed distance in the soil, is necessary.

The TDR method of the determination of the soil bulk electrical conductivity is based on the assumption that the applied electromagnetic pulse loses its energy due to the electrical conductivity of the soil. Thus, from the measurement of attenuation of the pulse being propagated in the considered soil,  $EC_a$  can be found according to Eq. (3). All the necessary information for the calculation of the apparent conductivity of the soil is in the TDR trace reflected from the TDR sensor rods, *ie* the magnitudes of the electromagnetic pulse at the beginning and end of the distance  $L$  it covers in the soil, and time,  $t$ , between the related reflections.

### 3.3.2. Experimental verification of the soil electrical conductivity measurement

A set of 9 samples of soil material having gradually differentiated sand and clay content was investigated. Air-dry samples were wetted with solutions of KCl in 5 steps to cover the range of water content from air dryness up to saturation.

Measurements of the soil apparent electrical conductivity,  $EC_{a-TDR}$ , were performed with application of the Time-Domain Reflectometry. Also parallel reference readings of the soil bulk electrical conductivity,  $EC_{a-4p}$ , were taken with the four-electrode probe. LOM/mts - TDR soil water content, temperature, salinity meter and ELCON/4el soil bulk electrical conductivity meter from Easy Test [29] were used respectively. The procedure was repeated for solutions having different salinities (concentrations of KCl).

Results obtained with the discussed attenuation-based TDR measurements of the soil electrical conductivity,  $EC_{a-TDR}$ , of the investigated soil samples, as derived from TDR pulse attenuation accordingly to Eq. (3), disagreed with the reference data,  $EC_{a-4p}$ , determined using the four-electrode reference method. The results of soil electrical conductivity measurements using these two methods are compared in **Fig. 5**.

To explain the discrepancy it was assumed that more than the single, above-mentioned reason of the pulse attenuation should be taken into account.

Electromagnetic waves undergo attenuation when propagating for the following reasons:

- energy is partly radiated into the surrounding (the soil),
- energy is partly dissipated (converted to heat) during dielectric polarization of the material it propagates in (solid particles + soil water)
- energy is dissipated due to electrical conductivity of the material (soil water) it propagates in.

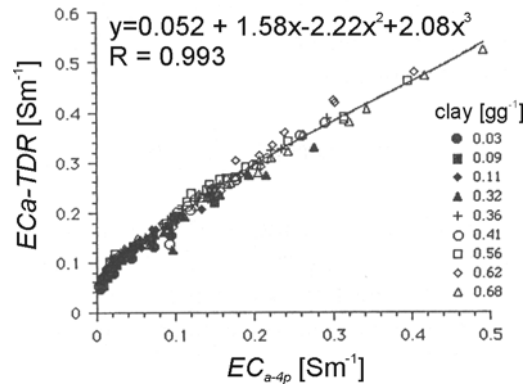


**Fig. 5.** Bulk electrical conductivity,  $EC_{a-TDR}$ , of the investigated soil samples obtained using TDR pulse attenuation method accordingly to Eq. (3), versus reference data,  $EC_{a-4p}$ , determined using four-electrode reference method

The attenuation of the pulse is described by the imaginary part,  $\varepsilon''$ , of the soil dielectric permittivity, according to Eq. (3). When  $EC_a$  reaches magnitude close to zero, like in case of dry or wet but not salty soil, then  $\varepsilon''$  reaches a finite, nonzero magnitude. This implies discordance of the  $EC_{a-TDR} - EC_{a-4p}$  relationship due to a remarkable intercept caused by the dielectric losses in the soil.

The  $EC_{a-TDR}$  versus  $EC_{a-4p}$  line seems to justify the above explanation. Its shape revealed nonlinearity. Fitting a polynomial to the  $EC_{a-4p}(EC_{a-TDR})$  relationship (see

**Fig. 6)** made the TDR attenuation-based method applicable for the determination of the soil bulk electrical conductivity.

Malicki *et al.* [62] introduced a term: salinity index,  $X_s$ , which is defined as follows:

$$X_s = \frac{\partial EC_a}{\partial \varepsilon} \quad (13)$$

It can be determined electrically from simultaneous readings of  $EC_a$  and  $\varepsilon$ , for expressing soil salinity status in relative terms as a moisture-independent variable. They found its applicability for soils having water content from 0.12 to saturation. The values of  $X_s$  determined for silty loam, silt, river sand, quartz sand and loamy sand is presented in **Table 3**.

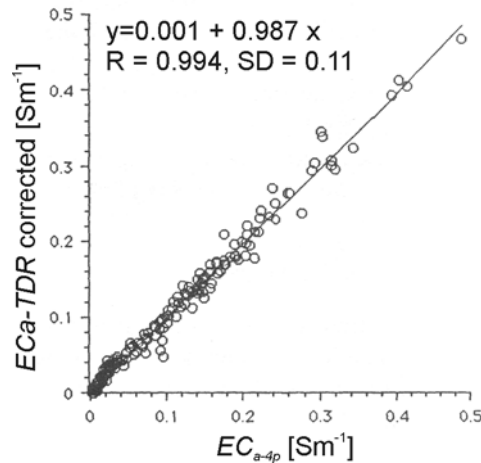


**Fig. 6.** Comparison of the bulk electrical conductivity of the investigated soils,  $EC_{a-TDR}$ , with the reference data,  $EC_{a-4p}$ , after correction accordingly do the polynomial of **Fig. 5**

**Table 3.** Salinity indices for various soils (after Malicki *et al.* [62]),  $EC_s$  [ $dSm^{-1}$ ] is the electrical conductivity of a solution used to moisten soil samples

Soil	Salinity index, $X_s$
Silty loam	$X_s = 0.0205 + 0.0098 EC_s$
Silt	$X_s = 0.0091 + 0.0081 EC_s$
River sand	$X_s = 0.0000 + 0.0136 EC_s$
Quartz sand	$X_s = 0.0016 + 0.0126 EC_s$
Loamy sand	$X_s = 0.0049 + 0.0110 EC_s$

Notice that at  $C_s = 0$ , *ie* when distilled water was used to moisten the soil, the salinity index possesses a certain baseline magnitude,  $X_{si}$ , which is assumed to result from initial salinity,  $C_{si}$ , of water, coming from residual soluble salts present in the soil. Even if distilled water, having practically zero conductivity, is used as the input solution,  $X_s$  remains greater than zero. This seems to be because the matrix of any soil possesses some soluble components, such as residual salts, carbonates, silica, etc., which can contribute to the initial conductivity of the soil water extract (*ie* distilled water as the input solution). Therefore electrical conductivity of soil water defined as the soil salinity,  $EC_w$ , is always greater than zero.

### 3.3.3. Summary

Direct calculation of bulk electrical conductivity of the soil from attenuation of the electromagnetic pulse leads to significant error.

The TDR attenuation-based method for the determination of the soil bulk electrical conductivity can be applied after fitting an appropriate correction to the  $EC_{a-4p}(EC_{a-TDR})$  relationship according to the polynomial from **Fig. 5**.

Salinity index, defined as the derivative of bulk electrical conductivity to bulk electrical permittivity, which can be determined simultaneously by TDR measurements, can be applied as a moisture-independent electrical variable to express relative changes in the soil salinity without entailing any calibration.

## 3.4. Choice of frequency of the electric field in dielectric measurement of soil water content in saline soils

Water concentration in soil (soil water content) and soil temperature are the quantities of strong temporal and spatial variability, while the concentration of solid phase (soil density) as well as the density of its elements (particle density) is practically stable.

Changes of electrical capacity of a capacitor with soil as the dielectric are attributed to the soil water content changes because the dielectric constant of water (equal to 81 at 18 °C) dominates the dielectric constant of soil solid phase (equal to 4 ÷ 5) and air (equal to 1). Considering above, the electric measurement of soil water content is done on the base of the correlated dielectric constant (Gardner *et al.* [32], Malicki [51], Malicki and Skierucha [59], White *et al.* [101]). Such a solution to the problem is not ideal. The presence of ions in the “soil water” causes the conduction electric current. Therefore soil has dual nature. Simultaneously it possesses the properties of an insulator characterized by the dielectric constant of water, soil solid phase elements and air, as well as a conductor characterized by the electrical conductivity of an electrolyte (it is

assumed that the conductivity of soil solid phase and air is negligible). Therefore the soil dielectric permittivity is a complex value with the real part conditioned by its water content and imaginary part by its salinity. The presented discussion refers to the conditions when the dielectric measurement of soil water content is not influenced by the conductivity of the electrolyte in it. The objective of the considerations below is the determination of the frequency of the electric field applied to the soil that would allow interpreting its reaction only on the basis of water and solid phase in it.

### 3.4.1. Frequency dispersion of the electrolyte dielectric permittivity

Dielectric permittivity,  $\varepsilon$ , of an electrolyte is a complex value dependent on the frequency of the applied electric field,  $f$ . Its real,  $\text{Re}(\varepsilon)$ , and imaginary  $\text{Im}(\varepsilon)$  parts have the form (Chelkowski [14], Hasted [37]):

$$\text{Re}(\varepsilon) = \varepsilon' \quad (14)$$

$$\text{Im}(\varepsilon) = \varepsilon'' + \frac{EC_w}{\omega\varepsilon_0} \quad (15)$$

where:  $\varepsilon'$  and  $\varepsilon''$  are real and imaginary parts of the complex dielectric permittivity of water, respectively,  $EC_w$  – electrical conductivity of the electrolyte [ $\text{Sm}^{-1}$ ],  $\omega$  – angular frequency of the applied electric field (equals to  $2\pi f$ ) [ $\text{s}^{-1}$ ],  $\varepsilon_0$  – is the dielectric permittivity of free space [ $\text{Fm}^{-1}$ ].

The real and imaginary parts of the complex dielectric permittivity are modeled by Cole-Cole formulas [14,37]:

$$\varepsilon' = \varepsilon_\infty + \frac{(\varepsilon_s - \varepsilon_\infty) \left[ 1 + (\omega\tau)^{1-h} \sin \frac{h\pi}{2} \right]}{1 + (\omega\tau)^{2(1-h)} + 2(\omega\tau)^{1-h} \sin \frac{h\pi}{2}} \quad (16)$$

$$\varepsilon'' = \frac{(\varepsilon_s - \varepsilon_\infty) \left[ (\omega\tau)^{1-h} \cos \frac{h\pi}{2} \right]}{1 + (\omega\tau)^{2(1-h)} + 2(\omega\tau)^{1-h} \sin \frac{h\pi}{2}} \quad (17)$$

where:  $\varepsilon_\infty$  is the relative water dielectric permittivity when  $\omega > \tau^{-1}$ ,  $\varepsilon_s$  is the relative dielectric permittivity of water when  $\omega = 0$ ,  $\tau$  is the relaxation time of

water orientation polarization [s],  $h$  is the parameter describing interaction of water dipoles:  $0 < h < 1$ . After substituting (17) in (15) we can have  $\text{Im}(\varepsilon)$  for the electrolyte:

$$\text{Im}(\varepsilon) = \frac{(\varepsilon_s - \varepsilon_\infty) \left[ (\omega\tau)^{1-h} \cos \frac{h\pi}{2} \right]}{1 + (\omega\tau)^{2(1-h)} + 2(\omega\tau)^{1-h} \sin \frac{h\pi}{2}} + \frac{\sigma_e}{\omega\varepsilon_0} \quad (18)$$

The absolute value of the complex dielectric permittivity of electrolyte,  $k$ , is:

$$k = |\varepsilon| = \sqrt{[\text{Re}(\varepsilon)]^2 + [\text{Im}(\varepsilon)]^2} \quad (19)$$

Presenting the values from Eq. (16) and Eq. (19) for different  $w$  gives the information about the frequency dispersion of  $\varepsilon'$  and  $k$ , *ie* the dependence of the related values on the frequency of the applied electric field (Malicki [54]).

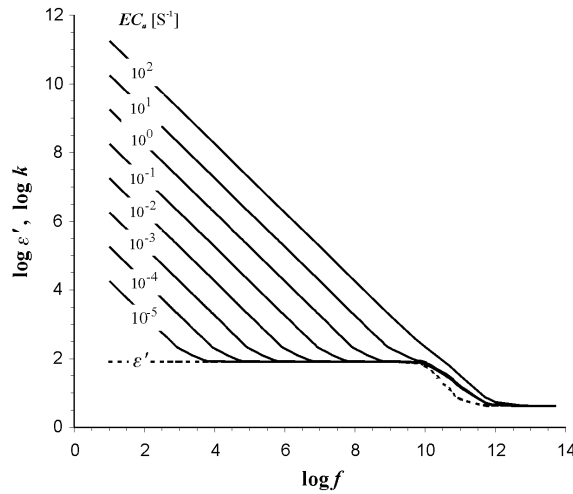


**Fig. 7.** Frequency dispersion of the real part,  $\varepsilon'$ , and module,  $k$ , of the complex dielectric constant of the electrolyte for different conductivities

**Fig. 7** shows the frequency dispersion of the module,  $k$ , of the complex dielectric permittivity of an electrolyte and the dispersion of its real value,  $\varepsilon'$ , for the electrolyte of variable conductivity,  $EC_a$ . The assumptions in the presented

calculations were taken from Hasted [37]:  $\varepsilon_0 = 8.854 \cdot 10^{-12} [\text{Fm}^{-1}]$ ,  $\varepsilon_s = 81$ ,  $\varepsilon_\infty = 4.23$  (Hasted [37]),  $h = 0.013$  (Hasted [37]),  $\tau = 9.3 \cdot 10^{-12}$  s.

It is evident that for the defined frequency range and variability of electrical conductivity,  $k = \varepsilon'$ . This means that the imaginary part of the dielectric permittivity of the electrolyte,  $\text{Im}(\varepsilon)$ , is negligible and the electrolyte behaves as a dielectric (insulator). The right limit of this frequency range depends on the dielectric loss (relaxation) of water particles and is about  $10^{10}$  Hz, and the left limit depends on the value of the electrolyte electric conductivity,  $EC_w$ .

Applying the sufficiently high frequency of the electric field,  $f_{\min}$ , to the sensor, it would be possible to release the dielectric measurement of soil water content from the influence of the electric conductivity, if the electric conductivity of the electrolyte present in the soil does not exceed  $10 [\text{Sm}^{-1}]$  (according to James *et al.* [45]). This frequency can be found after correlation of frequency values at the inflection point of the curves with the respective values of  $EC_w$ :

$$\lg f_{\min} = 8.5 + \lg \sigma_e \quad (20)$$

Accounting for the fact that the electric conductivity of the soil at saturation with the electrolyte is about  $5 \div 15$  times lower than the conductivity of the electrolyte (Malicki and Walczak [61]),  $f_{\min}$  determined for the electrolyte refers also to the soil.

The presented discussion can be repeated in other way. Both components of the complex dielectric constant (6) can be represented by loss angle,  $\delta$ , tangens of which is the ratio of the imaginary to real part.

$$\delta = \arctg \left( \frac{\text{Im}(\varepsilon)}{\text{Re}(\varepsilon)} \right) \quad (21)$$

The frequency dispersion of the real part,  $\varepsilon'$ , of the complex dielectric constant and the loss angle,  $\delta$ , for the electrolyte having different conductivity values are presented in **Fig. 8**. The figure, based on the Cole-Cole formulas, takes into account the electrical conductivity of the electrolyte ( $EC_w/2\pi f \varepsilon_0$  from equation (6)).

For the defined frequency range, dependent on the electrical conductivity,  $EC_w$ , of the applied electrolyte, the loss angle decreases from  $90^\circ$  to zero. Therefore for the frequency close to 1 GHz the complex dielectric constant of electrolyte reduces to its real part,  $\varepsilon'$ , only when the tested material does not have too high electrical conductivity.

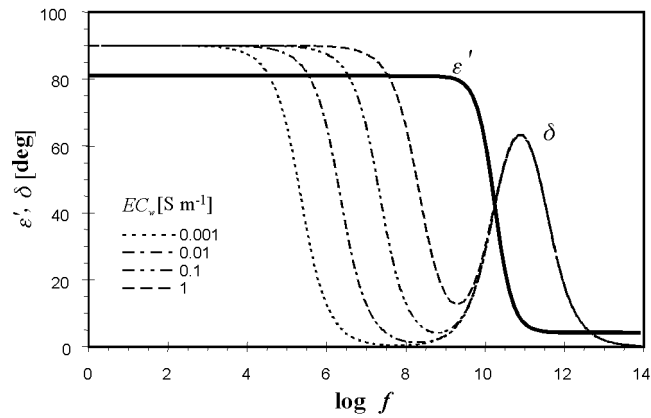


**Fig. 8.** Frequency dispersion of the real part,  $\epsilon'$ , of the complex dielectric constant and the loss angle,  $\delta$ , for the electrolyte for its various electrical conductivities,  $EC_w$

The time-domain reflectometry as applied to the measurement of water content and salinity of porous materials implements the property described above.

#### 3.4.2. Summary

1. The lower electric conductivity of the electrolyte present in the soil, the lower is the lower frequency limit, where the electrolyte behaves as pure water (dielectric, insulator), which enables the dielectric measurement of soil water content without the influence of its electric conductivity.
2. If the electrical conductivity of the soil electrolyte does not exceed the value of  $1 \text{ [Sm}^{-1}\text{]}$ , using the sufficiently high, but not higher than  $10^{10} \text{ Hz}$ , frequency of the applied electric field, the ion conduction is dominated by orientation polarization of soil water particles.

#### 4. THE INFLUENCE OF SOIL ELECTRICAL CONDUCTIVITY ON THE SOIL WATER CONTENT VALUES MEASURED BY TDR METHOD

Topp et al. [90] did not find the influence of soil salinity, or soil electrical conductivity,  $EC_a$ , on the the electromagnetic wave velocity of propagation for mineral soils wetted with NaCl and CaSO<sub>4</sub> solutions of conductivity values practically found for soil solutions. However they found the increase of TDR measured water content,  $\theta_{TDR}$ , measurement error for high saline soils. The explained is as a result of high attenuation of the TDR pulse and the problems with finding the correct reflection point.

Dalton et al. [19] measured simultaneously water content and electrical conductivity in the range  $0.03 \div 0.14$  [ $S\cdot m^{-1}$ ] of saturated soil samples ( $\theta = 0.34 \pm 0.01$ ) using the TDR method. They found that TDR determined soil water content is not influenced by the soil electrical conductivity.

In the electromagnetic field of high frequency the soil electric conductivity does seem to influence the velocity of EM propagation. **Fig. 8** shows that in the defined frequency range the loss angle decreases to the values close to zero. This means that for the frequencies in this range the imaginary part of the complex dielectric permittivity (6) is negligible. Consequently for the TDR measurement technique of soil content determination based on the measurement of the electromagnetic wave propagation velocity in the soil can be simplified from Eq. (4) to Eq. (2). The following chapter will practically verify these conclusions.

##### 4.1. Material and method

The soil material consisted of two soils (**Table 4**) and their mixtures prepared in the proportion, so as to have the density of soil samples equally distributed in the range  $1.23 - 1.91$  [ $g\cdot cm^{-3}$ ].

**Table 4.** The parameters of the soils used for the preparation of soil mixtures.

Localization	Soil type (FAO)	Level	Depth [cm]	$\rho$ [ $g\cdot cm^{-3}$ ]	$\rho_s$ [ $g\cdot cm^{-3}$ ]	Soil texture % (FAO)			C [%]
						sand	silt	clay	
Markuszów	Orthic	Bh1	40-60	1.58÷1.80	2.64	85	12	3	0.89
	Podzol								
Janów Lub.	Eutric	Bh	20-30	1.14÷1.53	2.43	1	31	68	0.35
	Cambisol								

The measurements were performed in laboratory conditions. The measured soil parameters were: soil water content,  $\theta$ , and bulk density,  $\rho$ , performed by thermogravimetric method; soil refractive index,  $n = \sqrt{\varepsilon}$ , and soil apparent electrical conductivity,  $EC_a$ , performed by the reflectometric method [29]; electrical conductivity,  $EC_w$ , of the solution of KCl used for wetting the soil samples.

The air dry soil was sieved through 2 mm holes and moistened by the KCl solutions of the conductivity values,  $EC_w$  [ $S\cdot m^{-1}$ ]: 0.00, 0.127, 0.488, 0.825 and 1.17. This way the soil apparent conductivity,  $EC_a$ , values were in the range  $0.04 \div 0.5$  [ $S\cdot m^{-1}$ ]. The soil samples were moistened uniformly and were placed in glass containers cautiously to have the soil sample of uniform density.

#### 4.2. Results and discussion

The results of the measurements performed on the prepared soil samples can be presented in tabular form (**Table 5**) as ( $n$ ,  $\theta$ ,  $\rho$ ,  $EC_w$ ). The influence of the soil electrical conductivity in the TDR refractive index determination can be checked using by multiple regression method.

$$n = a_0 + a_1\theta + a_2\rho + a_3EC_w \quad (22)$$

where:  $a_0 - a_3$  are empirical coefficients and  $EC_w$  is the electrical conductivity of the KCl solutions.

**Table 5.** The results of multiple regression method (22)  $S_{yx}$  is the standard error of estimate

$a_3 \neq 0$		$a_3 = 0$	
$n = a_0 + a_1\theta + a_2\rho + a_3EC_w$		$n = a_0 + a_1\theta + a_2\rho$	
$R^2$	0.99	$R^2$	0.99
$S_{yx}$	0.138	$S_{yx}$	0.139
no of samples	225	no of samples	225
$a_0$	0.536	$a_0$	0.539
$p(a_0)$	<0.01	$p(a_0)$	<0.01
$a_1$	8.819	$a_1$	8.792
$p(a_1)$	<0.01	$p(a_1)$	<0.01
$a_2$	0.575	$a_2$	0.569
$p(a_2)$	<0.01	$p(a_2)$	<0.01
$a_3$	-0.031		
$p(a_3)$	0.164		

The results of  $R^2$ ,  $S_{yx}$  and the coefficients  $a_0$ ,  $a_1$  and  $a_2$  have similar values in the both cases. The  $p$ -value for  $a_3$   $p(a_3) \gg 0.01$  and it can be concluded that the electrical conductivity of the solution (determining the soil salinity) influences the TDR determined soil refractive index in the statistically not significant way.

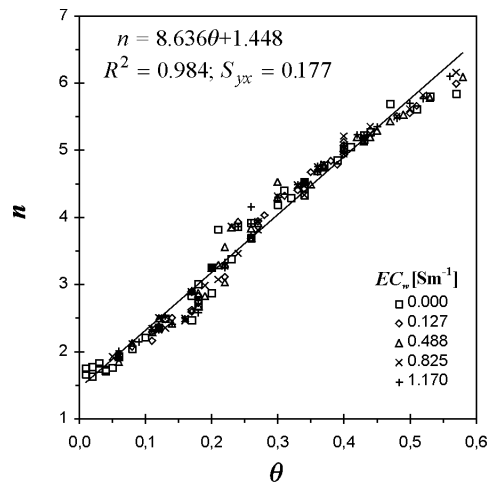


**Fig. 9.** The relation  $n(\theta)$  for soil samples moistened by KCl solutions of different electrical conductivities,  $EC_w$

Consequently the TDR determined water content does not depend on soil electrical conductivity in the soil salinity range covered by the experiment.

**Fig. 9** presents the relation  $n(\theta)$  for the analyzed soil samples wetted by the KCl solutions of different electrical conductivity values,  $EC_w$ . In the range of  $0 \div 1.17$  [ $S \cdot m^{-1}$ ], that is in the range corresponding to the natural soil salinity values, the soil electrical conductivity does not influence this relation. Practically this means, that reflectometric measurement of soil water content by the TDR method is not sensitive to the soil electrical conductivity,  $EC_a$ , and its salinity.

## 5. EVALUATION OF DIELECTRIC MIXING MODELS OF MINERAL SOILS

The increasing popularity of Time Domain Reflectometry (TDR) technique in the dielectric determination of soil water content (Or and Wraith [72], Topp *et al.* [90]) implies the necessity of verification of the dielectric mixing models. The commonly used models describing the soil dielectric constant as the mixture of solid matter, water and air are:  $\alpha$  model (Birtchak [9], Bohl *et al.* [11], Steru [86]), the model proposed by *de Loor* [25] and empirical models (Malicki and Skierucha [59], Malicki *et al.* [58], Skierucha [78], Topp *et al.* [90]).

The soil water content sensor used in TDR method and presented schematically in **Fig. 10**, consists of two parallel metal rods (or three metal rods applied by Heimovaara [39], Wright and Or [105], Zegelin *et al.* [106]) of the length  $L$ , inserted into the tested soil [32,38,59]. The time,  $t$ , for the electromagnetic (EM) wave to cover the distance  $L$  may be calculated as the sum of propagation times along the individual soil phases (Kraszewski [48]):

$$t = t_s + t_a + t_w \quad (23)$$

where the indexes  $s$ ,  $a$  and  $w$  stand for solid, gas and water phases, respectively.

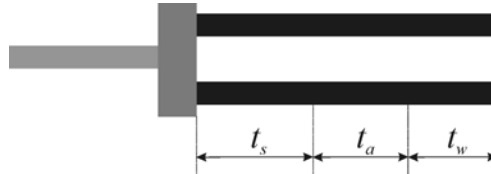


**Fig. 10.** TDR interpretation of soil as a three phases medium in dielectric mixing model  $\alpha$

In most practical conditions the velocity of EM wave propagation,  $v$ , in the soil may be presented as:

$$v = \frac{c}{\sqrt{\varepsilon}} = \frac{2L}{t} \quad (24)$$

where  $c$  is the velocity of light in free space,  $\varepsilon$  is the soil dielectric constant. The total propagation time,  $t$ , of EM wave can be expressed by dividing it into

elementary propagation times along the solid, water and air phases of the soil expressed by (23) by means of (24):

$$t = t_s + t_a + t_w = \frac{2L\sqrt{\varepsilon}}{c} = \frac{2L_s\sqrt{\varepsilon_s}}{c} + \frac{2L_a\sqrt{\varepsilon_a}}{c} + \frac{2L_w\sqrt{\varepsilon_w}}{c} \quad (25)$$

with:  $L_s$ ,  $L_a$ ,  $L_w$  are idealized by the presented model parts of the probe inserted into an elementary soil phase. Rewriting to last two elements of the Eq. (25), multiplying by the elementary cross-section  $S$  and then dividing by the whole volume of soil in the cylinder defining the sphere of influence of the TDR measurement method gives:

$$\sqrt{\varepsilon} = \sqrt{\varepsilon_s} \frac{V_s}{V} + \sqrt{\varepsilon_a} \frac{V_a}{V} + \sqrt{\varepsilon_w} \frac{V_w}{V} = \sqrt{\varepsilon_s} (1 - \phi) + \sqrt{\varepsilon_a} (\phi - \theta) + \sqrt{\varepsilon_w} \theta \quad (26)$$

or using the parameter  $\alpha$ , which summarizes the geometry of the medium with relation to the applied electric field (Roth *et al.* [77]):

$$\varepsilon = \left( (1 - \phi) \varepsilon_s^\alpha + (\phi - \theta) \varepsilon_a^\alpha + \theta \varepsilon_w^\alpha \right)^{\frac{1}{\alpha}} \quad (27)$$

which is the 3-phase dielectric mixing model  $\alpha$ , expressing the square root of the apparent dielectric constant of soil in the terms used by soil scientists:  $\phi$  – soil porosity and  $\theta$  – volumetric water content. Whalley [100] presented the similar discussion.

Following Birchak *et al.* [9], Alharthi and Lange [3] assumed  $\alpha = 0.5$ , which gives the Eq. (26). After introducing adsorbed water as a fourth phase Dobson *et al.* [28] determined  $\alpha$  by regression data for different frequencies (ranging from 1.4 to 18 GHz) and soil types (ranging from sandy loam to silty clay) and obtained  $\alpha = 0.65$ . The four-phase dielectric mixing model  $\alpha$ , accounting for the adsorbed to soil solid phase bound water has the following form:

$$\varepsilon^\alpha = (1 - \phi) \varepsilon_s^\alpha + (\phi - \theta) \varepsilon_a^\alpha + (\theta - \theta_{bw}) \varepsilon_w^\alpha + \theta_{bw} \varepsilon_{bw}^\alpha \quad (28)$$

where water exists in two phases: as free water,  $w$ , like capillary water and bound water,  $bw$ , like molecular or film water. Generally the  $\alpha$ -model of soil dielectric mixture may be presented as follows:

$$\varepsilon^\alpha = \sum_i V_i \varepsilon_i^\alpha \quad (29)$$

where  $V_i$  is the volumetric concentration of  $i$ -th phase and  $\varepsilon_i$  is the dielectric constant of this phase.

The four-phase model proposed by *de Loor* [25,26] and used by Dirksen and Dasberg [27] and Dobson and Ulaby [28] is:

$$\varepsilon = \frac{3\varepsilon_s + 2\theta_w(\varepsilon_w - \varepsilon_s) + 2\theta_{bw}(\varepsilon_{bw} - \varepsilon_s) + 2\theta_a(\varepsilon_a - \varepsilon_s)}{3 + \theta_w\left(\frac{\varepsilon_s}{\varepsilon_w} - 1\right) + \theta_{bw}\left(\frac{\varepsilon_s}{\varepsilon_{bw}} - 1\right) + \theta_a\left(\frac{\varepsilon_s}{\varepsilon_a} - 1\right)} \quad (30)$$

where the indexes  $s$ ,  $w$ ,  $bw$  and  $a$  refer to solid phase, water, bound water and air, respectively. This model describes heterogeneous mixture where foreign granules with dielectric constant  $\varepsilon_i$  are imbedded in a homogeneous and isotropic dielectric with dielectric constant  $\varepsilon$ . The imbedded foreign granules in Eq. (30) represent free water, bound water and air. The host medium is the solid phase.

The empirical models  $\varepsilon(\theta)$  and  $\varepsilon(\theta, \rho)$ , where  $\rho$  is the soil bulk density, form the formula of the appropriate regression curves [58,59,78,90]. The formula (31) presented below and discussed in Skierucha [78] will be used in this paper as the reference:

$$\varepsilon = (0,573 + 0,582\rho + (7,755 + 0,792\rho)\theta)^2 \quad (31)$$

where  $\rho$  [g/cm<sup>3</sup>] is the soil bulk density.

The verification of the discussed 3-phase and 4-phase models is presented in the following sections.

### 5.1. Material and methods

Sixteen mineral soils of different texture, volumetric water content and bulk and particle density were investigated (**Table 6**).

The following variables were measured: dielectric constant,  $\varepsilon$ , bulk density,  $\rho$ , particle density,  $\rho_s$ , and gravimetrically determined volumetric water content,  $\theta$ . Dielectric constant,  $\varepsilon$ , was determined using TDR (LOM/m from *Easy Test, Ltd.* [29]). The remaining variables were measured with the application of standard methods.

The solid phase dielectric constant,  $\varepsilon_s$ , was calculated from the formula (derived from the formula (27)):

$$\varepsilon_s = \overline{\varepsilon_s} = \frac{1}{n} \sum_i^n \left( \frac{(\varepsilon(\theta=0))^\alpha - \phi_i}{1 - \phi_i} \right)^{\frac{1}{\alpha}} \quad (32)$$

where  $\alpha=0,5$ .

The solid phase dielectric constant was calculated on the base of three-phase model  $\alpha$  applied to all soil samples from **Table 6** fitting the exponential function to the experimental data.

**Table 6.** Selected properties of the investigated mineral soils, where  $\rho$  [ $\text{gcm}^{-3}$ ] is the soil bulk density,  $\rho_s$  [ $\text{gcm}^{-3}$ ] is the soil particle density

No	Localization	Soil type (FAO)	Level (depth in cm)	Bulk density ( $\text{gcm}^{-3}$ )	Particle density ( $\text{gcm}^{-3}$ )	Texture % (FAO)		
						Sand	Silt	Clay
1	Parana. Brazil	Haplic Ferrasol	Ah (0-10)	1.27+1.60	2.62	82	6	12
2	Parana. Brazil	Haplic Ferrasol	Bws (120-140)	1.31+1.77	2.67	72	8	18
3	Grunewald. Germany	Haplic Luvisol	Bt (90-120)	1.35+1.55	2.53	2	75	23
4	Grunewald. Germany	Haplic Podzol	Bhs (30-45)	1.21+1.60	2.54	88	10	2
5	Elba. Italy	Chromic Luvisol	Ah (0-20)	1.34+1.64	2.63	46	31	23
6	Elba. Italy	Chromic Luvisol	Bt (150-180)	1.33+1.73	2.65	35	31	34
7	Elba. Italy	Luvic Calcisol	Ah (0-20)	1.25+1.68	2.57	50	26	24
8	Elba. Italy	Luvic Calcisol	Btk (80-100)	1.14+1.52	2.53	26	28	46
9	Werbkowice	Haplic Chernozem	Ap (0-20)	1.18+1.40	2.28	2	52	46
10	Parana. Brazil	Rhodic Ferrasol	Ah (0-10)	1.01+1.37	2.88	4	16	80
11	Parana. Brazil	Rhodic Ferrasol	Bws (140-160)	1.04+1.24	2.88	3	16	81
12	Ohlendorf. Germany	Haplic Luvisol	Bt (60-80)	1.31+1.62	2.70	2	75	23
13	Ohlendorf. Germany	Arenic Cambisol	C (70-120)	1.59+1.70	2.63	98	2	0
14	Markuszów	Orthic Podzol	Bh1 (40-60)	1.58+1.80	2.64	85	12	3
15	Czesławice	Orthic Luvisol	Ck (150)	1.25+1.61	2.48	0	68	32
16	Janów Lubelski	Eutric Cambisol	Bh (20-30)	1.14+1.53	2.43	1	31	68

For dry soil ( $\theta=0$ ) only solid and air phases are present, therefore knowing the porosity of the most dry soil from the tested samples it is possible to estimate the  $\varepsilon_s$  as the average of all tested mineral soil samples according to Eq. (32).

This extrapolation gives the average value of dielectric constant soil solid phase equal to 4.72, which is in agreement with the published data (Dirksen and Dasberg [27], Friedman and Robinson [31]). The detailed statistics of the performed calculations are in **Fig. 11**.

It is assumed that for each soil type there is a transition water content value,  $\theta_{WP}$ , which makes the distinction between soil water as bound or free. This water content can be determined from the empirical formula (Wang and Schmutge [99]) as:

$$\theta_{WP} = 0,0674 - 0,00064 \cdot SAND + 0,00478 \cdot CLAY \quad (33)$$

where *SAND* and *CLAY* are percents of sand and clay in the tested soils. The index *WP* stands for wilting point as Wang and Schmugge [99] correlated the transition water content with the wilting point water content.

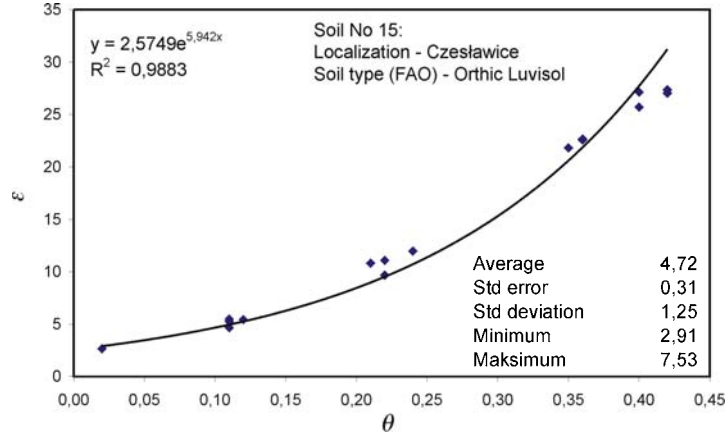


**Fig. 11.** Determination of the dielectric constant of soil solid phase using extrapolation and three-phase soil dielectric mixing model  $\alpha$ .

Further discussion concerning 4-phase models assumes:

- If  $\theta > \theta_{WP}$ , the soil dielectric constant is represented by the 3-phase models, that is the formula (27) for the  $\alpha$ -model, and the formula (30) for the *de Looor* model at  $\theta_{bw}=0$ .
- If  $\theta \leq \theta_{WP}$ , the soil dielectric constant is represented by the 4-phase models, that is the formula (28) for the  $\alpha$ -model, and the formula (30) for the *de Looor* model, at  $\theta_{bw} = \theta$  and  $\varepsilon_{bw} = \varepsilon_s + (80,2 - \varepsilon_s) \frac{\theta_{bw}}{\theta_{WP}}$ , where  $\varepsilon_s$  is the soil solid phase dielectric constant, according to (32) for  $\alpha=0,5$ .

## 5.2. Results and discussion

The relation between the soil dielectric constant,  $\varepsilon_s$ , and soil water content,  $\theta$ , is presented in **Fig. 12**. It comes that for water content below 0.3 the values calculated from the empirical model (31) are higher than the measured ones. This is particularly evident for samples with high clay content (**Table 6**, no. 10, 11 and 16), *ie* for clay content more than 60%. High clay content is positively correlated with the amount of bound water surrounding soil solid particles (Or and Wraith

[72]). These particles of water have the dielectric constant lower than that of free water. Therefore the model (27) is not adequate for clayey soils.

The value of dielectric constant of bound water,  $\varepsilon_{bw}$ , increases with the distance from the solid particles. Dirksen and Dasberg [27] confirmed this for soils of high specific surfaces.

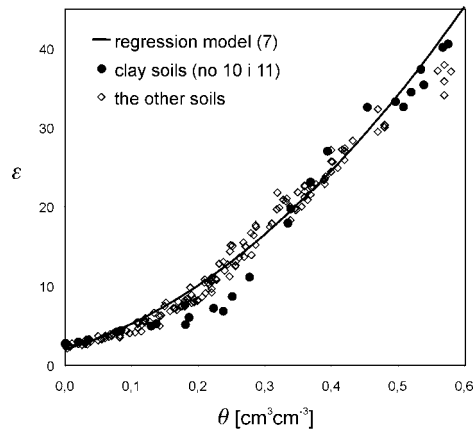


**Fig. 12.** Relation between the soil relative dielectric constant,  $\varepsilon$ , and soil volumetric water content,  $\theta$ , for the investigated mineral soils. The solid line represents the empirical model (31) calculated for the average bulk density of the soil samples  $1.42 \text{ [gcm}^{-3}\text{]}$

The comparison of  $\varepsilon$  values calculated from the 3-phase model (27) and measured by TDR device is presented in **Fig. 13**. There are two distinct ranges of  $\varepsilon$ , below and above the transition value of  $\varepsilon_{TDR} \cong 15$ , and this distinction generally does not depend on the value of the parameter  $\alpha$ .

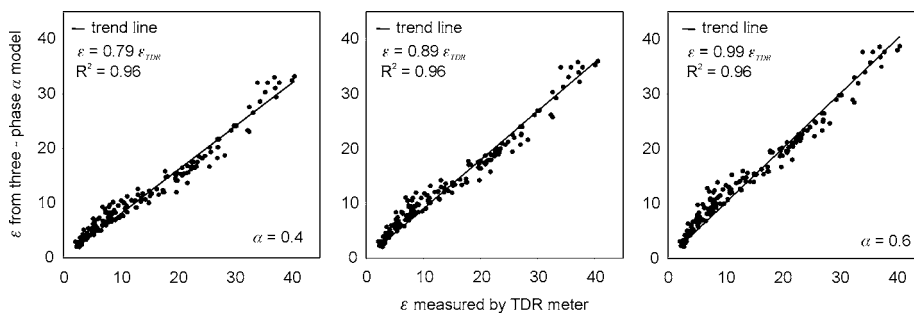


**Fig. 13.** Comparison of soil relative dielectric constants of the investigated soil samples measured by TDR method (horizontal axis) and calculated from 3-phase model  $\alpha$  (27) for different values of  $\alpha$  parameter.

Below the transition value, the soil dielectric constants calculated from the model are higher than the measured ones. For each  $\alpha$  parameter the distribution of data is similar ( $R^2=0.96$ ), the slope of the trend line is near 1 for  $\alpha=0.6$ . For  $\varepsilon$  greater than the transition value, the 3-phase  $\alpha$  model generates numbers close to the measured ones.

The empirical regression model (31), accounting for the soil density, does not eliminate the characteristic decline of data around the transition value of  $\varepsilon$ , although it makes it smaller (**Fig. 14**). The inclusion of soil bulk density to the empirical model of  $\varepsilon(\theta)$  significantly increases the accuracy of TDR soil water content determination (Malicki *et al.* [58], Skierucha [78]).

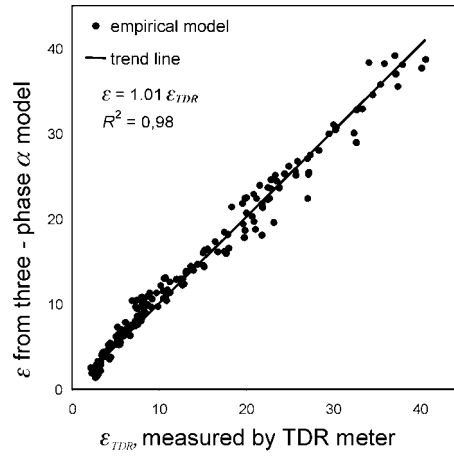


**Fig. 14.** Comparison of the soil dielectric constants measured by TDR method (horizontal axis) and calculated by the empirical model (31) accounting for soil bulk density.

The 4-phase models (28) and (30) account for the presence of soil bound water,  $\theta_{bw}$ , the magnitude of which can be expressed as:

$$\theta_{bw} = x \cdot S \cdot \rho \quad (34)$$

where  $x$ [m] is the distance from the solid phase surface and  $S$ [m<sup>2</sup>/g] is the soil specific surface depending mainly on the soil clay content. According to Or and Wraith [72] and Sposito [84] the bound water is formed by no more than 3 monomolecular layers of water, where the single layer thickness is  $3 \times 10^{-10}$ [m].

The dielectric constant of the bound water is lower than that of capillary water because of hindering effect of solid phase induced to water dipoles. The relation

between the bound water dielectric constant and the distance from the solid phase surface is unknown.

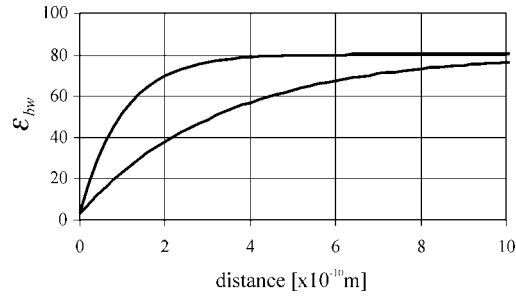


**Fig. 15.** Values of dielectric constant of bound water,  $\epsilon_{bw}$ , related to the distance,  $x$ , from the phases interface

Or and Wraith [72] assume the exponential function, similar to the presented below (**Fig. 15**):

$$\epsilon_{bw} = 80,2 - 77 \cdot e^{-kx} \quad (35)$$

where  $k$  is the parameter influencing the change of  $\epsilon_{bw}$  with the distance of water particles from the phases interface.

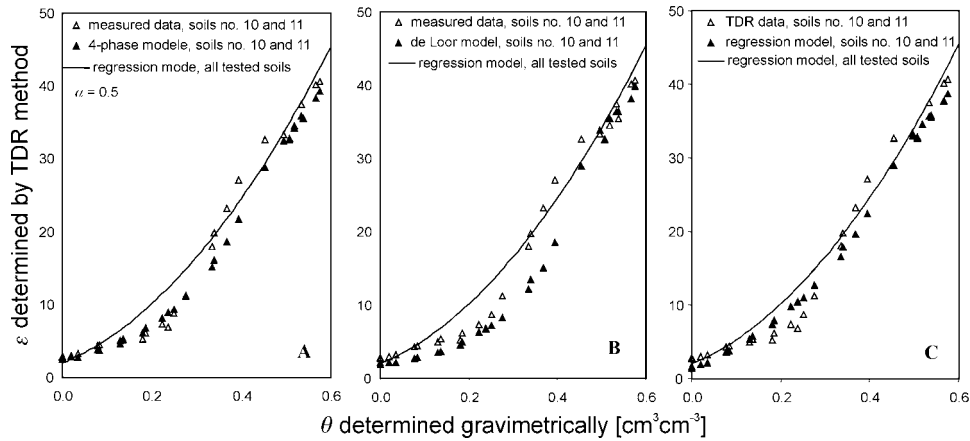


**Fig. 16.** Effects of the 4-phase models for the investigated clay soils (Table 6, no. 10 and 11): A – for model  $\alpha$ , B - for *de Looor* model and C – effect of regression model (31) accounting for soil bulk densities, the solid line represents model (31) for  $\rho = 1,42$  [gcm<sup>-3</sup>]

To verify the observations concerning the influence of bound water on the  $\varepsilon(\theta)$  relation the soils 10 and 11 (**Table 6**) are examined. They have the highest clay content from among the investigated soils and the transition water content is distinct on the  $\varepsilon(\theta)$  curve (**Fig. 12**). The value of transition water content,  $\theta_{WP}$ , is calculated from the formula (33) presented after [99]. The assumptions presented earlier in the “Material and methods” section are applied to 4-phase models (28) and (30) for two selected soils (**Fig. 16**). The regression model shows higher values as compared to the measured ones for water contents below 0.35 (**Fig. 16C**).

The data calculated from the modified 4-phase models follow the measured data in the range where the regression model produces higher values. In the range of  $\varepsilon < 15$  the 4-phase models work in agreement with the TDR measured data. Better correlation is achieved after application of  $\alpha$  model than the model of *de Loor*. For all tested soils the values of  $\varepsilon$  produced by 4-phase modified  $\alpha$  model as compared to the TDR measured ones are presented in **Fig. 17**.

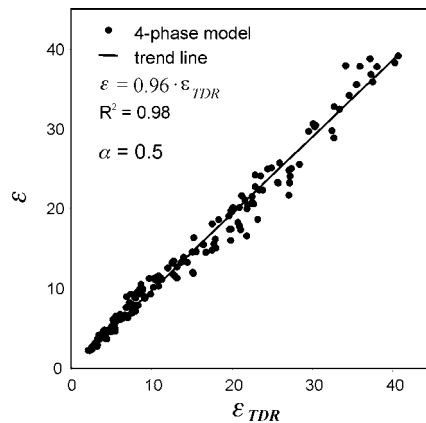


**Fig. 17.** Comparison of the analysed soil dielectric constant measured by TDR method (horizontal axis) and calculated from the 4-phase model  $\alpha$

Scatter of data in **Fig. 17** is comparable with that from the empirical model (31) accounting for the soil bulk density.

### 5.3. Conclusions

- Effect of bound water on the dielectric mixing model can be accounted for if clay content is known.

- The modified model  $\alpha$  with the clay content as the corrective parameter of bound water works equally well as the regression model with soil bulk density as the corrective parameter.

## 6. TEMPERATURE EFFECT ON SOIL DIELECTRIC PERMITTIVITY- DESCRIPTION OF LABORATORY SETUP AND APPLIED SOFTWARE

The purpose of the study, which uses the below described laboratory setup, is to determine the temperature influence on the soil bulk dielectric permittivity,  $\varepsilon_b$ , calculated from the measurement of the EM velocity of propagation in the soil using TDR technique. The final effect is aimed at the adaptation of existing physical models to account for the soil dielectric permittivity change caused by the change of its temperature for mineral soils of variable texture and bulk electrical conductivity. The developed model will help to interpret the influence of selected soil physical parameters on its dielectric properties and will be used in calibration of soil water content and conductivity reflectometric meters.

The soil bulk dielectric permittivity,  $\varepsilon_b$ , change with temperature is not fully explained yet (Or and Wraith [72]), but analysing equations (37) and (38) it can be assumed that:

- $\varepsilon_b$  decreases with temperature increase because  $\varepsilon'$  decreases following the temperature effect of soil free water,
- $\varepsilon_b$  increases with temperature increase following the release of bound water molecules,
- $\varepsilon_b$  increases with temperature increase following temperature induced increase of soil electrical conductivity,  $\sigma_{dc}$ .

Reaching the described objective is requires the collection of experimental data of the selected soil physical properties and developing the general physical model of the temperature effect on soil dielectric permittivity. The tested material consists of mineral soils of variable texture and specific surface area.

The complexity of applied experimental methods requires the application of automatic measurement system. It consists of a central computer controlling the sequence and time schedule of the measurement from individual sensors and the temperature in the temperature chambers. The individual sensors are equipped with intelligence in the form of microcontrollers that react on the commands from the central unit and take over the control on the measurement process. The measured data from the individual sensors of non-electrical quantities are converted into digital form and sent back to the central unit for storage.

The collected data feed the general physical model of the form  $\varepsilon = f(\theta, T, EC_a, \rho, S)$ , where the arguments of the presented function are: soil water content, temperature, apparent electrical conductivity, bulk density and specific surface area, respectively.

## 6.1. Description of the laboratory setup

Reflectometric measurements for the determination of the change of soil samples bulk dielectric permittivity with temperature, water content and electrical conductivity were performed using the setup presented in **Fig. 18** and **Fig. 19** and described in detail in Skierucha [81]. Below there is a short description of the measurement system.

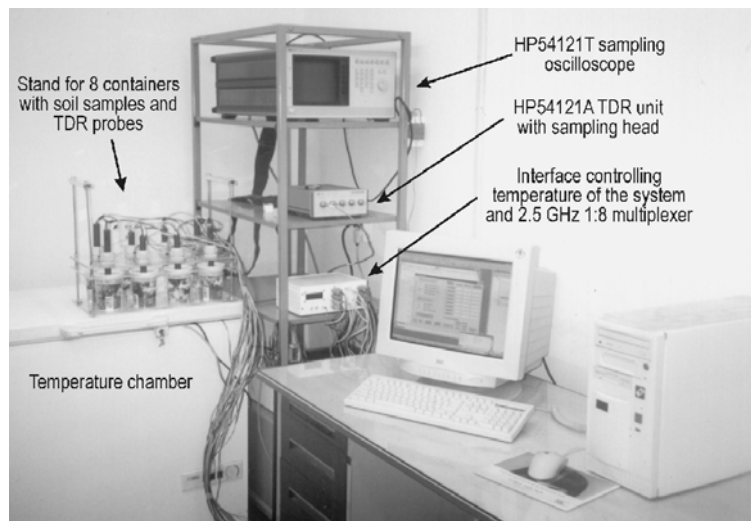


**Fig. 18.** The experimental setup for the determination of temperature effect on soil dielectric permittivity determined by TDR method

The setup consists of three functional modules controlled by PC computer:

- oscilloscope frame HP54120 with the TDR unit HP54121T,
- self designed and manufactured interface connecting TDR probes to the TDR unit by eight position 0.01 - 2.4 GHz multiplexer [42], reading selected temperature sensors and controlling the temperature chamber,
- temperature chamber consisting of a freezer, a fan-heater inside it and an additional fan to minimize temperature gradients inside the chamber.

PC compatible computer controlling the dedicated interface by means serial RS232C interface and the oscilloscope by universal GPIB interface, is connected to Internet to monitor the performance of the experiment in the remote way. The application software was written in Visual Basic to provide a user friendly interface for the operator. Temperature of the soil samples was controlled by switching on and off the fan-heater located at the bottom of the temperature

chamber and the freezer, only one working at a time. An independent temperature sensor connected to the main security switch was applied to disconnect all power devices in the system in case of reaching upper limit temperature,  $T_z = 65^\circ\text{C}$ , inside the chamber.

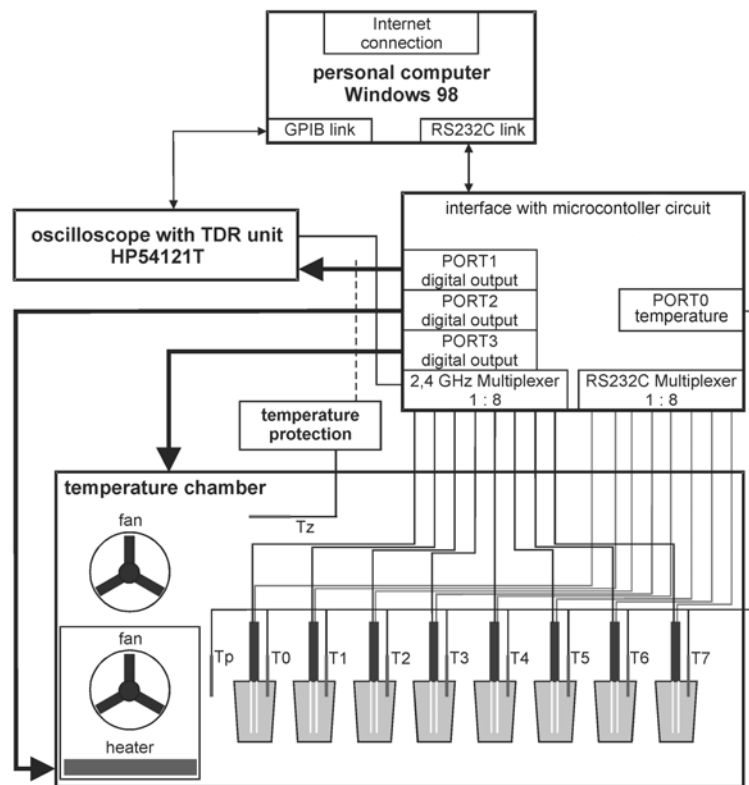


**Fig. 19.** Block diagram of the laboratory setup for the determination of temperature effect on soil dielectric permittivity

Each TDR measurement started when the air temperature inside the chamber,  $T_p$ , the temperature of the measured soil sample,  $T_0, T_1, \dots$  or  $T_7$ , and the regulation temperature reached the same value with  $\pm 0.4^\circ\text{C}$  tolerance. The decrease of the temperature tolerance was possible but it would cost the significant increase of time to stabilize the temperature in the soil sample and the chamber. The complete measurement cycle at six temperature values, from  $5^\circ\text{C}$  to  $55^\circ\text{C}$  in  $10^\circ\text{C}$  increments, for the set of eight soil samples took about 12 hours and starting from the 4-th cycle the measurable decrease of TDR water content

values of soil samples was noticed, which was attributed to the evaporation of water from wet soil samples.

The applied TDR probes were standard Easy Test, Ltd. [29] two wire probes enhanced with the electronics (microcontroller, digital output temperature sensor, analog-to-digital converter and serial interface) for independent measurement of the probe temperature and soil electrical conductivity. The construction of such a “smart sensor” is presented in **Fig. 20**.

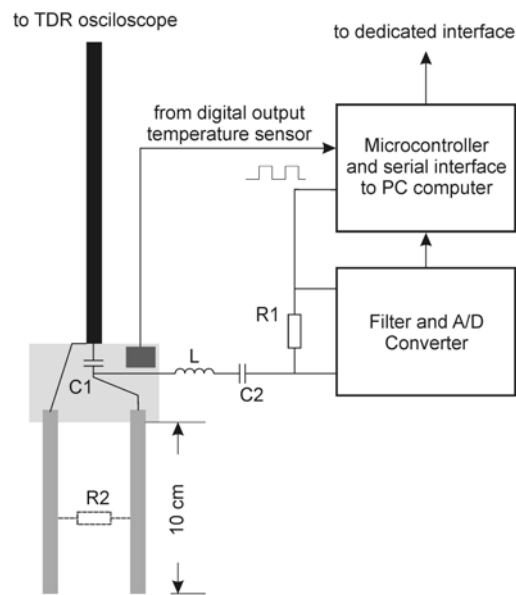


**Fig. 20.** Block diagram of the TDR probe with the electronics for soil electrical conductivity and temperature measurements

The electrical conductivity of the soil sample,  $EC_a$ , measured from the voltage drop on the reference resistor  $R1$  connected in series with the soil equivalent resistor  $R2$ . Low frequency conductivity,  $EC_a$ , of the soil samples were determined from the formula:  $EC_a = C/R2$ , where  $C$  is a calibration constant determined individually for each TDR probe by the measurement in NaCl solution of known conductivities.

The source voltage for electrical conductivity measurement is a square wave, generated by the microcontroller, of 100 kHz frequency that does not polarize the electrode-soil system, the inductance  $L$  is for separation of high frequency TDR signal from much lower frequency square wave and the capacitance  $C2 \gg C1$  is a DC block between the electrode-soil system and the measurement circuitry.

The user interface on the main computer controlling the experiment is presented in **Fig. 21**. It consists of several fill-in places, which meanings are explained beside. Before the measurement starts, the user should input the initial parameters: upper and lower limit regulation temperature and the temperature step of regulation.

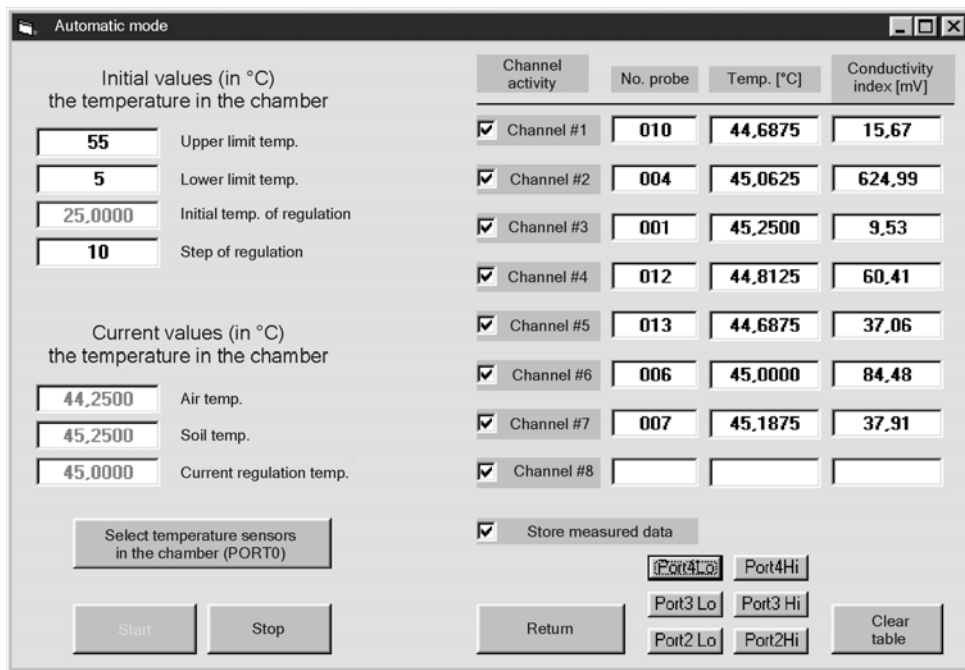


**Fig. 21.** Application window presenting the state of the conducted experiment

The values presented in **Fig. 21** inform that the measurement temperatures of soil samples will be in the range from 5°C to 55°C in 10°C steps. Also the active channels should be selected and choose the name of the output file for data storage. During the experiment the individual windows with current results are continuously updated. The measurement takes place when the values of air temperature in the temperature chamber ( $T_p$ ), temperature of the tested soil samples ( $T_0$ ,  $T_1$ , ... or  $T_7$ ) and the current temperature of regulation reach the same value with  $\pm 0.4$  °C. Decreasing the tolerance is possible but it costs the significant increase of time for the temperature stabilization in the temperature chamber. For the initial values from **Fig. 21** the complete measurement cycle covering the temperature range from 5°C to 55°C is done in about 12 hours.

The measurement sequence for each active probe is done at the defined (in the application window from **Fig. 21**) regulation temperature. After completing the measurement from the active probes, the regulation temperature changes and the controlling program performs the algorithm of temperature stabilization around the new value. Then, after reaching temperature stabilization in the chamber, the measurement sequence of active probes starts again.

The condition of temperature homogeneity in the temperature chamber requires the continuous mixing of air inside the chamber. This is accomplished by fans working all the time in the chamber during the work of the measurement system. The temperature of regulation and the sequence the samples measurement is broken by the user.

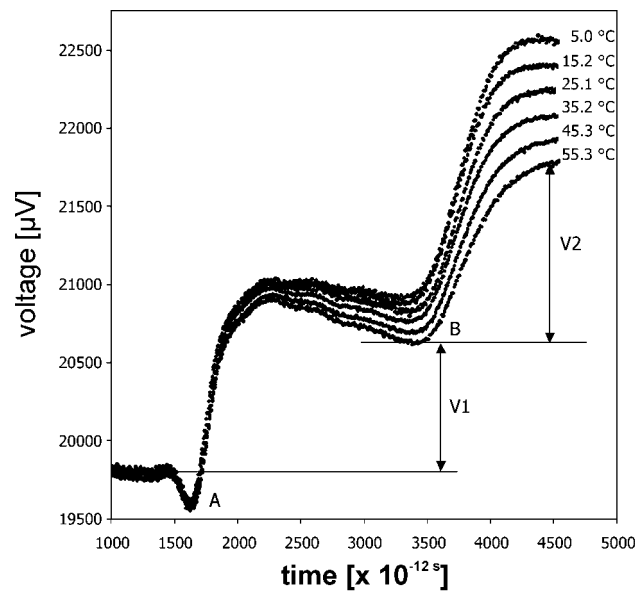


**Fig. 22.** Set of reflectograms registered by the presented setup for the same soil sample in different temperatures.

The system control computer is equipped with the digital GPIB (General Purpose Interface Bus) interface [64] for controlling the HP54121T oscilloscope equipped with the TDR unit [40]. The software modules included in GPIB interface card enable to program the GPIB interface from Visual Basic programming language, especially storage of the graphical representation of the reflectograms presented on the oscilloscope screen to the text file. The analysis of this reflectograms is done after importing the generated text files into the spreadsheet for determination of two parameters using later for calculation of the

soil sample volumetric water content and apparent electrical conductivity (**Fig. 22**):

- propagation time of the pulse in the parallel waveguide of the measurement TDR sensor, *ie* the time between the points A and B, for determination of volumetric water content of the soil sample (Dalton and van Genuchten [20], Malicki and Skierucha [59]),
- voltage ratio  $V_2/V_1$ , for determination of apparent electric conductivity,  $EC_a$ , the soil sample (Giese and Tiemann [33]).

The interface built on the base of the microcontroller PIC16F874 [65] is the interpretation of commands from PC compatible computer (the experiment control unit) by RS232C serial interface. The interface reacts on the following commands:

- setting/resetting digital outputs of PORT1 for switching on/off the sampling oscilloscope HP54121T (by a semiconductor switch),
- setting/resetting the digital output of PORT2 for switching on/off the heater in the temperature chamber (by a semiconductor switch),
- setting/resetting the digital output of PORT3 for switching on/off the power to the temperature chamber to stop cooling it (by a semiconductor switch),
- controlling the 1-Wire interface [18] by PORT3, for the reading of temperature in the containers with soil samples in the chamber,
- selection and management of the serial RS232C multiplexer channel for the communication with the chosen probe,
- management of communication between the interface and PC compatible control unit,
- selection of the microwave multiplexer 2.4 GHz channel.

For simultaneous automatic registration of a number of probes the system uses two multiplexers. The broad bandwidth 2.4 GHz multiplexer is the proprietary construction described by Skierucha [80] and briefly presented in this publication in the point 10.4.2. It uses an integrated circuit made of GaAs technology. This switching circuit mounted on specially designed PC board proved its superior performance over other type of high frequency signals switching.

RS232C multiplexer communicates among the interface and the measurement probes. It is possible to omit the PIC16F874 interface and connect a single measurement probe directly to the RS232C computer interface. Then the measurement will be performed on the connected probe. The performance of the PIC16F874 interface is transparent from the point of view of a measurement probe.

The 1-Wire link uses Dallas DS18B20 semiconductor temperature sensors described in [18]. The sensors can be connected in parallel to limit the cable length and number of wires in a cable. The temperature conversion lasts about 700 ms and the analog to digital converter integrated in the sensor in connection with the applied digital signal transfer protocol make the sensor a smart device.

Before taking measurement from a sensor it must be addressed, *ie* transmit a serial number in the form of digital signals to all the sensors connected in parallel. The next command activates only the addressed sensor, the other are not operating. The additional advantage of 1-Wire temperature sensors is small power consumption, supply current of the sensor is taken from the digital communication line. The only drawback of 1-Wire system is a complicated communication protocol for completing the commands in defined time sequence, which requires the application of a dedicated microcontroller.

The schematic description of the TDR probe with integrated electronic circuitry for temperature and electrical conductivity measurement in is presented in **Fig. 20**. The digital and analog parts are integrated in one enclosure with the TDR probe. The commands coming from PIC16F874 interface or directly from the PC compatible computer (by RS232C serial link) are decoded and executed by the embedded microcontroller PIC16F872. It controls the 1-Wire link for temperature measurement, RS232C link for serial communication with higher-level device and 16-bit analog to digital Sigma/Delta converter [4].

The measurement of the soil electrical conductivity consists in the measurement of the voltage drop on the reference resistor R1. The magnitude of this voltage drop depends on the apparent resistance of the soil located between the steel rods of the TDR probe. The analyzed voltage drop is forced by the rectangular signal of 0.5 duty cycle and frequency 100 kHz, generated by the PIC16F872 microcontroller. Application of alternate signal, symmetrical around the ground voltage enables to avoid electrical polarization of the electrodes-soil setup, which would produce measurement errors. The probe temperature measurement is necessary for temperature correction of electrical conductivity measured values and overall temperature correction of the electronics elements in the probe. The temperature sensor is placed inside the probe enclosure (filled with epoxy resin). The experiment for testing the temperature effect on the dielectric permittivity of soil uses also other temperature sensors, placed together with the TDR probe rods in the tested soils. They are applied due to the presence of temperature gradients between soil and the TDR probe enclosure (the temperature difference between the probe and soil reaches  $\pm 1$  °C. This fact caused the application of additional sensors placed directly in the tested soil samples (the sensors T0, T1, ..., T7 in **Fig. 19**). The advantage of the presented approach of the soil electrical conductivity measurement is that the measurement is performed in

close vicinity of the analyzed object, which eliminates errors associated with the measured analog signal transmission along the wires. Now, the signal with the measurement results is digitally transmitted to the data processing unit (PC compatible computer or PIC16F874 interface) by means of the RS232C serial link.

The temperature chamber is the specially adopted freezer. It has a heater and two fans installed inside, which ensure continuous air movement and minimization of temperature gradient inside. Remotely activated heater in the temperature chamber creates the danger of non-controlled temperature increase and eventually fire. This may happen when for example the controlling program hangs-up for some reason when the heater is on. An independent temperature measurement system in the chamber protects the whole system against this danger. The protection has the upper temperature limit set to the value which exceeded will reset the PIC16F874 microcontroller in the interface and set the digital outputs at PORT0, PORT1, PORT2 to the values corresponding to off state of the external devices, including the heater in the temperature chamber.

## **6.2. Summary**

The presented system automatically registers data from the complex setup consisting not only on the data measurement devices but also actuators that control the measurement conditions. The applied hardware and software are applied for testing the temperature effect of physical parameters of the tested materials as well as the performance of the electronic devices. The system has been designed for the analysis of temperature effect on the soil dielectric permittivity. The results of this research are not the subject of the above study.

## 7. TEMPERATURE PROPERTIES OF SOIL DIELECTRIC PERMITTIVITY

Application of time domain reflectometry to monitor soil water content in long time periods revealed significant fluctuations of water content readings correlated with the soil temperature.

The aim of the study is to determine the influence of temperature on soil bulk dielectric permittivity,  $\varepsilon_b$ , measured by TDR method and indirectly on soil water content calculated from  $\varepsilon_b$ . The end result is the verification of physical models describing the change of soil dielectric permittivity with temperature for soils of different type, water content and salinity. The presented models will help to interpret the influence of selected soil physical parameters on its electromagnetic properties and will improve the calibration procedure of the reflectometric soil water content meters.

The measurements performed on mineral soils collected from Lublin region, Poland, by specially constructed experimental setup confirmed the temperature effect of  $\varepsilon_b$ , causing the TDR soil water content measurement error. The experimental data confirm the theory of the soil dielectric permittivity,  $\varepsilon_b$ , temperature effect as the result of two competing physical phenomena:  $\varepsilon_b$  increases with temperature increase following the release of bound water from soil solid particles with soil temperature increase and  $\varepsilon_b$  decreases with temperature increase following the temperature effect of free water molecules. However the applied four component dielectric mixing models do not fully reflect all examined soils temperature behaviour, and the temperature correcting formula based on model  $\alpha$  does not work properly. The proposed temperature correcting formula is based on the observed temperature behaviour of  $\varepsilon_b$  at a specific water content for each of the analysed soil, named equilibrium water content,  $\theta_{eq}$ . The temperature effect for this soil water content is not observed, which means that at  $\theta_{eq}$  the both competing phenomena mentioned earlier compensate each other. The equilibrium water content,  $\theta_{eq}$ , is correlated with the soil specific surface area. The temperature correcting formula, adjusting the TDR measured soil water content values of the analysed soils to the respective values at 25°C, decreases the standard deviation around the mean values about two times as compared to not corrected data.

### 7.1. Introduction

Measurement of soil water content using time domain reflectometry (TDR) has become increasingly popular because of simplicity of operation, accurate and rapid measurement, usually there is no need for soil individual calibration, the

process of measurement is non-destructive, portable systems are available and the method gives ability to automatize and multiplex probes (Baker and Allmaras [7], Malicki and Skierucha [59], Topp *et al.* [90]). The bulk apparent dielectric permittivity,  $\varepsilon_b$ , of the soil is calculated on the base of the propagation velocity of electromagnetic (EM) waves along the probe forming a waveguide consisting of two or more parallel metal rods fully inserted into the analyzed soil. The dielectric permittivity of water is much higher than the other soil constituents because of the unique dipole nature of water molecules. Therefore having the soil dielectric permittivity from the TDR measurements it is possible to determine indirectly the amount of water in the soil.

The dielectric permittivity,  $\varepsilon$ , of soil as well as other dielectric materials or mixtures with molecules forming permanent dipoles, like water molecule, are subjected to orientation polarization (Chełkowski [14]) in the imposed EM field. The permanent dipoles need finite time, called relaxation time,  $\tau$ , to keep up with the alternating EM field. When the frequency the field increases, the molecule with the permanent dipole response lags in phase. Therefore the permittivity of such dielectric material is a complex value (Litwin [50], von Hippel [96]):

$$\varepsilon = \varepsilon'(\omega) - i \left( \varepsilon''(\omega) + \frac{\sigma_{dc}}{\omega \varepsilon_0} \right) = \varepsilon'(\omega) (1 + i \tan \delta) \quad (36)$$

where:  $i = \sqrt{-1}$ ,  $\sigma_{dc}$  is the electrical conductivity of the sample at low frequency,  $\varepsilon_0 = 8.85 \cdot 10^{-12} [\text{Fm}^{-1}]$  is a dielectric permittivity of free space. Its real part,  $\varepsilon'(\omega)$ , is in-phase with the imposed EM field, while the imaginary part,  $\varepsilon''(\omega) + \sigma_{dc} / \omega \varepsilon_0$ , is out-of-phase. The loss tangent,  $\tan \delta$ , describing the overall loss of energy in the dielectric material is defined as:

$$\tan \delta = \frac{\varepsilon''(\omega) + \frac{\sigma_{dc}}{\omega \varepsilon_0}}{\varepsilon'(\omega)} \quad (37)$$

This energy loss is associated with the out-of-phase components of soil complex dielectric permittivity;  $\varepsilon''(\omega)$  attributed to dipole reorientation at high frequency of the applied EM field, while  $\sigma_{dc} / \omega \varepsilon_0$  to ionic conduction at low frequency of the EM field.

It was shown by von Hippel [96] that for porous materials having negligible magnetic properties the bulk dielectric permittivity of the material,  $\varepsilon_b$ , can be determined from the velocity,  $v$ , of propagation of EM wave, as:

$$\varepsilon_b = \left(\frac{c}{v}\right)^2 = \frac{\varepsilon'(\omega)}{2} \left[1 + \left(1 + \tan^2 \delta\right)^{1/2}\right] \quad (38)$$

When  $\tan \delta \ll 1$ , what happens for the frequency of imposed EM field in the range of about 1 GHz (Heimovara [39], Malicki and Skierucha [60]), the equation (38) simplifies to:  $\varepsilon_b \cong \varepsilon'(\omega)$ , which means that the bulk dielectric permittivity of the soil can be replaced by its real component. The detailed description of TDR technique and the soil water content meters based on it, are presented in other sources [7,20,27,58,59,61,92,100].

In the first applications of TDR technique [90] for soil water content determination the influence of temperature on the TDR determined  $\varepsilon_b$  was neglected as not significant. When field TDR meters for soil water content monitoring in longer time periods were introduced, the significant fluctuation of measured data, correlated with soil temperature, were noticed. Also, it was found (Halbertsma *et al.* [36], Skierucha [79]) that the temperature effect on TDR determined soil water content,  $\theta_{TDR}$ , depends on the amount of water in the soil and the soil texture. For sandy, silt and peat soils  $\varepsilon_b$  decreased with temperature increase. There was no temperature effect reported for clay soil. Other authors (Or and Wraith [72], Wraith and Or [105]) reported that  $\theta_{TDR}$  increased with temperature for silty loam soil for all soil water content, however another silty loam soil showed the increase of  $\theta_{TDR}$  for relatively low water contents and its decrease with temperature increase for relatively higher water contents.

The soil bulk dielectric permittivity,  $\varepsilon_b$ , change with temperature is not fully explained yet [72], but analysing equations (37) and (38) it can be assumed that:

- (a)  $\varepsilon_b$  decreases with temperature increase because  $\varepsilon'$  decreases following the temperature effect of soil free water,
- (b)  $\varepsilon_b$  increases with temperature increase following the release of bound water molecules,
- (c)  $\varepsilon_b$  increases with temperature increase following temperature induced increase of soil electrical conductivity,  $\sigma_{dc}$ .

The purpose of this study was to determine the temperature influence on the soil bulk dielectric permittivity,  $\varepsilon_b$ , calculated from the measurement of the EM velocity of propagation in the soil using TDR technique. The final effect was aimed at the adaptation of existing physical models to account for the soil

dielectric permittivity change caused by the change of its temperature for mineral soils of variable texture and bulk electrical conductivity. The developed model will help to interpret the influence of selected soil physical parameters on its dielectric properties and will be used in calibration of soil water content and conductivity reflectometric meters.

## 7.2. Temperature effect of dielectric permittivity of soil free water

Corrections of the TDR determined water content data related to the temperature effect of dielectric permittivity of free water was examined in [49,79]:

$$\theta_{25} = \frac{\theta_{TDR}(T)}{1 + n_{fw}[d(T) - 1] \cdot \frac{d\theta}{dn}} \quad (39)$$

where:  $\theta_{TDR}(T)$  and  $\theta_{25}$  are the TDR determined at  $T$  temperature and corrected to 25 °C soil water content data,  $n_{fw} = \sqrt{\varepsilon_{fw}} = 8.851$  is free water refractive index at 25 °C,  $\varepsilon_{fw}$  is dielectric permittivity of free water at 25 °C,  $d(T)$  is the known relationship between dielectric permittivity and temperature of free water (CRC [17]):

$$n_{fw}(T) = n_{fw} \cdot d(T) = 8.851 \cdot d(T) \quad (40)$$

$$[d(T)]^2 = 1 - 0.4536 \cdot 10^{-2}(T - 25) + 0.9319 \cdot 10^{-7}(T - 25)^2 \quad (41)$$

and  $d\theta/dn$  is the derivative of TDR calibration function. Another correction suggested in Pepin *et al.* [74] adjusted the TDR determined soil water content,  $\theta_{TDR}$ , readout by  $0.00175\theta_{TDR}/^{\circ}\text{C}$ . The both corrections did not reflect the influence of soil texture on the observed temperature effect.

It is evident (Halbertsma *et al.*[36], Pepin *et al.* [74]) that the physical processes involving other soil phases apart from only the liquid phase should be taken into account when interpreting the temperature effect on the soil  $\varepsilon_b$ .

Applying 3-phase soil model and assuming that the refractive indexes of soil solid and air phases do not significantly depend on temperature, the soil refractive index  $n_T$  may be expressed in function of temperature as:

$$n_T = \theta n_w + f_a n_a + f_s n_s + \theta n_w (d(T) - 1) = n_{20} + \Delta n(T) \quad (42)$$

where:  $n_w$  is the free water refractive index at 20 °C,  $n_{20}$  is the soil refractive index at 20 °C,  $\Delta n(T)$  is its temperature dependent correction,  $f_a$ ,  $f_s$  are volumetric fractions of soil air and solid phases, respectively.

The soil water content,  $\theta = \theta_{20}$ , in Eq. (42) is determined gravimetrically in laboratory conditions or using TDR soil water content measurement method applied for the soil at 20°C, *ie* in TDR meters calibration conditions. The values of the refractive index,  $n_T$ , for soils are determined at  $T$  temperature can be corrected to the values at 20 °C,  $n_{20}$ , according to the Eq. (42), which can be rewritten as:

$$n_{20} = n_T - \theta_{20} n_w (d(T) - 1) \quad (43)$$

As the dielectric soil water content measurement is based on the calibration formula  $\theta = f(n)$ , the TDR calculated soil water content depend on its temperature:

$$\theta_T = \theta(n_T) = \theta(n_{20} + \Delta n(T)) \quad (44)$$

For linear shape of the calibration formula the following is true:

$$\theta_T = \theta(n_{20} + \Delta n(T)) = \theta_{20} + \frac{d\theta}{dn} \Delta n = \theta_{20} + \frac{d\theta}{dn} \theta_{20} \cdot n_w (d(T) - 1) \quad (45)$$

Rewriting the Eq. (45) we can receive the TDR determined soil water content,  $\theta_{20}$ , corrected to its value at 20°C:

$$\theta_{20} = \frac{\theta_T}{1 + n_w (d(T) - 1) \cdot \frac{d\theta}{dn}} \quad (46)$$

The above corrections based on the temperature change affecting the soil free water and applied to the soil water content values determined by TDR measurement method will be verified below using experimental data.

### 7.3. Materials and methods

The influence of temperature on the refractive index,  $n$ , of the EM waves was tested on the saturated peat soil and three mineral soils with texture presented in **Table 7**: sand, silt and clay.

The values of the refractive index of the tested mineral soils were determined by the laboratory TDR meter [29], and a field TDR meter FOM/mts was used for the measurement of  $n$  in the peat soil. The measured values of water content,  $\theta$ , were recalculated to the desired values of the refractive index,  $n$ , on the base of the applied calibration function  $\theta=f(n)$  [29]. The field measurements were performed in spring on the non tilled saturated soil. The TDR probes were installed below the ground water level (22 – 36 cm), *ie* at the depth of 60 cm. During the measurement period the soil temperature increased almost two times, from 6,3°C do 11,7 °C, in continuous saturated conditions (the ground water level did not drop below 60 cm). Therefore, it can be assumed that the observed changes of the EM velocity of propagation, and the values of the refractive index,  $n$ , of the soil resulted only from the change of the soil temperature.

**Table 7.** Selected physical parameters of the tested soils

No.	Localization	Soil type (FAO)	Depth [cm]	$\rho$ [g·cm <sup>-3</sup> ]	$\rho_s$ [g×cm <sup>-3</sup> ]	CEC	C [%]
1	Wytyczno (sand)	Gleyic Podzol	30 - 40	1.53 ÷ 1.64	2.61	1.4	0.4
2	Tarnawatka (silt)	Eutric Regosol	20 - 30	1.30 ÷ 1.62	2.7	11.8	0.1
3	Kępa (clay)	Eutric Fluvisol	15 - 25	1.08 ÷ 1.40	2.66	24	1.2
4	Rhinluch Germany	Eutric Histosol	20 - 30	0.12	1.4	-	51.4

A two-rod TDR sensors, LP/m from Easy Test, Ltd. [29], with the rods of 0.8 mm in diameter, 53 length and 5 mm distance between the rods, were applied for the TDR laboratory measurements. The soil samples were stored in PVC cylinders of 10 cm in diameter and 5 cm height. The temperature of the soil samples was measured by thermocouples. A TDR probe was installed horizontally in each cylinder with a soil sample, at the middle of its height. A thermocouple was installed at the same level. Containers with soil samples and the probes were sealed to avoid evaporation of water during the measurement process (about 3 hours), placed in a microwave for homogenous heating and then the velocity of EM propagation in the heated soil sample were measured.

#### 7.4. Results and discussion

Due to the well known temperature effect of  $n(T)$  (CRC [17]) and the need to verify the measurement instrumentation and the correction formulas (43) and (46), the measurements were performed also on pure water.

The calibration formula (47) used in TDR soil water content meters from Easy Test, Ltd. [29] was applied to calculate to evaluate the temperature effect,  $n_T$ , for pure water.

$$\theta = 0,175 \cdot n - 0,57 \quad (47)$$

Substituting  $\theta = \theta_T$  and  $n = n_T$  we have:

$$n_T = 3,25 + 5,7 \cdot \theta_T \quad (48)$$

where  $\theta_T$  i  $n_T$  are temperature dependent result of soil water content measurement with the TDR meter and the temperature dependent soil refractive index, respectively.

The conditions necessary to meet for the non-temperature effect water content measurement are:  $dn/dT \approx \Delta n / \Delta T = 0$  and  $n(20^\circ \text{C}) = 8,95 \pm E_n$ , where  $E_n$  represents the absolute measurement error of  $n$ . The results of the correction formulas are presented in **Fig. 23** and **Table 8**. They show that the corrections according to (43) and (46) almost meet the discussed conditions.

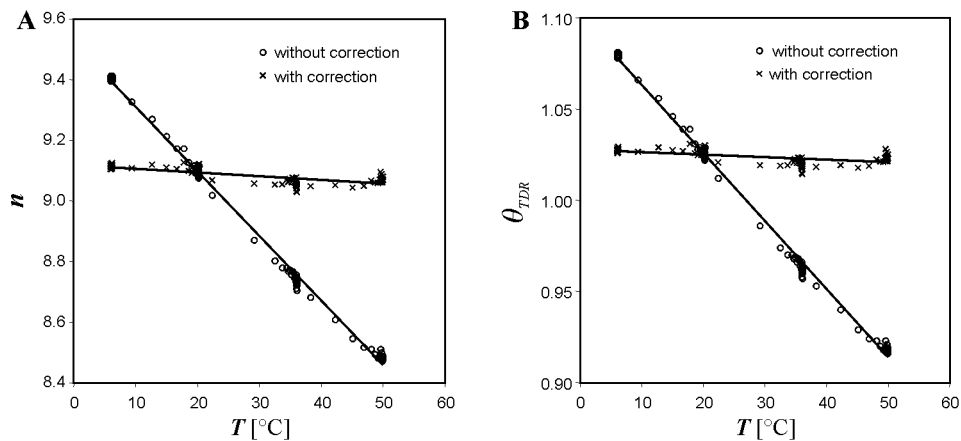


**Fig. 23.** The effect of the applied temperature corrections for TDR measurement in water: (43) – for the measured refractive index,  $n$  (part A), and (46) – for the calculated volumetric water content,  $\theta_{TDR}$  (part B)

The relative,  $\Delta n/\Delta T$ , and absolute,  $\Delta n$ , changes of the refractive index in the whole span of analyzed temperature of water,  $6 \div 50$  °C, is presented in the table **Table 8**, below. It shows that for water the temperature corrections according to Eq. (43) and Eq. (46) on the refractive index,  $n$ , and volumetric water content,  $\theta_{TDR}$ , determined by TDR method are acceptable.

**Table 8.** Corrected and non-corrected temperature errors of the measurement of the refractive index,  $n$ , for water and the TDR measured values of its content,  $\theta_{TDR}$

Measurement	$\Delta n$ for		$\Delta \theta$ for	
	$\Delta n/\Delta T$	$6 \leq T \leq 50$ °C	$\Delta \theta/\Delta T$	$6 \leq T \leq 50$ °C
without correction	-0.0213	- 0.9798	-0.0037	- 0.9798
After correction on $n$ according to Eq. (42)	-0.0012	0.0414	-0.0001	0.0414

The temperature change of the refractive index,  $n$ , for peat soil having constant volumetric water content equal to 0.87 in saturated conditions is presented in **Fig. 24**. During the measurements the peat soil temperature changed from 6 °C to 12 °C.

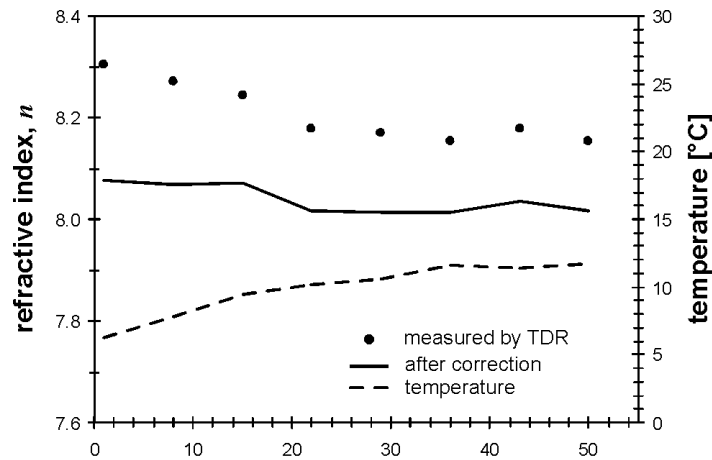


**Fig. 24.** Influence of temperature on the refractive index,  $n$ , for peat soil and the results of applied corrections

The temperature fluctuations caused the corresponding changes of the refractive index from  $n(6$  °C) = 8.30 to  $n(12$  °C) = 8.14. The correction according

to Eq. (43) significantly decreased the influence of temperature and the corrected values were:  $n(6\text{ }^\circ\text{C})=8.06$  do  $n(12\text{ }^\circ\text{C})=8.02$ .

**Table 9** shows the regression coefficients for the relation  $n(T)$  applied for the measurements on mineral soils, illustrated in **Fig. 25**. These coefficients reflect the susceptibility of the refractive index on temperature  $dn/dT$ .

For the presented measurements and tested soils this susceptibility changed in the following range:

$$-0.0105 < \frac{dn}{dT} < 0.0008 \text{ deg}^{-1} \quad (49)$$

depending on the soil water content and soil type.

**Table 9.** Regression coefficients in the relation  $n(T)=a_0+a_1T$  for the tested mineral soils without and after the application of correction (43)

	$\theta$	$a_1$		$a_0$	
		without correction $\times 10^{-5}$	with correction $\times 10^5$	without correction	with correction
sand	0.006	30	40	1.65	1.65
	0.171	-250	90	3.06	2.99
	0.344	-1050	-370	4.98	4.84
silt	0.019	80	120	1.70	1.69
	0.324	-370	280	4.52	4.65
	0.425	-490	360	5.47	5.64
clay	0.021	50	90	1.72	1.71
	0.244	30	520	3.26	3.36
	0.492	4	990	5.66	5.86

**Fig. 25** presents the results of measurements on three mineral soils described in **Table 7**, each of them having three different water contents. The temperature influences significantly on the soil refractive index,  $n$ , and this influence increases with the soil volumetric water content.

For clay soil the refractive index,  $n$ , change with temperature is different than for sand or silt soil. It does not decrease with the temperature increase. This behavior can be explained by the release of molecular water (bound by clay soil particles) with temperature increase. The dielectric constant of bound water is about 20 times lower than free water (Dirksen and Dasberg [27]) and its value is comparable to the value of dielectric constant of ice,  $\epsilon_e$  about 3.2.

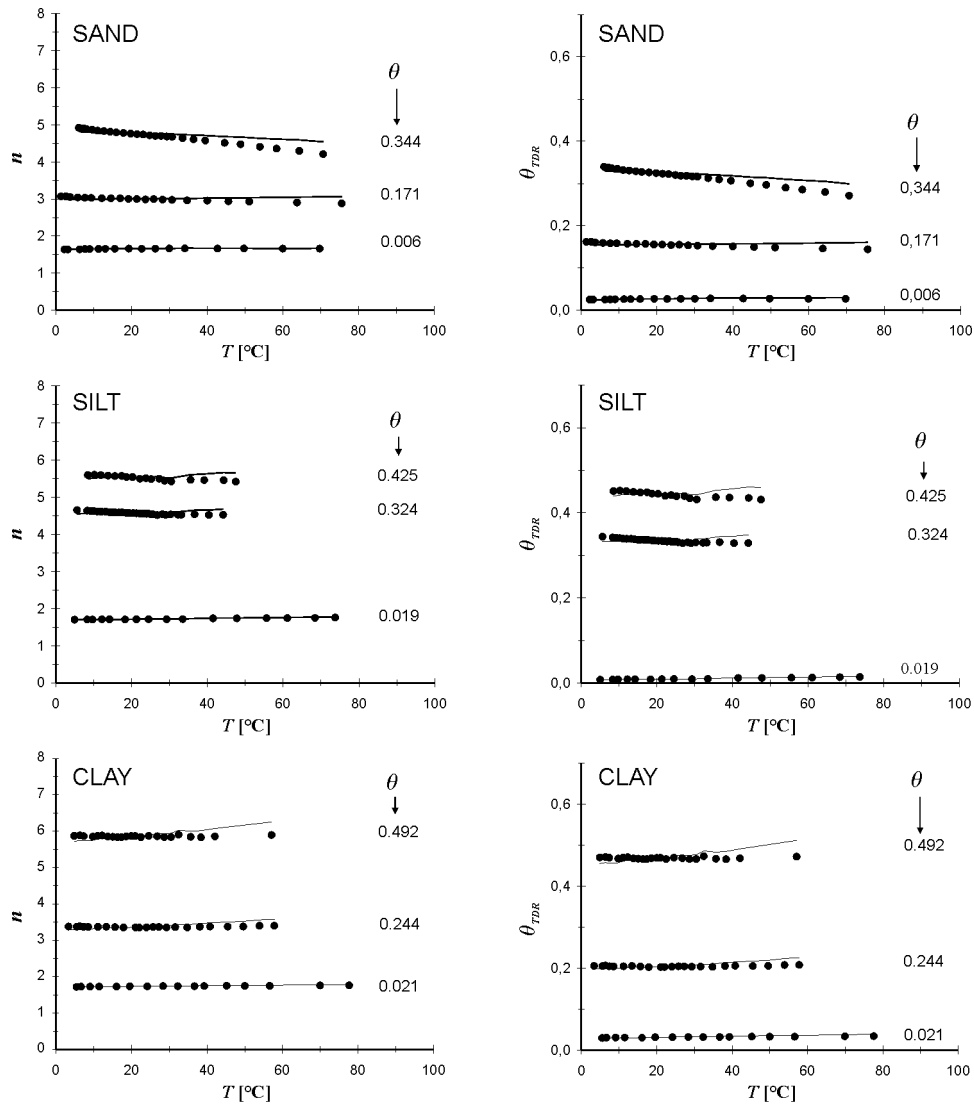


**Fig. 25.** The temperature effect on the soil refractive index,  $n$ , and the soil volumetric water content,  $\theta_{TDR}$ , determined by TDR method for three mineral soils: sand, silt and clay and the results of the applied corrections according to Eq. (43) and Eq. (46). On the right side there are values of water content,  $\theta$ , determined by thermo-gravimetric method. • - TDR determined values, line - correction on  $n$  and  $\theta$ .

Therefore there might be two competing phenomena that take place in the soil subjected to the temperature change:

- the soil refractive index for wet soil decreases with the temperature increase following the decrease of the water refractive index of free capillary water in the soil,
- the soil refractive index increases with the temperature because of the increase of free water particles and the simultaneous decrease of bound water particles.

Susceptibility of the refractive index,  $n$ , for soil on temperature causes the error of reflectometric soil water content measurement values,  $\theta_{TDR}$ . Taking into account the calibration function of the TDR meter according to [29]:  $n=1,491+7,675\theta$ , the equation:

$$\frac{d\theta}{dT} = \frac{d\theta}{dn} \frac{dn}{dT} \quad (50)$$

and (49) the range of the temperature error of the soil water content determined by TDR meter,  $\frac{d\theta}{dT}$  :

$$-0,0014 < \frac{d\theta}{dT} < 0,0001 \text{ deg}^{-1} \quad (51)$$

For extreme situations, for example for saturated sand soil, the increase of the soil temperature  $\Delta T=50^\circ\text{C}$  will be reflected by the decrease of TDR meter soil water content readout of  $\Delta\theta=0,0014 \cdot 50 \cdot 100\%=7\%$  related to the corresponding value determined by thermo-gravimetric method.

The temperature influence on the soil dielectric constant, and indirectly on the reflectometric measurement of soil water content depends on its water content and its texture. The influence of temperature on the TDR measured value may be taken into account or not, which depends on the assumed accuracy of measurements and type of the measured soil. In extreme conditions, *ex* for saturated sand soil, where bound water is almost not present, this error should be accounted for. The available TDR soil water content measurement devices may simultaneously measure temperature of the same soil sample. In this case the application of proposed temperature correction of is easy to implement and also required.

The temperature effect of TDR soil water content values for clay soils needs more detailed considerations due to complex physical processes connected to the presence of bound water. Also the effect of soil electrical conductivity may play important role.

### 7.5. Temperature effect of soil bound water

The discussion of the release of bound water from the solids with the temperature is presented in [72] and [105], where the authors applied Debye model [24] for polar liquids and liquid viscosity dependence on temperature,  $T$ , for bound water molecules at the distance  $x$  from the solid surface to present their relaxation frequency (**Fig. 26**):

$$f_{rel}(x, T) = \frac{kT \exp\left(-\frac{1}{T} \left(\frac{a}{x} + d\right)\right)}{8\pi^2 r^3 c} \quad [\text{Hz}] \quad (52)$$

where  $k = 1.38 \cdot 10^{-23} \text{ [JK}^{-1}\text{]}$  is the Boltzman constant,  $T[\text{K}]$  is the temperature,  $a=1621 \text{ [\AA K]}$ ,  $d=2.047 \cdot 10^3 \text{ [K]}$  and  $c=9.5 \cdot 10^{-7} \text{ [Pa s]}$  are constants used for the model simplification,  $r=2.5 \text{ [\AA]}$  is the radius of water molecule.

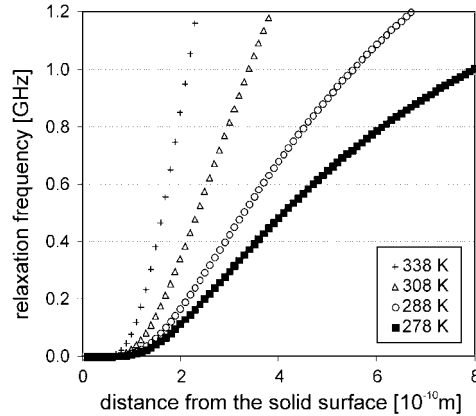


**Fig. 26.** Relaxation frequency of water molecules in relation to the distance from the solid surface and temperature according to (52) on the base of Debye model [24]

The water molecules that are close to the solid surface are less mobile in the imposed EM field as the ones far away from it, which is expressed in **Fig. 26** by lower relaxation frequency. For a given temperature the more distant the water molecules are from the solids, the higher relaxation frequency they have. The

increase of temperature increases their kinetic energy that raises the relaxation frequency and they become more mobile in the imposed EM field. The bound water molecules released from the solid surface become now free water molecules with higher value of the real part of the complex dielectric permittivity.

It can be added here that the release of water from the solids results in the increase of  $\varepsilon'$  and decrease of  $\varepsilon''$  in (37) describing the loss tangent of dielectric material. This phenomenon leads to a new equilibrium with more free water in expense to bound water.

Following Boyarskii *et al.* [12], Or and Wraith [72] and Wraith and Or [105], only a few layers of water covering soil particle are subjected to the change of relaxation time in relation to relaxation time of free water. Boyarskii *et al.* [12] report the analysis of nuclear resonance spectra of bound water films in clay showing the approximated relation between relaxation time of bound water, and thickness of the film covering soil particles. The relaxation time of bound water drops rapidly with the number of layers covering soil particle and it seems that only one or two layers have significantly longer relaxation times than that of free water.

The average rise time,  $t_r$ , of TDR pulses is about  $0.3 \cdot 10^{-9}$  s (Heimovaara [39], Malicki and Skierucha [59]). This time relates to the frequency bandwidth,  $bw$ , of TDR soil water content meters with the following formula given in Strickland [87]:

$$bw = \frac{0.35}{t_r [\text{ns}]} \approx 1.2 [\text{GHz}] \quad (53)$$

The authors of [72,105] recognized this frequency limit as the cut-off frequency,  $f^*$ , that distinguishes water molecules between free and bound. Water layers having dielectric relaxation frequencies lower than the cut-off frequency were considered as bound water having lower dielectric permittivity than for free water.

Rearrangement of (52) for a given TDR cut-off frequency,  $f^*$ , and temperature,  $T$ , leads to the simplified relation for the calculation of the thickness,  $x(T)$ , of bound water layer:

$$x(T) = \frac{a}{-d + T \ln \left( \frac{kT}{8\pi^2 r^3 c f^{*2}} \right)} \quad (54)$$

The purpose of the above discussion was the calculation of the temperature dependent volume fraction of bound water,  $\theta_{bw}(T)$ . Wang and Schmutge [99] show that the quantity of bound water in soil increases with the increase of clay fraction in it. This is due to large specific area of clay surface compared to other soil fractions. The bound water volume fraction of the soil is the product of solid phase surface,  $S$ , temperature dependent thickness of bound water layer,  $x(T)$ , and bulk density,  $\rho$ , as follows:

$$\theta_{bw}(T) = x(T)S\rho \quad (55)$$

Having determined the dependence of bound water volume fraction of soil,  $\theta_{bw}(T)$ , on temperature using equation (55), it is now possible to find the overall temperature dependence of bulk soil dielectric permittivity,  $\varepsilon_b$ , by application of dielectric mixing models. Among many dielectric mixing models describing soil as the mixture of solids, liquid, gas and also bound water phase there are two the most used: model  $\alpha$  (Birtchak *et al.* [9], Dirksen and Dasberg [27], Roth *et al.* [77]) and model *de Loor* (de Loor [25], de Loor [26], Dirksen and Dasberg [27], Dobson and Ulaby [28]).

Model  $\alpha$  treats the soil as the mixture of volume fractions of four phases described in the mathematical form:

$$\varepsilon_b^\alpha = (1-\phi)\varepsilon_s^\alpha + (\phi-\theta)\varepsilon_a^\alpha + (\theta-\theta_{bw})\varepsilon_{fw}^\alpha + \theta_{bw}\varepsilon_{bw}^\alpha \quad (56)$$

where:  $\varepsilon_b$ ,  $\varepsilon_s$ ,  $\varepsilon_a$ ,  $\varepsilon_{fw}$ ,  $\varepsilon_{bw}$  are respective values of bulk soil, solid, gas, liquid and bound water phases dielectric permittivity, and  $\theta$ ,  $\phi$  and  $\theta_{bw}$  are volume fractions of liquid, pore and bound water respectively in the soil,  $\alpha$  is a curve-fitting parameter that can be interpreted as a measure of geometry of the medium with relation to the applied electric field (Roth *et al.* [77]). Roth *et al.* [77] found that an average value of  $\alpha=0.5$  for three phase model while for four phase model  $\alpha=0.65$ .

Four-phase soil model of *de Loor* is based on Maxwell equations and it describes the homogenous mixture of substances with different dielectric permittivity with the host solid phase medium. It can be described in following form:

$$\varepsilon_b = \frac{3\varepsilon_s + 2\theta_{fw}(\varepsilon_{fw} - \varepsilon_s) + 2\theta_{bw}(\varepsilon_{bw} - \varepsilon_s) + 2\theta_a(\varepsilon_a - \varepsilon_s)}{3 + \theta_{fw}\left(\frac{\varepsilon_s}{\varepsilon_{fw}} - 1\right) + \theta_{bw}\left(\frac{\varepsilon_s}{\varepsilon_{bw}} - 1\right) + \theta_a\left(\frac{\varepsilon_s}{\varepsilon_a} - 1\right)} \quad (57)$$

The four phase models (56) and (57) were applied in Skierucha [82] to show that they reflect the influence of the bound water phase in TDR water content measurements in the soils with high clay content.

### 7.6. Soil conductivity influence on temperature effect of soil dielectric constant

Literature reports and the own research of the authors (Malicki and Skierucha [60], Skierucha [78], Topp *et al.* [90]) show that soil electrical conductivity does not influence in the statistically significant way the TDR determined soil bulk dielectric permittivity,  $\varepsilon_b$ , and consequently the soil water content calculated from it. However recent studies (Topp *et al.* [92]) prove that the imaginary component of the soil relative permittivity (36), which includes high and low frequency contributions, can have measurable effect on  $\varepsilon_b$ . It is commonly known that electrical conductivity of the medium increases with temperature. Assuming that the relaxation frequency of soil solid and gaseous phases dielectric permittivity,  $\varepsilon_s$  and  $\varepsilon_a$ , are higher than its liquid phase, the  $\varepsilon_b$  determined by TDR method, covering the frequency range up to about 1.5 GHz, depends only on the soil liquid phase. This assumption is fundamental for reflectometric determination of soil water content. Following the discussion in Or and Wraith [72] it is possible to present the frequency,  $f$ , dependence of real and imaginary part of salt-water mixture dielectric permittivity,  $\varepsilon'$  and  $\varepsilon''$ , as well as the velocity of propagation,  $v$ , of electromagnetic wave along the TDR probe rods inserted in this mixture for different temperatures and apparent electrical conductivities,  $EC_a$  (**Fig. 27**). The values of  $\varepsilon'$  and  $\varepsilon''$  are calculated from Debye model [24]:

$$\varepsilon'(f) = \varepsilon_{hi} + \frac{\varepsilon_{low} - \varepsilon_{hi}}{1 + \frac{f}{f_{rel}}} \quad (58)$$

$$\varepsilon''(f) = \frac{(\varepsilon_{low} - \varepsilon_{hi}) \frac{f}{f_{rel}}}{1 + \frac{f}{f_{rel}}} + \frac{EC_a}{2\pi f \varepsilon_0} \quad (59)$$

where:  $\varepsilon_{low}$  and  $\varepsilon_{hi}=4.23$  are real parts of  $\varepsilon$  at low and hi frequency,  $f_{rel}$  is relaxation frequency.

The dependence of  $\varepsilon_{low}$  on temperature is described by (40) and (41),  $f_{rel}(T)$  can be expressed by the empirical formula given by Stogryn [88]:

$$f_{rel} = \frac{(49,25 + T)(45 + T)}{255,04 + 0,7246T} \cdot 10^9 \text{ [Hz]} \quad (60)$$

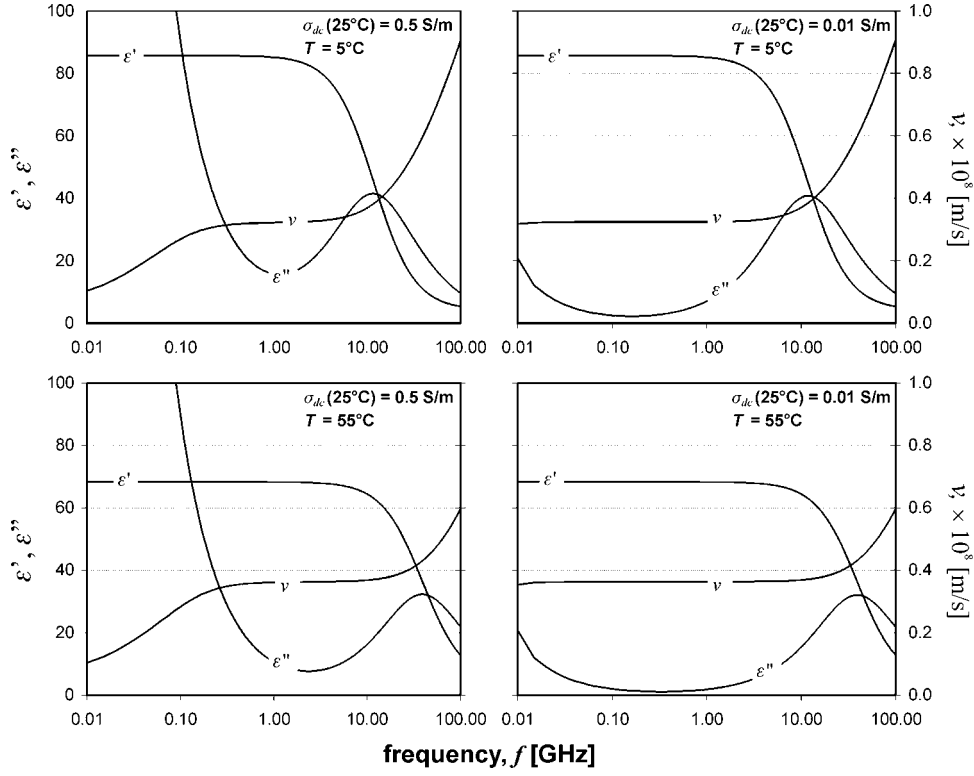


**Fig. 27.** Frequency dependence of real,  $\varepsilon'$ , and imaginary,  $\varepsilon''$ , parts of complex dielectric permittivity of salt-water mixtures for two values of electrical conductivity of the solution:  $EC_a = 0.01$  and  $0.5 \text{ [Sm}^{-1}\text{]}$ , at two temperatures:  $T = 5$  and  $55^\circ\text{C}$  of the solution

The temperature dependence of  $EC_a$  is as follows (Hasted [37]):

$$\sigma_{dc}(T) = \sigma_{dc}(25^\circ\text{C}) \exp[-\Delta(2,033 \cdot 10^{-2} + 1,266 \cdot 10^{-4} \Delta + 2,464 \cdot 10^{-6} \Delta^2)] \quad (61)$$

where:  $T$  is in  $^\circ\text{C}$  and  $\Delta = (25^\circ\text{C} - T)$ .

The velocity of propagation,  $v$ , of electromagnetic wave in a dielectric medium is determined as follows (von Hippel [96]):

$$v(f) = \frac{c}{\sqrt{\frac{\varepsilon'(f)}{2} \left[ 1 + \sqrt{1 + \left( \frac{\varepsilon''(f)}{\varepsilon'(f)} \right)^2} \right]}} \quad (62)$$

where  $c$  is the velocity of light in free space.

The increase of temperature of the salt-water mixture increases the frequency range around the frequency 1 GHz, where the velocity of propagation of electromagnetic wave along the waveguide, used in TDR technique, does not change. Therefore the temperature effect on the electrical conductivity of soil, resulting mainly from ionic conductivity of soil electrolyte should not influence the bulk temperature effect of soil dielectric permittivity.

## 8. THE ACCURACY OF SOIL WATER CONTENT MEASUREMENT BY TDR TECHNIQUE

Time Domain Reflectometry (TDR) method for the measurement of soil water content becomes popular for the simplicity of operation, accuracy and the non-destructive, as compared to other methods, way of measurement [5,6]. This measurement technique takes advantage of three physical phenomena characteristic to the soil:

As in the indirect methods of measurement, the TDR water content measurement values are burdened with correlation imperfections between the measured values, *ie* soil refractive index  $n = \sqrt{\varepsilon}$  and the real value of soil water content,  $\theta$ . It is assumed that the “real value” of soil water content is its value measured by the reference thermo-gravimetric method. The other sources of errors are: the hardware and software imperfections of the measuring device (which measures the time distance between the reflections of the electromagnetic pulse from the beginning and end of the TDR probe rods [59]) and TDR probe installation.

The user of TDR meter has limited possibility to minimize the influence of the hardware and software errors. He can only perform repeat measurements from the same probe and take the mean of the received data for further analysis. Care should be taken during TDR probe installation so as to avoid air gaps (Annan [5]), stones and roots between steel rods and the soil. The picture showing the reflections from the beginning and end of the probe inserted into the soil would be helpful. With some experience the user can decide if the measurement point is representative or not.

For the discussion about the correlation error it is useful to treat the soil as a three phase medium, where the following formulae applies (Roth *et al.* [77]):

$$1 = f_w + f_s + f_a \quad (63)$$

where:  $f_w$  is a fraction of water,  $f_s$  is a fraction of solids and  $f_a$  is a fraction of air in the soil.

Assuming that there are no relaxation effects of the external electromagnetic field on the soil, the following three-phase dielectric soil model is proposed (Birtchak *et al.* [9], Steru [86]):

$$\varepsilon^\alpha = \varepsilon_w^\alpha f_w + \varepsilon_s^\alpha f_s + \varepsilon_a^\alpha f_a \quad (64)$$

where:  $\varepsilon$ ,  $\varepsilon_w$ ,  $\varepsilon_s$  and  $\varepsilon_a$  are the dielectric constants of soil as a whole, soil water, soil solids, and air,  $\alpha$  is a constant interpreted as a measure of the soil particles geometry. On the base of the measured data collected on various soils, it has been found that for the three phases dielectric model of the soil the average value of  $\alpha$  constant is 0.5 [77].

From the equations (10) and (64) together with the relation:

$$\phi = 1 - \frac{\rho}{\rho_s} \quad (65)$$

between the soil porosity,  $\phi$ , density,  $\rho$ , and the solid phase density,  $\rho_s$ , and assuming after Roth *et al.* [77] that  $\alpha = 0,5$  the following equations can be derived:

$$n = \sqrt{\varepsilon} = \frac{\rho}{\rho_s} (n_s - 1) + \theta (n_w - 1) + 1 \quad (66)$$

$$n = \sqrt{\varepsilon} = n_s (1 - \phi) + n_w \theta + \phi - \theta \quad (67)$$

where:  $n = \sqrt{\varepsilon}$  is a soil refractive index, while  $n_s$  and  $n_w$  are respectively the refractive index of the solid phase and water of the soil (we assume that  $\sqrt{\varepsilon_a} = n_a = 1$ )

The equations (66) and (67) show that apart from the liquid phase, the solid phase influences the dielectric properties of the soil. The statistical significance of this influence and the resulting error of the TDR measured soil refractive index and the soil water content derived from it are discussed below.

### 8.1. Material and method

The measurements were performed on disturbed mineral and organic soil samples in laboratory conditions. The measured material consisted of: 395 soil samples of 19 mineral soils different in texture, organic carbon content ( $C$ ), bulk density ( $\rho$ ), and particle density ( $\rho_s$ ), 111 soil samples of 9 organic soils different in organic carbon content ( $C$ ), bulk density ( $\rho$ ), and particle density ( $\rho_s$ ), 157 soil samples of 9 soil mixtures of peat-silt and peat-sand with differentiated bulk density ( $\rho$ ), and particle density ( $\rho_s$ ). The detailed description of physical parameters of soil used in the experiment is presented in Skierucha [78]. Each of the soil sample had its water content,  $\theta$ , determined by the standard thermo-

gravimetric method and the soil refractive index,  $n$ , was measured by the devices produced by the EASY TEST, Ltd. from Lublin, Poland, on the license of the Institute of Agrophysics, Polish Academy of Sciences, Lublin [29].

## 8.2. Results and discussion

The correlation table calculated for the selected soil parameters is presented in **Table 10**.

**Table 10.** The squared values of the correlation coefficient,  $R$ , between the selected parameters of the analyzed set of data, no of cases 663.

$R^2$	$n$	$\theta$	$\phi$	$\rho_s$	$\rho$	$C$	$clay$
$n$	1.00						
$\theta$	0.92	1.00					
$\phi$	0.03	0.15	1.00				
$\rho_s$	0.02	0.13	0.53	1.00			
$\rho$	0.03	0.16	0.94	0.72	1.00		
$C$	0.03	0.14	0.58	0.91	0.72	1.00	
$clay$	0.04	0.07	0.46	0.02	0.49	0.11	1.00

The soil volumetric water content,  $\theta$ , is highly correlated with the refractive index,  $n$ , for the analyzed set of soil samples. The other soil physical parameters:  $\phi$ ,  $\rho_s$ ,  $\rho$  and  $C$  are not correlated with  $n$ . The soil texture represented by the clay content in the soil ( $clay$ ), analyzed only for mineral soils (395 cases), is not correlated with  $n$ , either. High correlation between  $\theta$  and  $n$  ( $R^2=0.92$ ) enables to estimate the soil water content in the indirect way by the measurement of the soil refractive index,  $n$ . The relation between  $n$  and  $\theta$  was calculated by fitting a regression line into the set of measured data ( $n, \theta$ ).

$$n(\theta) = a_0 + a_1\theta \quad (68)$$

where:  $n(\theta)$  is the soil refractive index determined by TDR method,  $\theta$  is the water content of the tested soil samples determined by thermo-gravimetric method,  $a_0$  and  $a_1$  are: offset and slope of the trend line fitted into the data pairs ( $n, \theta$ ). The formula (68), called as the TDR calibration line, was determined for the whole set of data (663 soil samples) and separately for each subset of data (**Table 11**).

The values of the offset,  $a_0$ , and the slope,  $a_1$ , are different for the selected soil types; both values are the smallest for organic soils and the highest for mineral soils. The statistical parameters  $R^2$  and  $S_{yx}$  calculated for all 663 soil samples indicate worse correlation than for the individual soil types.

**Table 11.** Regression parameters  $n(\theta)$  for the tested soils ( $R^2$  – squared value of the correlation coefficient,  $S_{yx}$  – standard error of estimation).

soil type	no. of cases	density [g cm <sup>-3</sup> ]	porosity	$a_0$	$a_1$	$S_{yx}$	$R^2$
mineral	395	1.01 ÷ 1.80	0.32 ÷ 0.65	1.421	8.976	0.219	0.977
peat-sand and peat-silt mixtures	157	0.59 ÷ 1.43	0.46 ÷ 0.74	1.200	8.008	0.217	0.976
organic	111	0.12 ÷ 0.65	0.53 ÷ 0.91	0.776	7.932	0.260	0.981
all soil samples	663	0.12 ÷ 1.80	0.32 ÷ 0.91	1.491	7.675	0.425	0.923

The values of  $R^2$  for mineral and organic soils have similar values, nearly as high as for soil mixtures (Fig. 28).

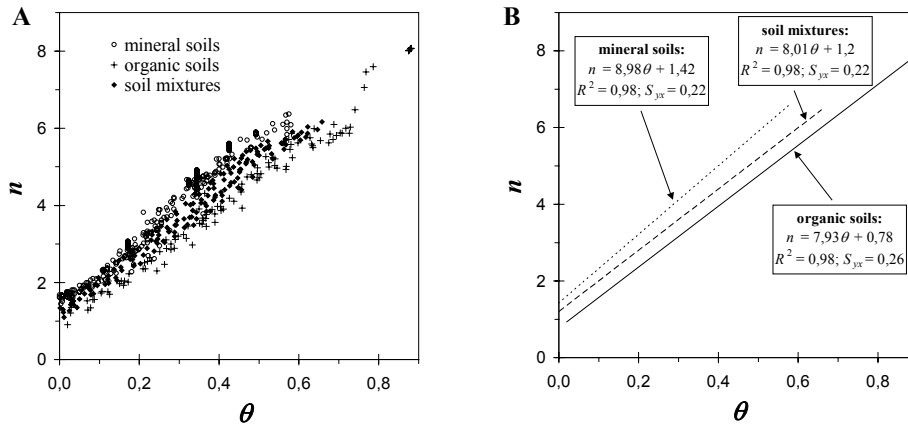


**Fig. 28.** Relation between the soil refractive index,  $n$ , and its water content,  $\theta$ , for mineral and organic soil samples as well as their mixtures. **A** - experimental data, **B** - regression  $n(\theta)$ .

Lower value of  $R^2$  and higher value of  $S_{yx}$  for the soil mixtures correspond with great differentiation of their density and porosity. Therefore it can be concluded that apart from soil water content,  $\theta$ , also soil density (or porosity) influences the soil refractive index,  $n$ , measured by TDR method.

The measured data were tested by multiple regression method (69) to determine the influence of analyzed soil properties on the value of the refractive index,  $n$ :

$$n = a_0 + a_1\theta + a_2\rho + a_3\phi + a_4\rho_s + a_5C + a_6clay \quad (69)$$

where:  $a_0 \div a_6$  are coefficients connected with different soil parameters:  $\theta$  - water content determined by the reference thermo-gravimetric method,  $\rho$  - bulk density,  $\phi$  - porosity,  $\rho_s$  - particle density,  $C$  - organic carbon content, *clay* - clay content in the analyzed samples.

The analysis of the *clay* significance in the equation (69) is performed only for mineral soils (395 cases). **Table 12** presents the values of the coefficients  $a_0 \div a_5$  and the parameters related to the *t-test* and *F-test* for all soil samples.

**Table 12.** The results of multiple regression analysis for all analyzed soil samples (no of cases - 663)

No.	Regression parameter	$a_0$	$a_1$ ( $\theta$ )	$a_2$ ( $\rho$ )	$a_3$ ( $\phi$ )	$a_4$ ( $\rho_s$ )	$a_5$ ( $C$ )	<i>p-value</i>	$R^2$	$S_{yx}$
1	$a_i$	1.491	7.675	-	-	-	-	<0.001	0.923	0.425
	$p_t$	<0.001	<0.001	-	-	-	-	-	-	-
2	$a_i$	0.289	8.504	0.846	-	-	-	<0.001	0.979	0.220
	$p_t$	<0.001	<0.001	<0.001	-	-	-	-	-	-
3	$a_i$	-0.279	8.500	0.792	-	0.244	0.005	<0.001	0.980	0.218
	$p_t$	0.092	<0.001	<0.001	-	<0.001	0.005	-	-	-
4	$a_i$	2.610	8.436	-	-2.463	-	-	<0.001	0.973	0.253
	$p_t$	<0.001	<0.001	-	<0.001	-	-	-	-	-
5	$a_i$	2.335	8.491	-	-1.857	-	-0.008	<0.001	0.976	0.240
	$p_t$	<0.001	<0.001	-	<0.001	-	<0.001	-	-	-
6	$a_i$	1.491	8.304	-	-	-	-0.020	<0.001	0.962	0.299
	$p_t$	<0.001	<0.001	-	-	-	<0.001	-	-	-

Each individual combination from the first column refers to the regression function (69) with arbitrary chosen number of parameters  $a_i$ . For each combination of independent data (*ie*  $\rho$ ,  $\theta$ ,  $\rho_s$  and  $C$ ) the *p-values* of respective  $a_i$  coefficients are calculated. The assumed significance level is 0.001. Except  $a_5$  in the third combination all coefficients have their *p-values* below 0.001, which proves that they are statistically significant.

Therefore the inclusion of  $\phi$  or  $\rho$  and  $\rho_s$  in the regression equation improves its parameters  $R^2$  and  $S_{yx}$ . This proves that the properties of soil solid phase influence the value of the soil refractive index,  $n$ , and consequently the velocity of EM wave propagation in the soil.

The values of *p* (referring to the *F-Snedecor test*) do not exceed 0.001 in all presented combinations. This does not agree with the zero hypotheses claiming that all coefficients in the analyzed multiple regression equation have zero values. Therefore each analyzed regression model is statistically significant. The reason

of this may be the high correlation between the variables  $n$  and  $\theta$ . The inclusion in the regression equation (69) the additional variables (*ie* introducing more degrees of freedom), apart of the soil water content,  $\theta$ , can only decrease the value of  $p$  parameter. The lower  $p_F$ , the goodness of fit in multiple regressions is better.

**Table 13.** The results of multiple regression analysis for individual groups of soil

No.	regression parameter	$a_0$	$a_1$ ( $\theta$ )	$a_2$ ( $\rho$ )	$a_3$ ( $\phi$ )	$a_4$ ( $\rho_s$ )	$a_5$ ( $C$ )	$a_6$ ( <i>clay</i> )	$p_F$	$R^2$	$S_{yx}$
Mineral soils (395 cases)											
1	$a_i$	1.422	8.976	–	–	–	–	–	<0.001	0.977	0.219
	$p_t$	<0.001	<0.001	–	–	–	–	–	–	–	–
2	$a_i$	1.502	9.134	–	–	–	–	-0.004	<0.001	0.981	0.198
	$p_t$	<0.001	<0.001	–	–	–	–	<0.001	–	–	–
3	$a_i$	0.604	9.014	0.561	–	–	–	–	<0.001	0.982	0.191
	$p_t$	<0.001	<0.001	<0.001	–	–	–	–	–	–	–
Organic soils (111 cases)											
1	$a_i$	0.776	7.932	–	–	–	–	–	<0.001	0.981	0.260
	$p_t$	<0.001	<0.001	–	–	–	–	–	–	–	–
2	$a_i$	0.844	7.951	0.238	–	-0.171	0.002	–	<0.001	0.982	0.255
	$p_t$	0.003	<0.001	0.173	–	0.152	0.461	–	–	–	–
3	$a_i$	0.876	7.946	–	-0.370	–	0.004	–	<0.001	0.982	0.256
	$p_t$	<0.001	<0.001	–	0.116	–	0.052	–	–	–	–
Soil mixtures (157 cases)											
1	$a_i$	1.200	8.008	–	–	–	–	–	<0.001	0.976	0.217
	$p_t$	<0.001	<0.001	–	–	–	–	–	–	–	–
2	$a_i$	-2.573	8.142	1.097	–	0.912	0.073	–	<0.001	0.994	0.107
	$p_t$	<0.001	<0.001	<0.001	–	<0.001	<0.001	–	–	–	–
3	$a_i$	3.448	8.190	–	-4.399	–	0.060	–	<0.001	0.993	0.121
	$p_t$	<0.001	<0.001	–	<0.001	–	<0.001	–	–	–	–

**Table 13** presents the results of multiple regression analysis for individual groups of soil. The selection of data into three individual groups (mineral, organic soils and their mixtures) significantly increases the correlation coefficient,  $R$ , and decreases the standard error of estimation,  $S_{yx}$ , between  $\theta$  and  $n$  in the linear relation  $n(\theta)$  in all groups as compared to all data. The introduction of the soil solid phase parameters into the multiple regression equation (69), *ie* its density,  $\rho$ , or porosity,  $\phi$ , additionally increased  $R$  and decreased  $S_{yx}$ . For each combination of independent variables the regression is statistically significant because the

values of  $p_F$  calculated for the respective case are always lower than the assumed error level (equal to 0.001).

The analysis of the soil texture significance in the regression (69), represented by clay content was performed in the group of mineral soils. It was found that the soil clay content texture significantly influences the regression equation coefficients (**Table 13**, case no 2 in the group of mineral soils). The importance of the soil clay content as an element in the regression is almost the same as the soil density. The regression  $n=f(\theta, \text{clay})$  gave the values of  $R^2$  and  $S_{yx}$  the same as for  $n=f(\theta, \rho)$  regression.

Taking into account the regression analysis with all analyzed soil samples it can be found that apart of the primary influence from the soil water content,  $\theta$ , on the value of the soil refractive index,  $n$ , also the soil solid phase modifies in the statistically significant way the relation  $n(\theta)$  by the soil density,  $\rho$ , and  $\rho_s$  (or the soil porosity,  $\phi$ ).

On the basis of the performed multiple regression analysis the following empirical formula were derived:

**Model I (Table 12, case no 1):**

$$n_I = 1.491 + 7.675\theta \quad (70)$$

**Model II (Table 12, case no 2):**

$$n_{II} = 0.289 + 8.504\theta + 0.846\rho \quad (71)$$

Taking into account the significance of the soil density in the  $n(\theta)$  relation, the following modification of the equation (68) is proposed:

$$n = (a_1 + a_2\rho) + (b_1 + b_2\rho)\theta \quad (72)$$

where the offset  $(a_1 + a_2\rho)$  and the slope  $(b_1 + b_2\rho)$  of the  $n(\theta)$  line are linear function of soil density.

The parameters  $a_1$ ,  $a_2$ ,  $b_1$  and  $b_2$  in the equation (72) were found with the use of the least square method giving the formulae:

$$n_{III} = 0.573 + 0.582\rho + (7.755 + 0.792\rho)\theta \quad (73)$$

referred to as the **model III**.

On the base of (66) and the set of measured data  $(n, \rho, \rho_s, \theta)$ , using the least square method for all analyzed data (663 soil samples), the values of the EM

refractive index of water,  $n_w = 8.676$ , and soil solid state,  $n_s = 2.177$ , were found. Introducing these values into (67), we have:

$$n_{IV} = 2.177 + 7.676\theta - 1.177\phi \quad (74)$$

referred to as the **model IV**.

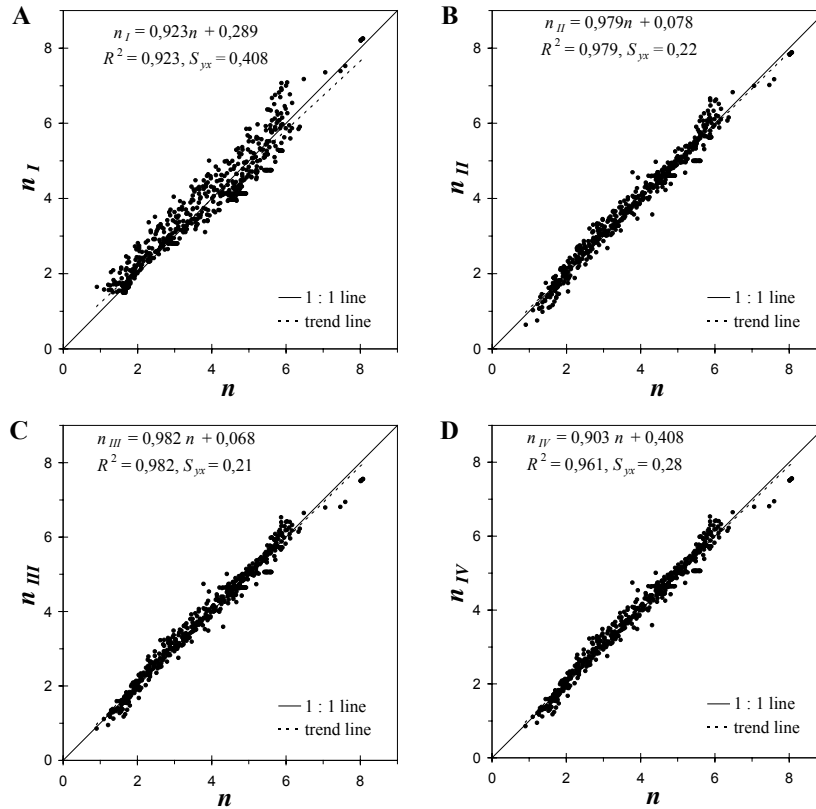


**Fig. 29.** Comparison of model values of the EM refractive index of the soil with the use of **A** – model I, **B** – model II, **C** – model III and **D** – model IV, with the values measured with TDR device (horizontal axis)

The water refractive index,  $n_w$ , in the temperature 20° C, in the frequency 1 GHz, is 8.95 (CRC [17]). The difference between the table and calculated experimental values of  $n_w$  suggests that its value decreases for water the soil. The

reason of this is the fact that water particles are bound by soil solid phase, which decreases the mobility of water dipoles.

The equations (70), (71), (73) and (74) present four models describing the soil refractive index,  $n$ , in the function of selected soil properties. These models were verified by the comparison of model calculated values of  $n$  with the experimental ones measured with the use of Time Domain Reflectometry technique. **Fig. 29** displays the results of this verification. The values of  $R^2$  and  $S_{yx}$  and the convergence of the trend line with the 1 : 1 line is the best for **model III**. This model generates the  $n$  values, which are closest to the measured ones. **Model I**, presently used as a calibration basis [29] in TDR soil water content measurement, generates values with the poorest correlation with the measured ones. **Models II** and **IV** are in the middle as far as goodness of fit is analyzed.

The best of the analyzed models is the **model III** described by (73). Taking into account the soil bulk density,  $\rho$ , decreases the standard deviation,  $S_{yx}$ , almost twice as much as in the **model I**, which has only soil water content,  $\theta$ , as the independent variable. **Model IV** with two independent variables: soil water content,  $\theta$ , and porosity,  $\phi$ , generates theoretical values of  $n$  slightly worse correlated with the measured values than **model III**.

The presented models allow determination of soil water content from the measurement of soil refractive index. The relation  $\theta(n)$ , with only one independent variable, can be found by conversion of (70), *ie* from the **model I**:

$$\theta_{TDR\_I} = 0.134n - 0.182 \quad (75)$$

Relation  $\theta(n, \rho)$  can be found by conversion of the (71), *ie* from the **model III**:

$$\theta_{TDR\_III} = \frac{n - 0.573 - 0.582\rho}{7.755 + 0.792\rho} \quad (76)$$

with two independent variables:  $n$  and  $\rho$ . The equation (76) is proposed as the calibration formulae of the TDR soil water content because of the best correlation of data.

**Fig. 30B** presents the comparison of the soil water content values,  $\theta_{TDR}$ , received from the **model III** with the reference values,  $\theta$ , and measured by the thermo-gravimetric method. The slope equal to one, almost no offset of the trend line and low value of the standard error of estimation,  $S_{yx}$ , verifies **model III** as the calibration equation of the reflectometric measurement of volumetric water

content. The similar values for **model I** presented in **Fig. 30A** show bigger dispersion of results generated by the actually used calibration function (70).

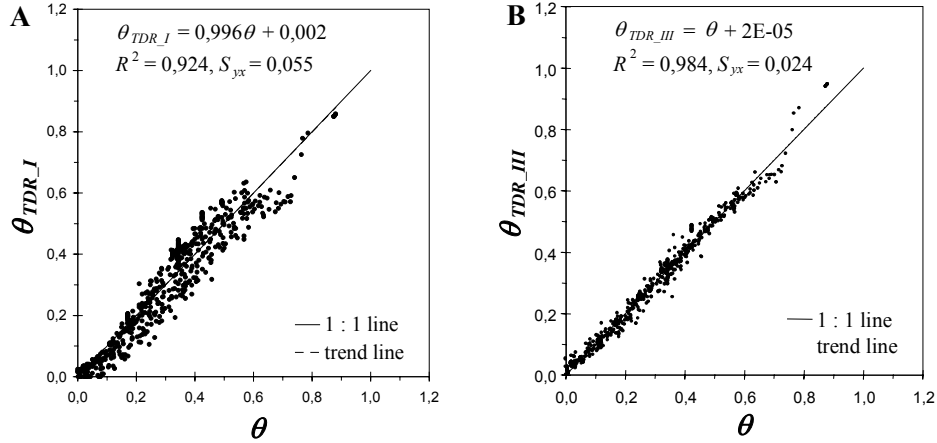


**Fig. 30.** Comparison of the values of soil water content,  $\theta_{TDR}$ , calculated from the measured values of soil refractive index,  $n$ , for **model I** – A and **model III** – B with the reference values determined by the thermogravimetric method

Equation (77) presents the soil water content values determined by TDR on the base of **model I** as the function of directly measured values of time distance between the appropriate reflections from the TDR probe.

$$\theta_{TDR} = 0.134 \frac{ct}{2L} - 0.182 \quad (77)$$

The derivative of (77) on time,  $t$ , is:

$$\Delta\theta_{TDR} = 0.134 \frac{c}{2L} \Delta t \quad (78)$$

where:  $\Delta\theta_{TDR} = (\theta_{TDR} - \theta)$  is the absolute error of the TDR measured soil water content, and  $\Delta t$  is the absolute error of the propagation time measurement. For the practical TDR sensor length  $L = 10^{-1}$  m, and the absolute error of time measurement  $\Delta t = 30 \cdot 10^{-12}$  [s], the absolute error of soil water content measurement resulted from the hardware and software imperfections of TDR meter is:

$$\Delta\theta_{TDR} = 0,2 \cdot 10^9 \cdot \Delta t = 0.006 = \pm 0.003 \quad (79)$$

The relative error of the soil water content measurement,  $\Delta\theta_{TDR}$ , calculated from the measurement of its refractive index,  $n$ , and originated from the constant error of the measuring device is:

$$\Delta\theta_{rel} = \frac{\Delta\theta}{\theta} = \frac{0,2 \times 10^9 \Delta t}{\theta} = \frac{0.006}{\theta} \quad (80)$$

The equation (80) presents the value of the relative error of  $\theta$  measurement, which results only from the measuring device. Its value depends on the soil water content, *ie* it tends to infinity for dry soil and for water it equals to 0.006. Introduction of an empirical correction on  $\theta_{TDR}$  for the solids and gas phases influence can not decrease the value of  $\Delta\theta_{rel}$  below the value presented in the equation (80).

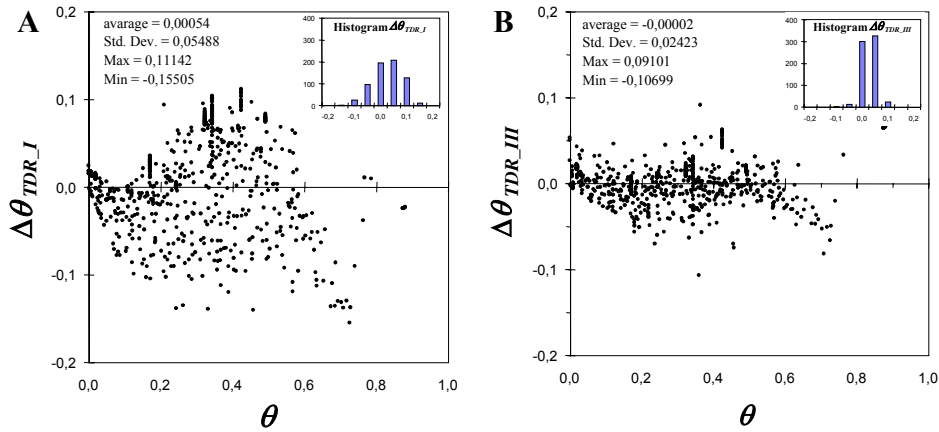


**Fig. 31.** The absolute error ,  $\Delta\theta_{TDR}$ , of the reflectometric soil water content measurement in relation of its real value,  $\theta$ , and the histograms of this error referring to the **model I**: **A** and the **model III**: **B**

**Fig. 31A** and **B** present the relation between the reflectometric soil water content measurement error,  $\Delta\theta_{TDR}$ , and its real value,  $\theta$ , for the **model I** and **III**. On the right top corners of these pictures there are the histograms of the errors. Smaller dispersion of data points and the shape of histograms confirm the importance of soil density as a factor influencing the error of TDR soil water content measurement.

From **Table 14** presenting the selected statistical parameters of the absolute errors referring to the models under investigation it is evident that the **model III** works much better than **model I**. Inclusion of the soil density in the **model III** resulted in decreasing the standard deviation of the TDR absolute error. Also the mean value of this error was closer to zero.

**Table 14.** Statistical parameters of the absolute errors for the models under investigation

Parameter	$\Delta\theta_{TDR\_I}$	$\Delta\theta_{TDR\_III}$
Mean value	0.00054	-0.00002
Standard deviation	0.05488	0.02423
Maximal value	0.11142	0.09101
Minimal value	-0.15505	-0.10699
Number of cases	663	663

Similar analysis was done for the relative error of TDR soil water content measurements.

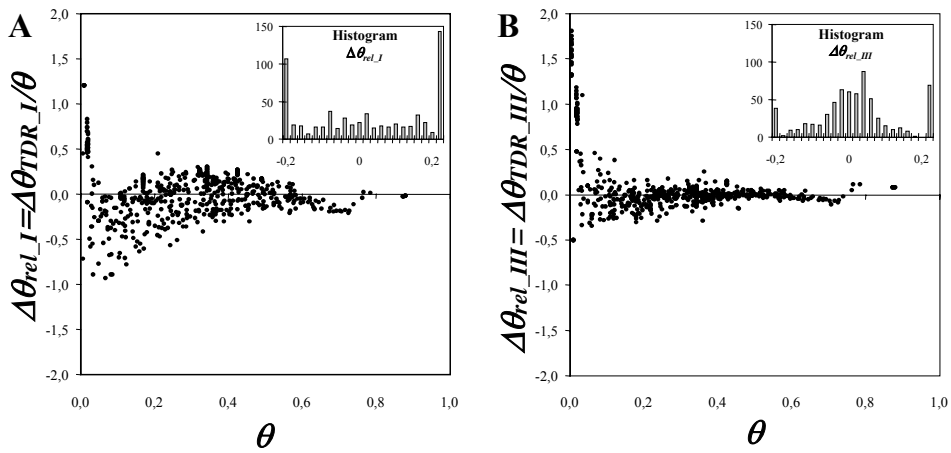


**Fig. 32.** The relative error,  $\Delta\theta_{rel}$ , of the TDR soil water content results as related to the real values of its water content,  $\theta$ , and the histogram of  $\Delta\theta_{rel}$  for soil water content values calculated for the **model I**: **A** and the **model III**: **B**

**Fig. 32** presents the relation between  $\Delta\theta_{rel}$  and  $\theta$  for the both models (in the same scale) as well as the histograms of the error  $\Delta\theta_{rel}$  for the **model I** and the **model III**. Ideally the histograms should look like the normal curve. The higher

values of  $\theta_{rel}$  for lower values of  $\theta$  can be explained by bigger influence of soil solid phase in the effective soil dielectric constant.

**Table 15.** Statistical parameters of  $\Delta\theta_{rel}$  for the set of data with all soil samples under test and the subset of data with soil samples of water contents  $\theta > 0.1$ .

Statistical parameter	$\Delta\theta_{rel}$	
	model I	model III
	<i>All soil samples under test</i>	
Mean	-0.0418	0.0317
Standard deviation	0.5112	0.3123
Variance	0.2613	0.0975
No of samples	388	388
Confidence Level (95%)	0.0511	0.0312
	<i>Soil samples with <math>\theta &gt; 0.1</math></i>	
Mean	-0.0036	-0.0102
Standard deviation	0.1830	0.0771
Variance	0.0335	0.0060
No of samples	328	328
Confidence Level (95%)	0.0198	0.0083

Water in dry soil exists mainly in the form of the particles adsorbed by solid phase. In this condition water molecules are not as easy to polarize as in free water condition. Therefore TDR soil water content measurement should underestimate the real values as compared to thermo-gravimetric method of soil water content determination. This effect should be more acute for fine soils.

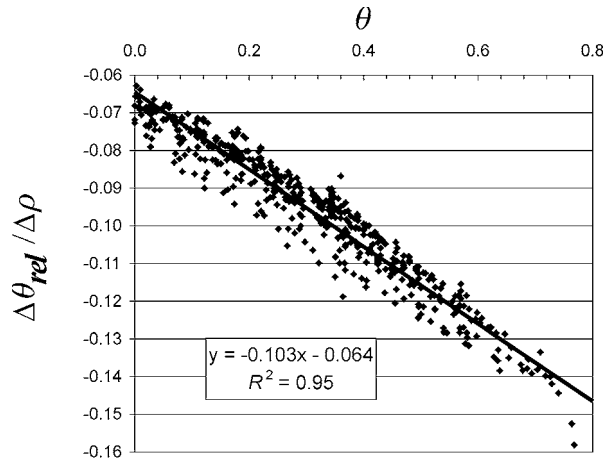


**Fig. 33.** Sensitivity of **model III** on the soil density,  $\rho$ , in relation to the soil,  $\theta$ .

Also the error coming from the hardware, which is constant is more visible for low water contents, according to (80).

The relative error of TDR water content values increases practically to infinity when soil water content tends to zero value.

**Table 15** presents the comparison of statistics for relative errors of TDR water content calculated from **model I** and **model III**. For soil water contents above 0.1 the standard deviation of  $\Delta\theta_{rel}$  is about four times smaller than for the whole range of  $\theta$ .

The sensitivity of TDR moisture on the soil density values calculated according to **model III** and expressed as  $\partial\theta_{TDR}/\partial\rho$  on the base of (76) is shown in **Fig. 33**.

We see that neglecting the change of soil density of  $0.1 \text{ g}\cdot\text{cm}^{-3}$  results in the TDR water content determined error of  $\Delta\theta_{TDR}=0,0064$  for dry soil and  $\Delta\theta_{TDR}=0,012$  for the soil with the water content value of 0.5.

### **8.3. Conclusions**

Soil solid phase influences the electromagnetic wave velocity (and consequently its dielectric constant) in soil in the statistically significant way. This influence makes the reflectometric technique, in soil water content measurement application, not selective. Soil density or porosity represents the solid phase influence on its dielectric constant measured by TDR. Inclusion of this influence in the calibration formulae of TDR method makes the reflectometric method of soil water content measurements more selective and decreases the absolute error of its measurement by the factor of two.

The error of TDR water content determination originates mainly from the correlation imperfections. The TDR hardware and software sources of TDR water content error may be visible in the lower range of soil water content values.

## 9. COMPARISON OF OPEN-ENDED COAX AND TDR SENSORS FOR THE MEASUREMENT SOIL DIELECTRIC PERMITTIVITY IN MICROWAVE FREQUENCIES

Real-time and non-invasive monitoring of physical and chemical properties of agrophysical objects, *ie* food products and agricultural materials, as well as the environment of their growth, storage and transportation is necessary to improve quality as well as quantity of agricultural production and to minimize the loss. The development of technology in the recent years has increased the number of methods and decreased the price of monitoring tools for application in Agriculture. Data transmission facilities, accurate and battery operated converters of physical and chemical properties into electrical signals and measurements in high frequency range are a few examples of the observed progress.

The important parameter for soil monitoring is its water content because water directly influences the other physical and chemical parameters of soil as a porous body. The indirect measurement of water content using its dielectric properties seems to be the right direction for the researchers. The objectives of the study are:

- comparison of two sensors for the determination of the complex dielectric permittivity,  $\epsilon^*$ , of soils: a three-rod TDR probe and an Open-Ended Coax probe,
- comparison of the hardware differences between the both systems for the measurement of  $\epsilon^*$  of porous materials working in time and frequency domains,
- long term objective is to design and build a prototype of a portable and not expensive meter for the measurement of  $\epsilon^*$  of porous materials working in the frequency domain.

The presented methods of the determination of the complex dielectric permittivity of materials are applications of dielectric spectroscopy, the branch of science aimed to identify relationships between dielectric properties of materials and their important quality characteristics and to develop scientific principles for measuring these characteristics through interaction of radio frequency and microwave electromagnetic fields with the agricultural materials and products.

Dielectric spectroscopy has some advantages over other physicochemical measurements: sample preparation is relatively simple, varieties of sample size and shapes can be measured, measurement conditions can be varied under a wide range of temperatures, humidity, pressure, etc., the technique is extremely broad band (mHz - GHz) thus enabling the investigation of diverse processes, over wide ranges of time and scale. Moreover the construction of a not expensive and

reliable meter working in the frequency range adjusted to the material under study can be a significant step towards the standardization of the measurement of the dielectric properties of agricultural materials and products.

The aim of the paper is:

- describe the main features of two methods of determination of  $\varepsilon^*$ : Open-Ended Coax Probe and Time Domain Reflectometry (TDR) methods,
- compare real and imaginary parts of  $\varepsilon^*$  determined from the measurement of three mineral soils,
- discuss the hardware differences of the meters working in the frequency domain (Open-Ended Coax Probe) and time domain (TDR).

When the electromagnetic wave leaves one medium, *eg* free space or a coaxial cable, to another, *eg* soil or other agricultural material, a part of its energy is reflected from the material and the rest is transmitted through it. This is due to the difference of the velocity of travel of electromagnetic waves in different media. When the material is lossy it will attenuate the electric signal or introduce the insertion loss.

The fundamental electrical property describing the interactions between the applied electric field and the material are described is the complex relative permittivity of the material  $\varepsilon^*$  (Kraszewski [47], Topp *et al.* [90]):

$$\varepsilon^* = \varepsilon' - j\varepsilon'' \quad (81)$$

where  $\varepsilon'$  is its real part, often called the dielectric constant, and  $\varepsilon''$  is its imaginary part,  $j$  is an imaginary unit.

Dielectric material has an arrangement of electric charge carriers that can be displaced or polarized in the external electric field. There are different polarization mechanisms in a material and each has a characteristic resonant frequency or relaxation frequency [43]. As the frequency increases the slower mechanisms do not contribute in the overall  $\varepsilon'$ . The imaginary part,  $\varepsilon''$ , will correspondingly have a local maximum at each critical frequency (**Fig. 34**).

There are different mechanisms of polarization of charge carriers in a material: electronic polarization, atomic, orientation and ionic polarizations.

Water is an example of a substance with strong orientation polarization. Ionic conductivity,  $EC$  [S/m], present at low frequencies only introduces losses into a material and the measured loss of material can be expressed as a function loss due to the dielectric polarization of the particles in the alternating electric field,  $\varepsilon_d''$ , and conductivity,  $EC$  (Topp *et al.* [90]):

$$\epsilon'' = \epsilon_d'' + \frac{EC}{2\pi f\epsilon_0} \quad (82)$$

where  $f$  is the frequency of the applied electric field,  $\epsilon_0$  is the dielectric permittivity of free space.

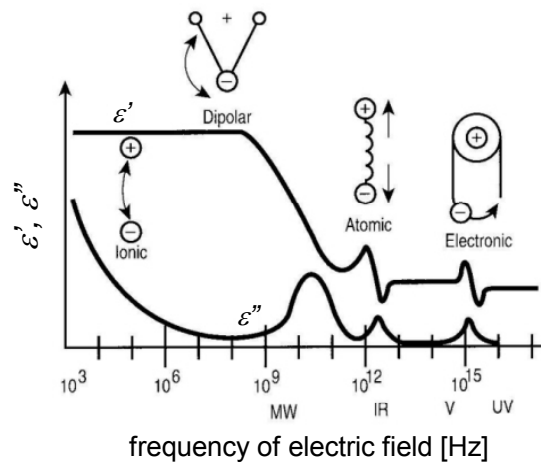


**Fig. 34.** Frequency response of dielectric mechanisms: MW, IR, V and UV are respectively microwave, infrared, visible and ultraviolet spectrum

Because water is present in all agricultural materials and its influence on the majority of agricultural properties is dominant, the specific property of water causing the orientation polarization is of primary area of interest of dielectric spectroscopy (Kraszewski [47]).

### 9.1. Hardware features of Time Domain Reflectometry method

Time Domain Reflectometry method for the determination of dielectric permittivity is widely accepted, especially for soil water content determination [90,59,61], for its advantages: simplicity of operation, accuracy and fast response, usually does not need calibration, is non-destructive, portable systems are available, is able to automatize and multiplex probes. The construction of TDR meter for determination of velocity of propagation of electromagnetic pulse in the material is much simpler than the frequency domain reflectometer. The basic elements of the meter are (**Fig. 35**): two pulse generators, delay unit, sampling head with data conversion facilities, a TDR probe (sometimes several multiplexed probes) and a microcontroller. The construction of the TDR meter needs a lot of

skills and professional instrumentation [59] to maintain stable parameters in field applications. The pulses travel times along the parallel waveguide in the measured media must be determined with the resolution of picoseconds (Baranowski *et al.* [8]). The measurement error of the pulse travel time along the probe rods equal to 10 ps will give the error of soil water content measurement of about 0.2%.

The applied frequency in Time Domain Reflectometry (TDR) method is not exactly defined as it can be done for Frequency Domain Reflectometry (FDR) represented by the Open-Ended Coax probe method. The application of a step pulse or a needle pulse of very short rise time,  $t_r$ , corresponds to the frequency range with the upper limit,  $f_{\max}$ , that can be calculated by the following engineering formula [87]:

$$t_r = 0.35 f_{\max}^{-1} \quad (83)$$

The probe in TDR method is a waveguide consisting of two or three parallel metal rods inserted into the tested medium.

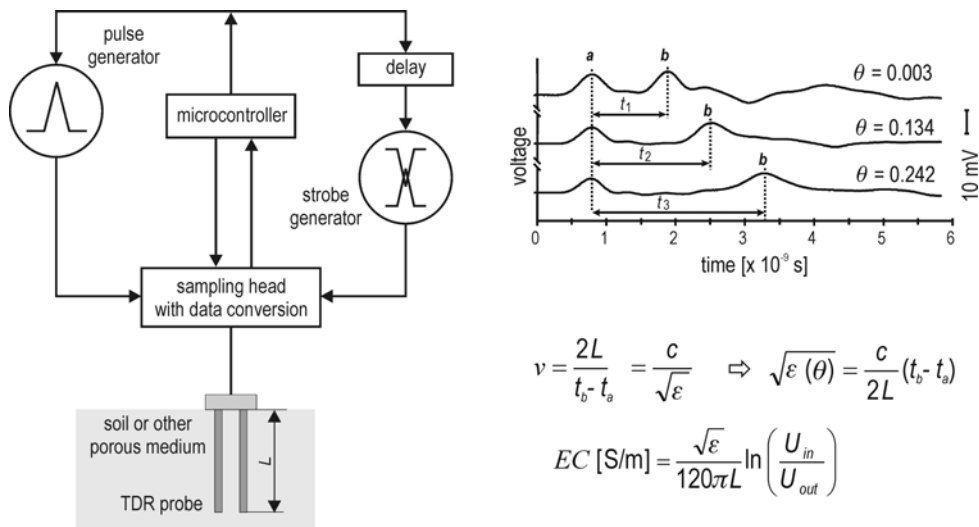


**Fig. 35.** Basic elements of the time domain reflectometer for determination of velocity of propagation of electromagnetic waves in porous media

The velocity of propagation of the pulse in this waveguide,  $v$ , is modified by the dielectric permittivity of the waveguide surroundings. In calculations it is usually assumed that the dielectric loss of the material does not influence the velocity of propagation of the pulse [90]. The real part of the medium complex

dielectric permittivity, the dielectric constant, is the indicator of its water content,  $\theta$ . For the probe length  $L$ , the apparent dielectric constant of the material,  $\epsilon$ , and indirectly its water content can be calculated [59] using the formula in **Fig. 35**, where:  $(t_b-t_a)$  is the measured time the pulse covers the distance  $2L$ ,  $c$  is the velocity of light in free space.

Most commonly used *EC* determination is based on *Giese and Tiemann* [33] approach:

$$EC = \frac{Z_0}{120\pi LZ_L} \quad (84)$$

where  $Z_0$  is probe impedance,  $L$  is probe length, and  $Z_L$  is the measured resistive load impedance across the probe embedded into the soil:

$$Z_L = \frac{Z_0}{[(2V_0/V_f) - 1]} \quad (85)$$

Lossy media attenuate the TDR reflected pulse and this makes the method practically useless for electrical permittivity of materials exceeding 4 dS/m, which is a high value for arable soils (Marschall and Holmes [63]). In saline soils the signal reflected from the end of the probe rods is completely attenuated (no amplitude at point  $b$  in **Fig. 35**). The measurement of the amplitude of the pulse reflected from the end of the probe, taken simultaneously to the pulse travel time, enables to determine the electrical conductivity of the soil,  $\sigma$ , and its salinity defined after Rhoades and Ingvalson [75] as the electrical conductivity of the extract of a saturated soil paste.

## 9.2. Open-Ended Coaxial Probe method

The measurement of dielectric properties of materials in frequency domain, with the application of microwave frequencies, needs expensive instrumentation. The basic elements of a simplified Vector Network Analyzer (VNA), working only in reflection mode, for determination of reflection parameter  $S_{11}$  is presented in **Fig. 36**. The device consists of a very stable frequency synthesizer generating sinusoidal waveforms of variable frequency feeding a sensor – Open-Ended Coax probe connected to the output/input port of the VNA. For a defined frequency the directional couplers sense the amplitudes and the phases of the waveforms produced by the generator and reflected from the probe. The detected difference in amplitude and phase depends on the dielectric properties of the tested material

at the end of the open-ended coaxial probe. The signals from the directional couplers are mixed with the signals from another generator, heterodyne, which frequency is adjusted by the phase detector. The reason for this frequency conversion is to have the constant frequency, not dependent on the synthesized frequency, of the signals reaching the measuring detector. The detected signals are characterized by constant frequency but their amplitudes and phase shifts do not change. The whole process of waveforms generation and detections is controlled by a microprocessor that changes the frequency of the synthesizer and registers the detected signals. All elements used in the presented system work in broad frequency range, from kHz to GHz, and they must have linear characteristics. Moreover, the measuring system accomplishes continuous recalibration to maintain parameters stable in time and temperature.

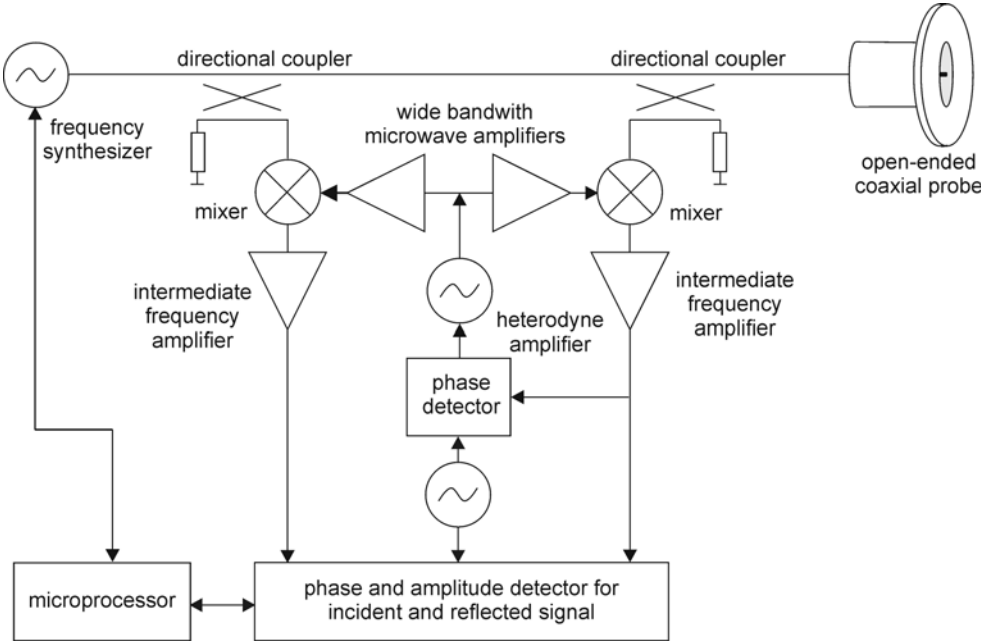


**Fig. 36.** Basic elements of the frequency domain reflectometer for determination of complex dielectric permittivity of porous media

Fundamental to use the Open-Ended Coax probe (**Fig. 37**) is an accurate model relating the reflection coefficient at its end to the permittivity of the material contacting with the probe. The lumped capacitance circuit model described by Stuchly and Stuchly [89] is applied in the presented example.

The applied lumped capacitance model of the probe assumes the presence of capacitance at the end of the probe. Its value depends on the complex dielectric permittivity of the material the probe was pressed to (**Fig. 37**). The complex value of the admittance of the probe end,  $Y_L^*$ , is:

$$Y_L^* = j\omega C_f + j\omega C_0 \varepsilon^* = j\omega(C_f + C_0 \varepsilon') + \omega C_0 \varepsilon'' \quad (86)$$

where:  $C_f$  represents the part of admittance that is independent from the dielectric sample,  $C_0$  is a part of admittance for air as dielectric.

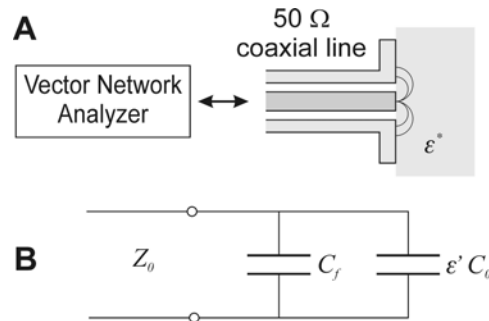


**Fig. 37.** A - Open-ended coaxial probe in the form of coaxial line open to the space with material of unknown dielectric permittivity  $\varepsilon^*$ , B - modeling the discontinuity of electromagnetic field by lumped capacitances  $C_f$  and  $C_0$

Before performing measurements on unknown materials the Open-Ended Coax probe should be calibrated on media with known dielectric properties, usually distilled water, methanol or air to find the values of  $C_f$  and  $C_0$ . The described measurement method and the lumped capacitance model were verified by measuring the dielectric permittivity of teflon. It was found that the  $C_f$  value is negligible and  $C_0$  calculated from (86) equals to the  $C_0$  coefficient of the correction polynomial obtained during calibration. Consequently the model (86) may be simplified to:

$$Y_L^* = \omega C_0 \varepsilon^* = j\omega C_0 \varepsilon' + \omega C_0 \varepsilon'' \quad (87)$$

The value of  $C_0$  describes the geometry of the probe and the frequency range of its application. The larger dimensions of the probe, the bigger its value and the better accuracy in applications for the materials of small values of dielectric permittivity, and simultaneously the high frequency range of measurement is

limited. This limitation comes from the fact that in case of materials of high dielectric permittivity and at high frequencies, the changes of the dielectric permittivity of the material causes very small changes of the phase shift of the reflection coefficient. This drastically decreases the accuracy of measurement and the need to apply calibration media of small value of dielectric permittivity.

### 9.3. Materials and methods

Dielectric permittivity of three soils was compared. **Table 16** presents the basic physical parameters of the tested soils.

**Table 16.** Localization and selected physical parameters of tested soil samples

No.	Locali- zation	Soil type	Density [gcm <sup>-3</sup> ]	Soil texture ISSS			Specific surface [cm <sup>2</sup> ·g <sup>-1</sup> ]
				sand	silt	clay	
				2-0,02 mm	0,02-0,002 mm	< 0,002 mm	
611	Olempin	Gleba brunatna	1.59	94	5	1	9
606	Wólka Kątna	Gleba murszowa	1.42	97	2	1	23
619	Sahryń	Czarnoziem	1.16	87	12	1	69

Dry soils were mixed with appropriate amount of distilled water to achieve four samples for each analysed soil with different water content values and taking care to get the homogeneous distribution of water in the soil samples. Twelve containers with soil samples covered with plastic foil (to minimize evaporation) were left for 24 hours in room temperature for water distribution in the samples in natural way. The gravimetric water content,  $\theta$ , and bulk density,  $\rho$ , were determined according to ISO standard 16586 [44] for each soil sample directly after the dielectric permittivity measurements were completed. The values of  $\rho$  in Table 1 are the mean for all applied water contents for each tested soil. Soil texture was determined by standard Bouyoucos method (Turski [93]). The values of soil specific surface,  $S$ , was determined with water vapour adsorption method (Ościk [73]).

Time Domain Reflectometry (TDR) and Open-Ended Coax Probe methods of determination of the complex dielectric permittivity of porous materials were applied.

TDR measurements were performed using the oscilloscope frame HP54120 with the TDR unit HP54121T, featured by 20 ps rise-time step pulse. The TDR probe was based on the standard coaxial connector (type N jack) with three

stainless steel wires soldered to the centre contact and two others symmetrically to the connector flange (**Fig. 38A**). The diameter of the rods was 2 mm, the distance to the central rod - 13 mm and the length of the rods - 114 mm. The characteristic impedance,  $Z_0$ , of the parallel waveguide measured from the reflection coefficient by the TDR unit was 165 ohm [2].

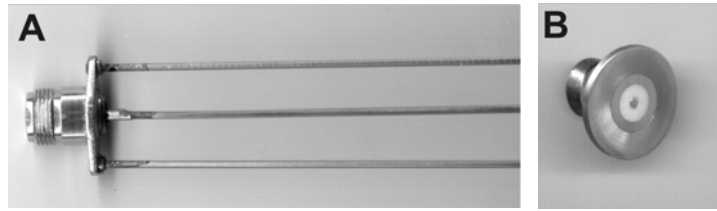


**Fig. 38.** The three-rod TDR probe – **A**, and an Open-Ended Coax probe – **B**, used in the measurement of dielectric permittivity of soils.

The data from the Open-Ended Coax probe were collected by the 20 kHz ÷ 8 GHz Rohde&Schwarz ZVCE Vector Network Analyzer (Blackham and Pollard [10], Stuchly and Stuchly [89]). It enables to calculate, on the base of the measured  $S_{11}$  parameter, the complex reflection coefficient and the complex admittance at the end of the probe. The probe was constructed on the base of type N coaxial connector machined flat at the side where it contacts with the tested material (**Fig. 38B**).

The Open-Ended Coax Probe method was verified by comparing the measured data to Cole-Cole model [10]. The Cole-Cole equation models the permittivity of free water and other polar substances:

$$\varepsilon^* = \varepsilon' - j\varepsilon'' = \varepsilon_\infty + \frac{\varepsilon_s - \varepsilon_\infty}{1 + (j\omega\tau_{rel})^{1-\alpha}} \quad (88)$$

where:  $\varepsilon_\infty$  is the relative high frequency permittivity,  $\varepsilon_s$  is the relative static permittivity and  $\tau_{rel} = 1/f_{rel}$  is the relaxation time (inverse of relaxation frequency  $f_{rel}$ ) of orientation polarization defined as the time at which the permittivity equals  $(\varepsilon_s + \varepsilon_\infty)/2$ ,  $\alpha$  is an experimental correction. The Cole-Cole model values of  $\varepsilon_\infty, \varepsilon_s, \tau_{rel}$  and  $\alpha$  are 4.45, 33.7,  $4.95 \times 10^{-11}$ s and 0.036, respectively.

#### 9.4. Results and discussion

The comparison of measured and the modeled data, using Cole-Cole model of complex dielectric permittivity of methanol is presented in **Fig. 39**.

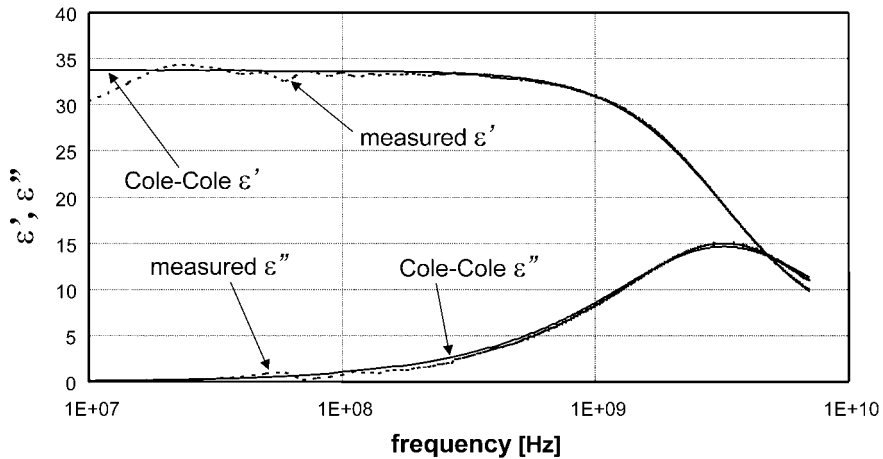


**Fig. 39.** Frequency change of real and imaginary parts of the complex dielectric permittivity of methanol for Cole-Cole modelled data and measured using open-ended coaxial probe

The measured and modeled data are very close to each other proving the applied measurement procedure to be adequate.

The comparison of the measured real and imaginary parts of the complex dielectric permittivity of the analysed soils is presented in **Fig. 40**.

The curves representing the relation  $\epsilon'(f)$  for soils of different water content,  $\theta$ , determined by gravimetric method, are collected by the Open-Ended Coax probe. In the lower frequency limit of 10 MHz the real part of the complex dielectric permittivity is relatively high. This is attributed to the influence of ionic double layers associated with colloidal soil particles. This effect is often referred to as the “Maxwell-Wagner” effect [41]. There was no orientation relaxation found in the measured frequency range from 10 MHz to 7 GHz because the tested soils have very small clay content. There is slight decrease of the measured  $\epsilon'$  with the frequency increase.

The real part of dielectric permittivity of tested soils,  $\epsilon'_{\text{Open-Coax}}$ , taken for the comparison with the soil bulk dielectric constant determined by TDR method,  $\epsilon_{b\text{-TDR}}$ , are values for 1 GHz frequency. There is high correlation between the

$\varepsilon'_{\text{Open Coax}}$  and  $\varepsilon_{b\text{-TDR}}$ , except for high water content, where the measurements in the frequency domain show higher values than time domain measurements.

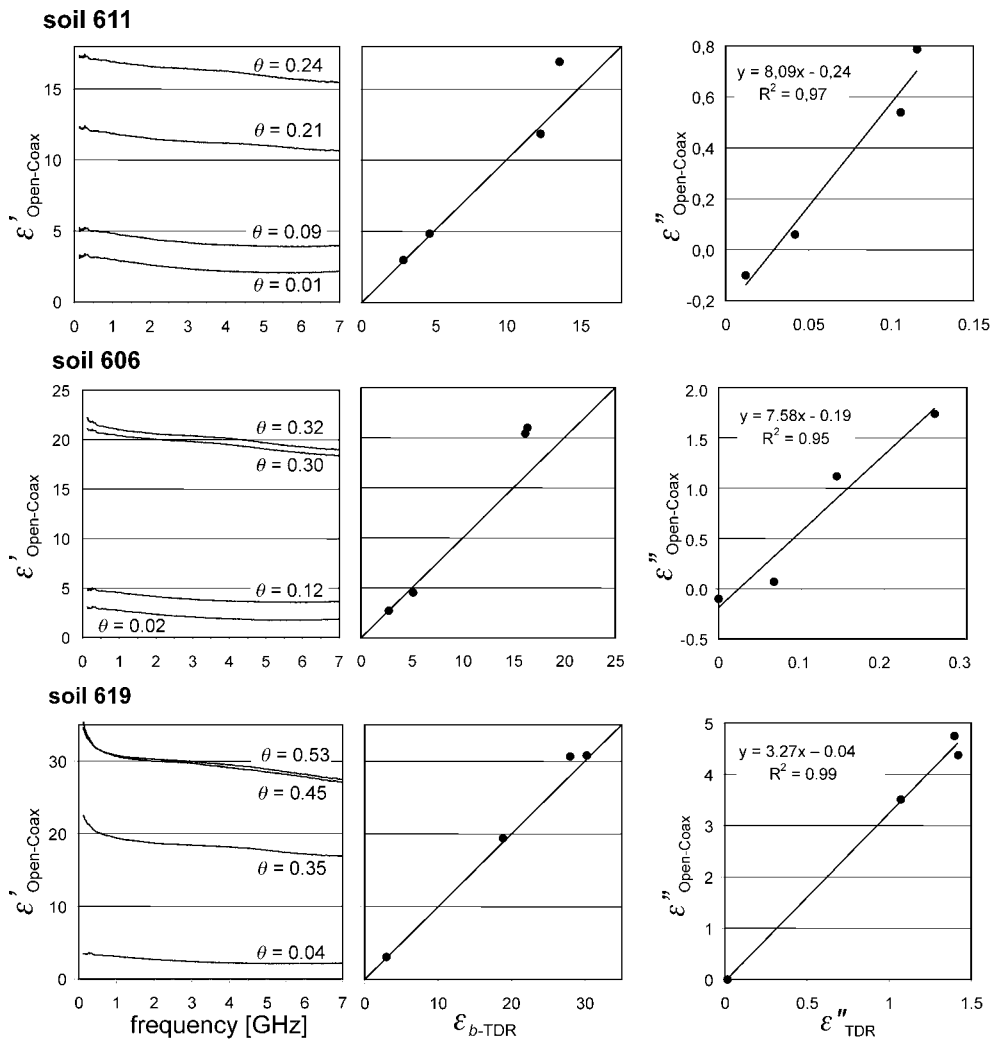


**Fig. 40.** Comparison of real,  $\varepsilon'$ , and imaginary,  $\varepsilon''$ , parts of the complex dielectric permittivity for the selected soils, calculated from the TDR and Open-Ended Coax probe measurements.  $\varepsilon_{b\text{-TDR}}$  is the bulk dielectric constant measured by TDR.

More difference between the measurements from the both probes can be found for the imaginary parts of the  $\varepsilon^*$ , where the values from TDR measurements

were much lower than for frequency domain. This inconsistency may result from two reasons:

- problems during the calibration of the Open-Ended Coax probe (the Vector Network Analyser calibration kit was not fitted for the performed measurements),
- the assumption that the dielectric loss,  $\varepsilon''$  in Eq. (82), was negligible in TDR measurements is false.

The both methods of the determination of the dielectric permittivity of porous materials have advantages and drawbacks. The parallel waveguide can have the length ranging from 5 cm to 50 cm or more and the tested material constitutes its propagation medium, therefore as opposite to the Open-Ended Coax method, the propagation velocity is an average along the probe rods and the volume of measurement is much larger. For small samples of material or in cases when it is not possible to insert the rods into it, the Open-Ended Coax method is more suitable. The frequency of the TDR measured  $\varepsilon_b$  is not precisely defined, as it is a superposition of sinusoidal waves making the final step or needle pulse. Also, for the frequencies in the range 0.5-1.5 GHz the real and imaginary parts of the dielectric permittivity do not change for the majority of agricultural materials. In the case of the Open-Ended Coax probe the user has the whole frequency spectrum for analysis.

The meters for the TDR and Open-Ended Coax measurements must work in high frequency to cover the physical phenomena associated with dipolar polarization of water molecules. The TDR meter working in time domain (**Fig. 35**) is much simpler to construct as compared to the meter working in frequency domain (**Fig. 36**), although both require much effort and test instrumentation. The temperature and long-term stable frequency conversion in the required range of change, from kHz to GHz, need the selection of electronic elements, which needs time and investments. However for the selected material only one frequency can be applied. The choice of this frequency can be determined by the preliminary tests with the use of the professional VNA.

## 9.5. Summary

- Real parts of  $\varepsilon^*$  of the tested soils, determined by the both measurement methods, are highly correlated and the measured values are close to each other. However for soil of high water contents the value of the real part  $\varepsilon^*$  determined by the Open-Ended Coax probe is higher than by TDR method. The imaginary parts are highly correlated but differ significantly.

- The difference of the imaginary parts of  $\epsilon^*$  of the tested soils needs additional research for explanation, it may result from the not adequate calibration tools applied.
- Open-Ended Coax and Time-Domain Reflectometry methods need further developments in the field of modeling (to provide models of tested media and identify the measured quantities with indicators of material properties) and hardware (to select appropriate geometry of applied sensors for different porous materials and to decrease the price of the meters).

## 10. MICROWAVE SWITCHES USED IN AUTOMATIC REFLECTOMETRIC SYSTEMS FOR SOIL WATER CONTENT AND SALINITY MEASUREMENTS

Due to advantages of reflectometric technique described earlier, this method was successfully applied in automatic field measurements. However, automatization of the soil water content and salinity measurement by means of TDR method requires switching of analyzing signal. Wide frequency bandwidth (above 1 GHz) makes it impossible to utilize conventional mechanical or solid state switches. The switching methods commonly used now in TDR technique are not satisfactory.

The measurement of soil water content by TDR method is popular and commonly acknowledged although its relatively short, *ie* 20 years old, history [90]. Automatization of this measurement is the natural consequence of its development and is forced by the economy as well as the demands of accuracy and reliability. TDR method of water content determination requires the application of complex electronic instrumentation working in microwave frequency range (above 1 GHz). In such high frequency the standard connections may be the source of signal distortions because they are the source of impedance discontinuity. This property is significant obstacle in automatization process of soil water content measurement by TDR. The condition to make automatic measurements from different channels is to be able to switch these channels between subsequent sensors.

### 10.1. Introduction

The mechanical switches commonly used by researchers (Baker and Allmaras [7], Topp *et al.* [90], van den Elsen *et al.* [95]) have very good frequency parameters but they have important drawbacks. The ideal switch should be not expensive, have as many channels as possible, low power consumption, unlimited number of switching, wide frequency range of operation (at least 2 GHz). The advantages of integrated switches made of GaAs is denoted in the comparative description (Skierucha [80]) of microwave switches used in TDR technique. This study presents the obstacles and the evolution of TDR microwave switches from mechanical to highly integrated solid-state microwave devices builds on the base of MMIC (Monolithic Microwave Integrated Circuit). The performed tests prove that the achieved solution fulfils the requirements of TDR soil water content determination method and performs better as compared with the ones tested earlier. The highly integrated microwave switch (MMIC - Monolithic Microwave

Integrated Circuit) recently introduced by Hittite [42] and its implementation in TDR soil water content measurement is described below.

The pulse from the generator (**Fig. 1**) applied in the TDR measurement system developed in IAPAS, Lublin has a needle shape with the rise and fall time equal to about 200 ps. Such a sharp pulse corresponds to the upper frequency,  $f_{HI}$ , limit of the generated signal calculated from Eq. (83) equal to 1.75 GHz.

For a TDR probe of 10 cm length the time,  $\Delta t$ , necessary for the pulse to cover the distance  $2L$  ( $L$  is the length of the TDR probe rods) in air is  $\Delta t = 2L\sqrt{\varepsilon_a}/c = 667 \cdot 10^{-12}$ [s], where:  $\varepsilon_a$  is the dielectric constant of air and  $c$  is the light speed in free space.

For given values of the TDR probe rods length and the rise time of the needle pulse the maxima of the reflectogram referring to the reflections of the initial pulse from the impedance discontinuities are easy to (**Fig. 41**).

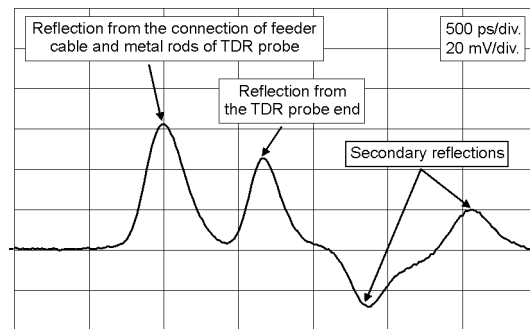


**Fig. 41.** TDR meter output – probe in air

Cutting the rods of the TDR probe below the length of 10 cm introduces additional technical problems in the reflectogram interpretation. The reflections become not separated and the travel time,  $\Delta t$ , measurement is burdened with an error. To keep the assumed accuracy it is necessary to generate a faster pulse and rebuilt the sampling head. In other words the bandwidth of the measurement system should be made wider. Introduction of additional elements, like high frequency signal switches, degrades the system performance and consequently its measurement accuracy even if these elements produce little reflections. In TDR technique even small reflections resulting from the impedance discontinuities are more severe because the signal passes it two times.

The best performance switches are mechanical ones. However they have disqualifying drawbacks in application to automatic measurement systems: they consume too much power, usually the number of switching is limited  $10^6$  and they

are expensive. The ideal TDR signal switch should not be expensive, should be economical both in price and power consumption, should have many switching channels, work in the bandwidth from DC up to at least 2 GHz and have other RF parameters similar to the mechanical ones. Radio frequency, or RF, refers to that portion of the electromagnetic spectrum in which electromagnetic waves can be generated by alternating current fed to an antenna. Radio frequency range is divided into bands starting from 3 Hz with the ELF (Extremely Low Frequency) that was used by the US Navy to communicate with submerged submarines and ending with EHF (Extremely High Frequency), which is the highest radio frequency band. EHF runs the range of frequencies from 30 to 300 GHz, above which electromagnetic radiation is considered to be low (or far) infrared light. This band has a wavelength of one to ten millimeters, giving it the name millimeter band.

The objective of the description below is to present the available microwave switches, their basic elements and the results of instrumental work performed in IAPAS, Lublin, Poland to build complex prototype SP16T bi-directional switches (single-pole-16-throw, *ie* a switch with one input/output and 16 outputs/inputs). One prototype switch was built with the use of MMIC (Monolithic Microwave Integrated Circuits) SPDT (single-pole-double-throw, *ie* a switch with one input/output and two outputs/inputs) constructed on FET gallium arsenide (GaAs) transistors, the other on miniature SPDT reed relays. Gallium arsenide is a semiconductor compound used in some diodes, field-effect transistors (FETs), and integrated circuits (ICs). The charge carriers, which are mostly electrons, move at high speed among the atoms. This makes GaAs components useful at ultra-high radio frequencies, and in fast electronic switching applications. GaAs devices generate less noise than most other types of semiconductor components.

The parameters describing the quality of microwave switch are: insertion loss, isolation and the Voltage Standing Wave Ratio (VSWR).

The insertion loss is the attenuation between input and output ports of the switch when embedded in a circuit, when the switch control voltage corresponds to the "ON" state of the output port.

The isolation is the attenuation between input and output ports of the switch when embedded in a circuit, when the switch control voltage corresponds to the "OFF" state of the output port. Insertion loss and isolation are usually expressed in dB.

VSWR indicates the degree of impedance match present at the switch RF port. In most cases, it is much easier to describe the impedance match in terms of return loss, dB. Return loss is equal to the amount of reflected power relative to the incident power at a port. Simply by measuring both incident and reflected power, the return loss can be measured and hence the VSWR can be calculated.

## 10.2. Electromechanical microwave switches

Electromechanical switches (**Fig. 42**) typically offer wider bandwidth, lower insertion loss, and lower VSWR specifications than solid-state switches. However, electromechanical switches have a shorter life cycle - typically 2 million switching cycles as opposed to 10 million for solid-state switches. Electromechanical switches also require switching times on the order of 25 ms, as compared to 25 ns for solid-state switches. The frequency bandwidth they work is from up to 26.6 GHz and can conduct as well as switch high power signals. The insertion loss at the frequency 2 GHz can be as low as 0.2 dB. The high price of electromechanical switches, high power consumption and limited number of switching cycles are the reasons for searching other solutions, especially between solid-state semiconductor devices.

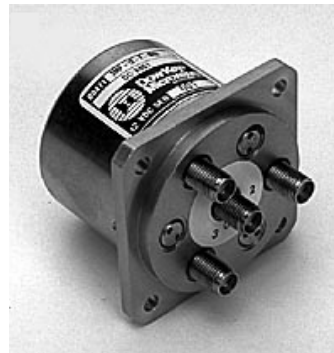


**Fig. 42.** Examples of electromagnetic microwave switches

Other basic components for use in TDR signal switching are reed relays encapsulated in the way to minimize insertion loss. The examples include RF reed relays from CoTo Technology [16] that can switch small power signals. They are equipped with coaxial shield made of copper alloy material that is terminated to two pins within the relay on each side of the switch. It is used to simulate the outer conductor of a coaxial cable for high frequency transmission. CoTo Technology's RF relays are designed to have broadband impedance as close as possible to 50 ohms.

The high frequency parameters of RF reed relays are not as good as PIN diodes or GaAs switches but the possibility to conduct DC signals and the simplicity of design decided to apply them in the prototype SP16T switch.

### 10.3. Semiconductor microwave switches

Switching microwave devices in microwave frequency range is performed with the use of PIN diodes [1], which for frequencies below 10 MHz perform as typical diode with small impedance in forward polarization and very high impedance in reverse polarization. The most important property of the PIN diode is the fact that it can, under certain circumstances, behave as an almost pure resistance at RF frequencies, with a resistance value that can be varied over a range of approximately  $1\ \Omega$  to  $10\ \text{K}\Omega$  through the use of a DC or low frequency control current. When the control current is varied continuously, the PIN diode is useful for leveling and amplitude modulating an RF signal. When the control current is switched “on” and “off” or in discrete steps, the device is useful for switching, pulse modulating, attenuating, and phase shifting of an RF signal. In addition, the PIN’s small size, weight, high switching speed, and minimized parasitic elements make it ideally suited for use in miniature, broadband RF signal control components. The capacitance of PIN diodes encapsulated in special *beam lead* enclosures can be as small as  $0.02\ \text{pF}$  providing very good isolation.

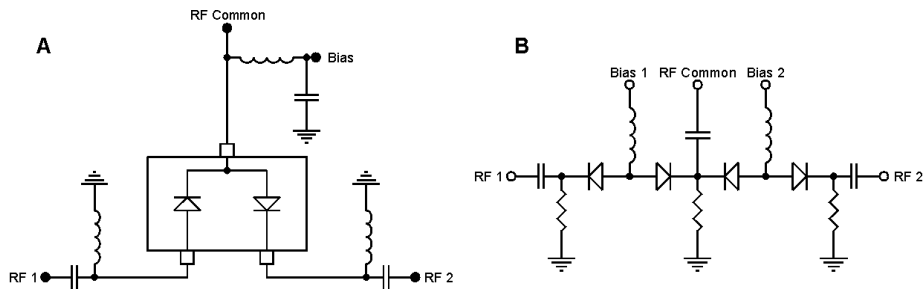


**Fig. 43.** Construction of SPDT switches built on PIN diodes: A – typical connections, B – serial connection of the diodes in a single channel increase isolation of the switch

**Fig. 43** presents connections for SPDT (single-pole-double-throw PIN diode switch). For higher isolation between channels the diodes are connected in series. When the bias voltage in **Fig. 43A** is negative the signal from RF1 passes the switch to the RF Common termination and the reverse polarized PIN diode isolates the signal on RF2, for positive bias the situation is opposite. The diagram in **Fig. 43A** diagram needs only one bias termination while two of them are required in the **Fig. 43B** diagram. Positive polarization of Bias 1 and negative of Bias 2 lets the signal from RF1 pass the switch while RF2 is isolated, and the opposite polarization of bias terminations results in passing RF2 and isolating

RF1. Two PIN diodes in series in each channel are for improving isolation in the case of negative polarization of the selected channel.

Collecting PIN switches to increase the number of switched channels implies the introduction of discontinuities of impedances at the connection point. The “star connection” of PIN diodes, when all except one diode are reverse polarized produces effective capacitance between the common point and the ground, which is the impedance discontinuity of capacitance character resulting in negative reflection.

The commonly available GaAs switches of SPDT type in MMIC technology enables to build more complex switches characterized by a very short switching time (nanoseconds), number of switching cycles is practically unlimited and consume very small power. Additionally they operate in the frequency range from DC, while PIN diode switches have low frequency limit to the value when PIN diode performs like a linear resistor. GaAs FET transistor has non-zero impedance (several ohms) in ON state and this can be a source of significant errors in cases when DC signals are transmitted.

#### 10.4. Materials and methods - prototype switches

##### 10.4.1. SP16T switches

Two switches were designed and constructed. Each of them has four layers “tree” structure presented in **Fig. 44**.

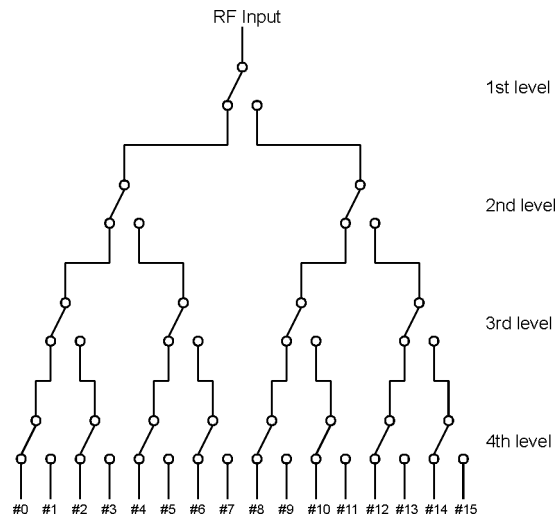


**Fig. 44.** Scheme of connections of the tested prototype SP16T switches

The basic element of one prototype is GaAs MMIC SPDT switch from Stanford Microdevices, type SSW-308 [85] in a small 8-pin surface mounted enclosure. It is used for switching signals in the frequency range from DC to 3 GHz with insertion loss lower than 1.2 dB. The prototype was constructed on double sided epoxy resign PC board of 0.7 mm width connecting the individual elements by 50  $\Omega$  strip lines.

The other prototype was constructed using RF reed relays [16] characterized by insertion loss of 0.3 dB at the frequency 0.5 GHz. It is suited for installation on 50  $\Omega$  transmission lines. The switch was mounted on 1.6 mm width epoxy resign PC board using strip lines of appropriate width of 50  $\Omega$ .

The testing measurements were done with the sampling oscilloscope HP54121T equipped with 20 GHz sampling head and a needle pulse generator of proprietary construction, which produces a needle pulse of 200 ps rise and fall times. The two-rods TDR probe (10 cm length rods, 1.5 mm in diameter and 15 mm distance between the rods) was applied for tests in the soil.

#### 10.4.2. SP8T fully integrated switch

The basic element of the prototype microwave switch is the integrated circuit HMC253QS24 from Hittite Microwave Corporation [42]. It is supplied from a single +5V voltage, has an built-in decoder controlled from standard TTL signals to chose one from eight available channels. It is sold in a cheap and surface mount package (QSOP type). The operation of the circuit is guaranteed in the frequency range 0-2.5 GHz. The basic parameters of the integrated circuit HMC253QS24, *ie* insertion loss of the selected channel and isolation are presented in **Fig. 45**.

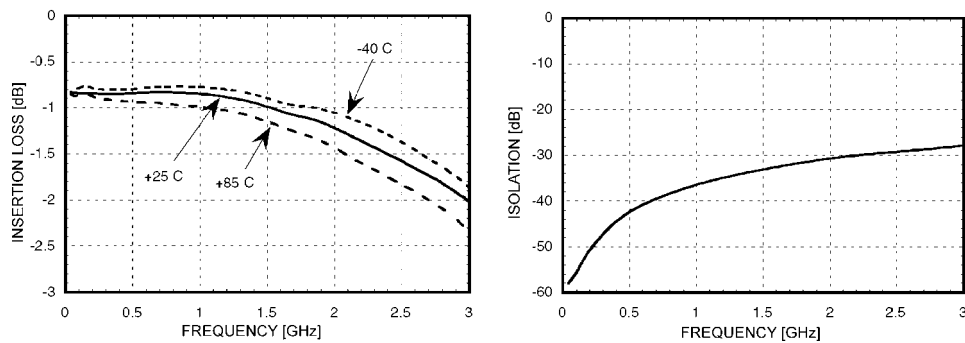


**Fig. 45.** Insertion loss and isolation between channels related to frequency for the MMIC device HMC253QS24 implemented in the prototype TDR switch

The significant aspect of the prototype switch is the topology of the PC board applied and the connectors for connecting TDR probes and a needle pulse from the generator similar to the one described by Malicki and Skierucha [59]. So as to minimize the impedance discontinuities along the way of the high frequency signal propagation from the generator to the probes, the strip lines of the PC board had  $50\ \Omega$  impedance. The picture displaying the both sides of the PCB board with the applied integrated circuit and radio frequency connectors of SMA type is presented in **Fig. 46**.

This value was equal to the impedance of the coaxial cables to the TDR probes and the generator. Also the precise SMA connectors were used. The PC board was prepared on three layer FR4 laminate, where the middle layer was connected to the system ground. The middle layer was used so as to decrease the  $50\ \Omega$  strip line width and to make the PC board mechanically resistant.

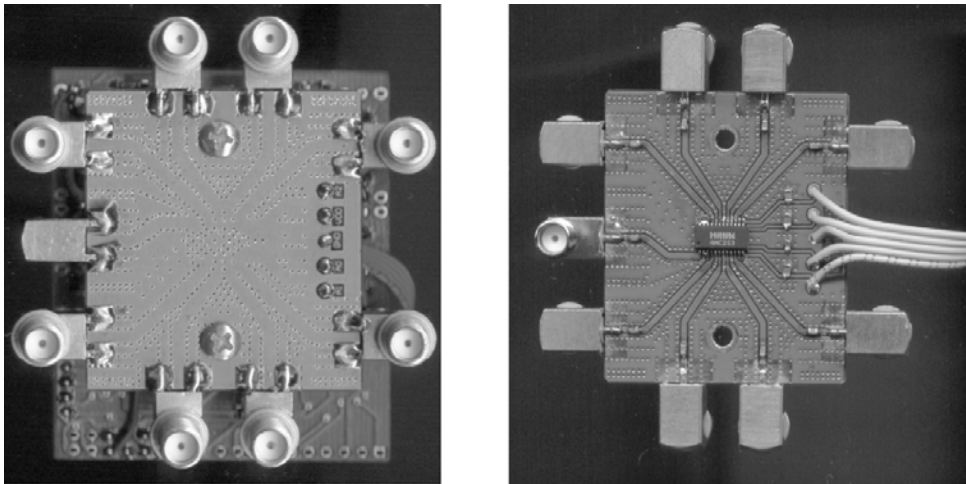


**Fig. 46.** Prototype one-to-eight microwave switch for the application in TDR soil water content meter

### 10.5. Performance of the developed RF switches in TDR applications

**Fig. 47** presents the comparison of the signals at the input and output of the prototype SP16T switches. The GaAs switch attenuates the input about 2.9 dB and the reed-relay switch – 3.3 dB.

These values are in agreement with the catalogue data, taking into account that the total signal attenuation of the ST16T switch is equal to the sum of attenuations (in decibels) from each of four levels shown in **Fig. 44**. The switches degrade the frequency response of the input signal According to Eq. (83) the

upper frequency limit 1.75 GHz decreased to 1.4 GHz and 1.5 GHz after passing the reed-relay and GaAs switches, respectively.

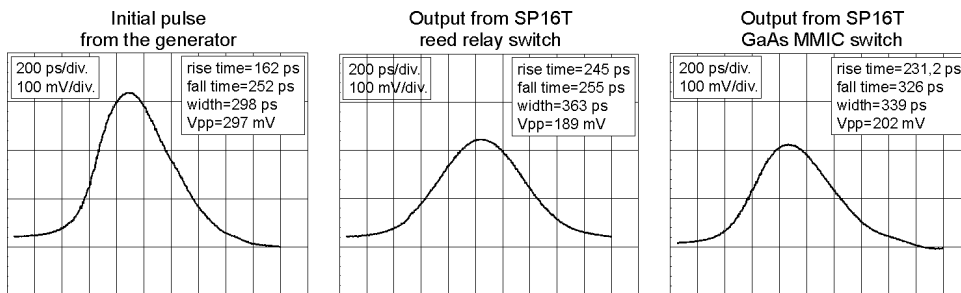


**Fig. 47.** Input pulse and output pulses from the tested SP16T switches

The comparison of reflectograms showing the reflections of the initial pulse from TDR probe in the soil, in the cases then there was no and with the switches connected, are presented in **Fig. 48**.

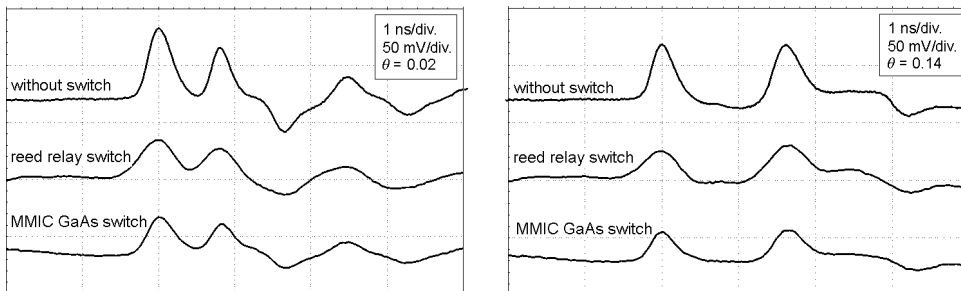


**Fig. 48.** The reflected signal attenuation introduced by the prototype reed relay and MMIC GaAs switches when the TDR probe was inserted into dry (left picture) and wet (right picture) sand

The reflections are more sharp and higher amplitude when there is no switch along the signal propagation path. The upper limit of the frequency range is lower for the reed relay switch because the reflected signals are less sharp than in the MMIC GaAs switch. However in both cases the reflections from the TDR probes are easily distinguishable even in dry sand.

It should be stressed that before the reflected signal produced by the generator is sampled, it must travel through the switch two times, towards the TDR probe and back to the sampling head. Therefore in the case of materials that attenuate the TDR signal (saline soils) the reflection from the TDR probe end will not be

visible for lower values of soil electrical conductivity than in the case without the switch. In practice the arable soil electrical conductivity does not exceed 4 dS/m and is not high enough to attenuate the TDR signal completely even in the presence of the tested switches.

The electrical connections between the electrical components of the switches should have electrical impedances equal to  $50 \Omega$ . Each element encountered along the TDR signal path propagation introduces impedance discontinuities responsible for secondary reflections that degrade the upper frequency limit and attenuate the signal. When the time window of the sampling head is located at the place of secondary reflections, they introduce additional measurement errors in phase and amplitude measurements. The signal reflected from the tested SP16T switches are presented in **Fig. 49**.

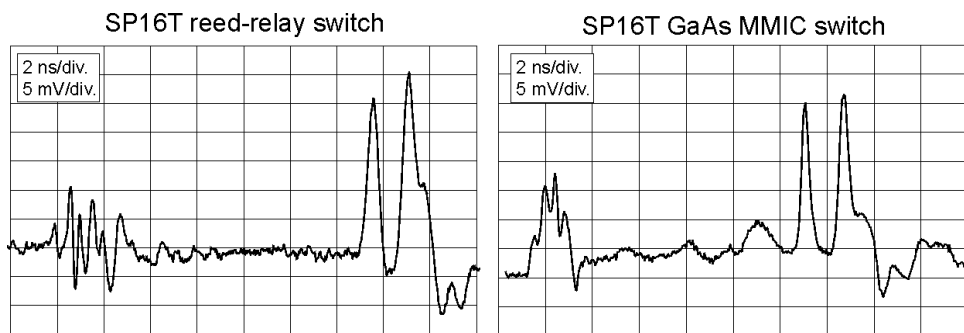


**Fig. 49.** Reflections observed from the tested SP16T switches and TDR probe in wet sand

The signal distortion at the beginning of the reflectograms represent the reflection from the switches, while the reflections from the TDR probe in wet sand are at the right side of **Fig. 49**. The maximal amplitude of reflected signal (17 mV) is for MMIC GaAs switch and it has inductive character with the increase of characteristic impedance after passing the switch.

The reflectograms showing reflections of the needle pulse electromagnetic wave from the rods of TDR probe are presented in **Fig. 50**. In the left column there are ones when the probe was connected directly to the TDR meter, in the right column the reflectograms were taken when the needle pulse propagated through the selected channel of the prototype switch.

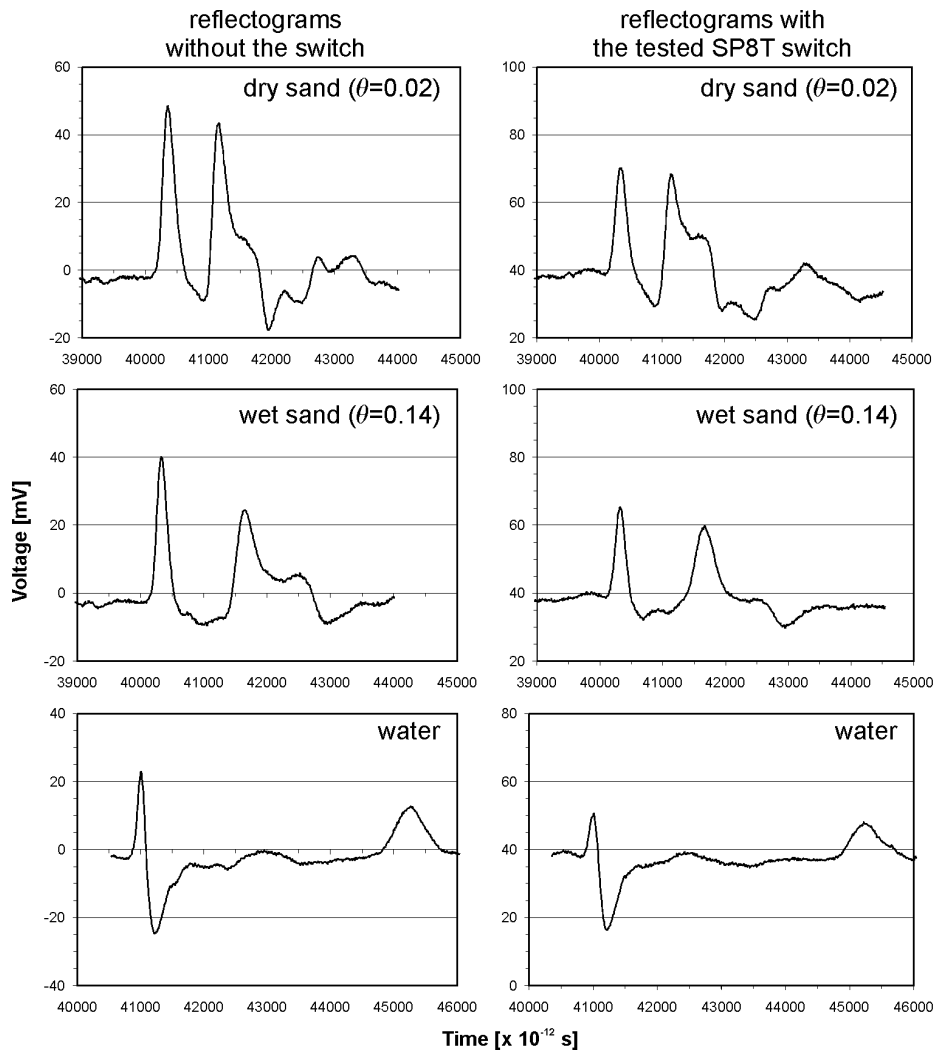


**Fig. 50.** Reflectograms presenting reflections of the needle pulse from the TDR probe rods with the application of the prototype MMIC switch (right column) and without it (left column). Left axis represents voltage in mV,  $\theta$  is the water content of the measured soil samples

The amplitude loss of the signal introduced by the prototype switch is about 3.5 dB, which corresponds to the values presented in Fig. 1. It should be noted that insertion loss in Fig. 1 refers to the one-way propagation through the switch.

In the TDR method the signal propagates through the switch twice (to the probe and back to the generator) and therefore it is attenuated two times.

The implemented prototype switch does not introduce the decrease of frequency band, which would be distinguished from the increase of rise and fall times of the pulses.

#### **10.6. Summary**

The tested prototype RF SP16T switch has frequency parameters good enough for application in reflectometric soil water content meters. However the attenuation of the signals caused by their insertion loss and energy loss caused by the discontinuity of impedances introduced by them in the  $50\ \Omega$  transmission lines may produce measurement errors. It seems that the connection of “tree” and “star” topologies would give better results.

The presented RF MMIC prototype SP8T switch is integrated in one small enclosure, which introduces smaller insertion loss. Return loss caused by discontinuity of impedances can be easier solved by careful design of the strip lines of the mounting PC board. As compared to the other switches used in the reflectometric technique they have lower power consumption and contain built-in convenient decoder for control signals. The integrated construction with eight channels available additionally increases the competitiveness of the applied microwave MMIC switch.

## 11. TDR SOIL WATER CONTENT, SALINITY AND TEMPERATURE MONITORING SYSTEM – DESCRIPTION OF THE PROTOTYPE

Selective measurements, without destructive interference to the measurement process and measured medium from unpredictable reasons are easy for interpretation but practically hard to accomplish. The unwanted sources of error when identified can be eliminated by application of a physically good model of the observed process or by empirical correction based on reference measurements. A lot of measurement errors happen during the wire-transmission of an analog signal from the sensor equipped by an appropriate transducer, converting the usually non-electrical signal to its electrical representation, to the measuring unit. To avoid wire-transmission errors modern measurement systems combine the measuring unit with the sensor-transducer element in the form of a smart transducer or smart sensor. Smart sensors are equipped with microcontrollers or digital signal processors capable to convert the measured signal to the digital form, performing individual calibrations and necessary corrections. Thus most of the data processing is completed at the sensor and the command and data communication with it usually performed in wireless way.

The main reasons for the development of automatic measurements systems are: the requirement objective readouts, without the unwanted interference from error sources including the influence of an experiment operator and economical reasons. The integral part of such a system is a data logger for autonomic data collection and storing. The recent development of telecommunication and associated electronics gives the new tools and means for the idea of automatic measurement of environmental physical and chemical properties, especially low power converters of non-electrical signals to easy for processing electrical signal, powerful microcontrollers integrated with analog-to-digital and digital-to-analog converters, timers, digital interfaces and abundant non-volatile memory.

The presented study shows the potential of the MIDL (Multi Interface Data Logger) data logger (**Fig. 51**), its functional features and the function in the automatic measurement system of physical and chemical parameters of soil and ground. The system has been developed in the Institute of Agrophysics in Lublin, Poland, as the direct answer for the need to collect data from ion-selective electrodes that measure the concentration of selected ions in the soil (Research Project 2 P04G 032 26 financed by the State Committee for Scientific Research). Also, the measurement devices developed, produced by the Institute of Agrophysics and used by a number of scientific soil laboratories [29] need a modern and hardware as well as software compatible data logger. The detailed

description of functional and technical parameters of this system as well as the details of start procedures is presented in respective manuals [66,67,68].

The MIDL – Multi Interface Data Logger follows up-to-date trends of electronics and informatics offering the users many features superior to the ones that have the old D-LOG data logger (see 12.3 in this monograph).



**Fig. 51.** Multi Interface Data Logger (in the middle between TDR soil water content, salinity and temperature meters) in the configuration for the measurement of 16 TDR FP/mts probes

It has been assumed that the MIDL data logger should provide:

- Ethernet 10Base-T Internet communication features,
- radio communication in the non-licensed 433MHz frequency band [74],
- supply by an external power source 6-12VDC,
- limited power consumption below 2W in the continuous work mode,
- communication interfaces for monitoring and configuration the device by means of a PC compatible computer, ie serial RS232C and infrared (IRDA) wireless digital data transmission,
- serial RS232C and RS485 work interfaces for connecting measurement devices,
- 4-bit output parallel port in TTL standard (to be compatible with the old measurement devices developed in the Institute of Agrophysics),
- user accessible universal connector for MMC (MultiMedia Card) memory card with the capacity up to 128MB memory,

- internal temperature sensor and real time clock,
- limited power consumption in the standard in the standard work mode, ie the energy used from 12VDC power source during 90 days should not exceed 2Ah, when the total script execution time is 3.6hours (including 0.33hours of RS232C or RS485 operation), the total radio communication – 7hours, the total time of the device in the watch mode (with the radio access periods of minimum 2seconds) – 2000 hours.
- temperature range of work –25°C to 85°C.

The picture with the prototype MIDL data logger system controlling two TDR meters, each with a multiplexer for connecting up to 8 TDR FP/mts probe in presented in **Fig. 51**.

### 11.1. Functional description

MIDL data logger consists of two functional versions, *ie* MASTER and SLAVE. The both versions are built on the base of the same hardware; SLAVE uses the whole hardware features while MASTER only the part of it. The functional features are distinguished by software automatically identifying the version.

MIDL can operate in various modes and **Fig. 52** presents the most complex mode where the system consists of a number of MASTER devices controlled by via Internet by PC compatible computers.

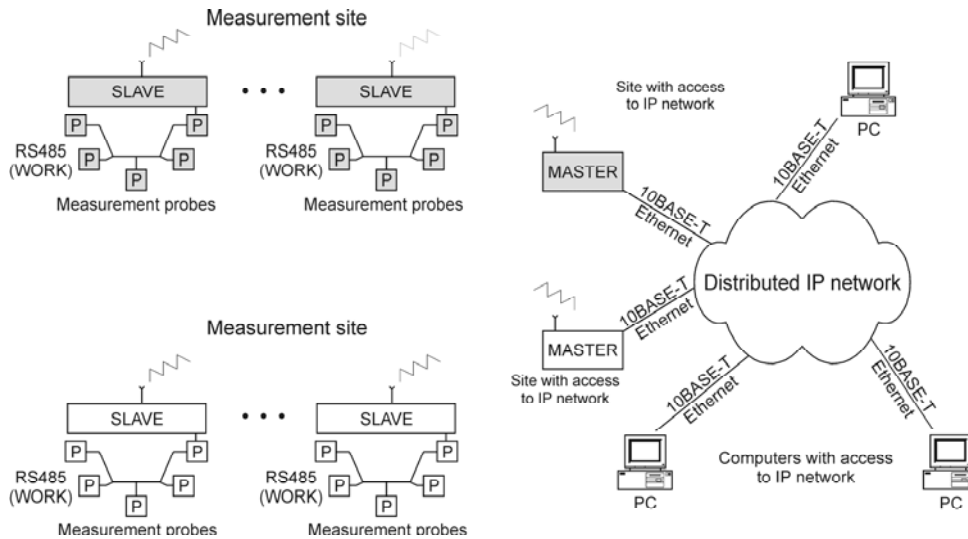


**Fig. 52.** Example setup of devices for soil and ground physico-chemical parameter monitoring system using wireless communication

MASTER modules are wireless transceivers (receivers and transmitters) of signals from Internet to radio signals between PC and the addressed SLAVE module. The wireless radio link works according to the accepted assumptions in the non-licensed frequency band of 433 MHz (Skierucha *et al.* [83], Wilczek *et al.* [104]). The SLAVE modules together with the connected measurement devices (by means of the serial interface RS485) are complete data acquisition systems. Each of them contains all the elements necessary to control the measurement process by the connected probes, store the collected data and communicate with the MASTER device to transmit the whole or a part of the storage memory to the PC, *ie* a separate supply source, microcontroller, real time clock and abundant (up to 128 MB) nonvolatile memory.

The access to MASTER and SLAVE devices is possible from any place accessible by the IP network and in case of Internet network – from any place in the world. The devices are protected by unique Internet addresses and access passwords. The range of the applied radio link is limited to about 500 meters in the case when there are no physical obstacles between the transmitting and receiving antennas. The applied radio link is built from commercially available, completely assembled and tested electronic modules [15]. During transmission and reception they consume small power (about 100 mW), they can be completely disconnected for a defined period to save power and quickly connected again. The communication speed is 9600 bits per second, and in case of large file transmission, *ie* above 1MB, is not economical due to limited energy in the supply battery. Another considered solution is to provide each SLAVE module with GPRS modem that enables much more fast connection with the Internet network. The basic drawback to apply GPRS modems is that they consume much more power than the presently applied 433 MHz modules. However it is possible to program the transmitting and receiving modems for short-time work, *ex* 10 minutes during 24 hours, to transmit the collected data to the base station (PC computer). Such a solution would guarantee large amount of data transmission and battery saving, which is a fundamental assumption of the presented data logger system. The described service of “wireless Internet” is presently provided by majority of mobile telecommunication providers.

Another example mode of operation of the MIDL system is the direct connection of the SLAVE modules to the cable Internet network, for example to perform measurements in a laboratory (**Fig. 53**). The access to the defined SLAVE module is possible from any computer connected with the Internet network and the software embedded in the SLAVE eliminates the conflicts that may occur by simultaneous access from many computers.

The simplest operation mode of the MIDL system is an autonomic mode. It consists in storing the experiment details (probes selection sequence, time

distance between the measurements, format of data storage) in the MMC memory card by means of MMC read/write interface connected to PC computer, using script commands (the list of script commands is presented in the part 11.7).

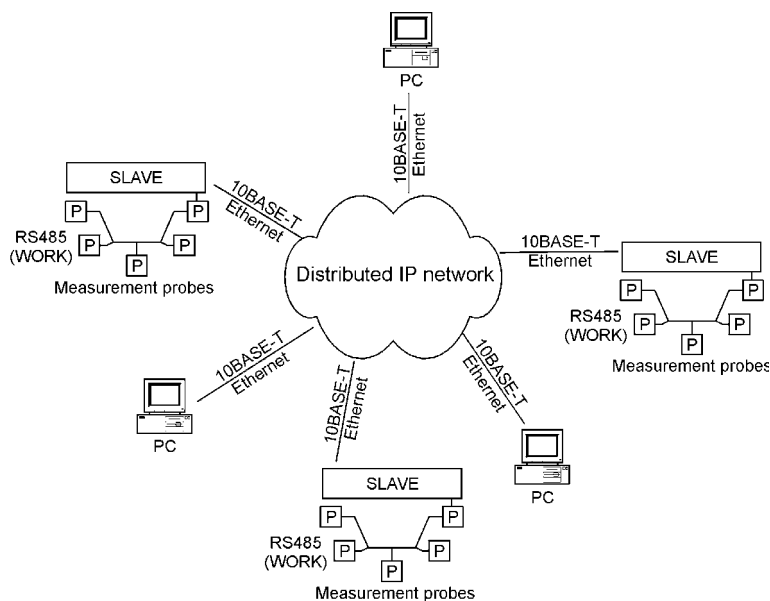


**Fig. 53.** Direct connection of SLAVE modules to Internet network

The access to the data is accomplished by the replacement of the MMC memory card filled with the collected data with an empty card. Due to large amount of memory available in MMC memory card its replacement is rare. The advantage of this mode of operation is small power consumption of the data logger.

## 11.2. SLAVE module

The basic version of MIDL data logger is SLAVE. Its simplified diagram is presented in **Fig. 54**.

The central element of the device is Control Unit. It is responsible for the supply distribution and coordination of the work of the remaining units on the base of the sequence of events written in the script file. For example when the Control Unit finds the command to set the device into the sleep mode, it disconnects supply to each module introducing the device into low power mode of work (about 100 mA) when no sensor is activated. After the defined period of

time the Real Time Clock module wakes-up the device, the Script Execution Interpreter reads the following commands, interprets them and executes sending commands to the work interface RS232C or RS485, setting the TTL outputs, reading the sensor data or storing the data into the MMC memory.

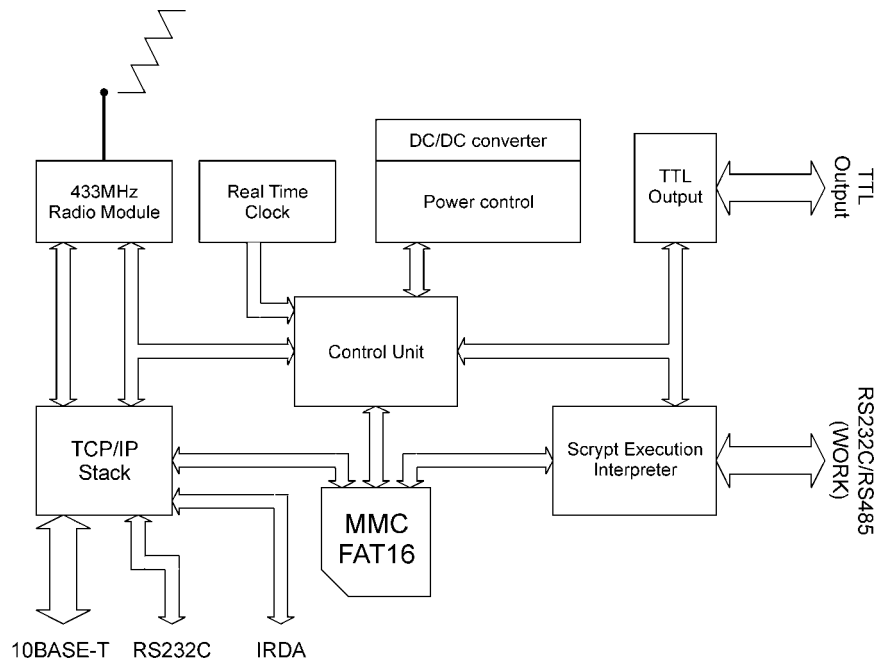


**Fig. 54.** Simplified functional diagram of the MIDL setup in SLAVE configuration

The access to data and to all configuration parameters of the device inscribed in the MMC memory card is possible by the 433 MHz radio link, RS232C serial and 10BaseT-Ethernet interfaces. All of them operates using IP protocol and the configuration of the device and the data access is the same for each interface.

The 433 MHz radio link enables a remote access to each SLAVE from the MASTER device. The operator activated the remaining interfaces directly at the device (*ex* by means of a notebook) after pushing the dedicated switch.

The characteristic features of the SLAVE device:

- cyclic execution of commands from the script file to control measurement from external probes,
- connection with the measuring probes by means of RS232C or RS485 interfaces,

- configuration, monitoring and readout of stored data by RS232C, 10BaseT-Ethernet and 433 MHz radio interfaces,
- the device management by means of TCP/IP network protocols,
- connection to the device by any FTP client and WWW browser,
- MMC memory handling using FAT16 file system (this means that MMC cards can be read directly by a PC compatible computer equipped with the MMC cars reader),
- the device works with minimal power consumptions for supply battery savings.

### 11.3. MASTER module

MASTER version of MIDL data logger is presented in **Fig. 55**.

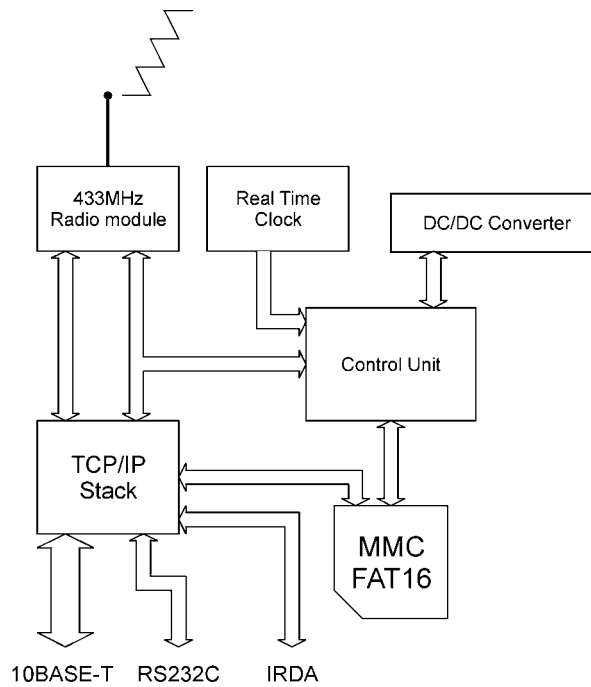


**Fig. 55.** Simplified functional diagram of the MIDL setup in MASTER configuration

MASTER serves as a bridge between the 10BaseT-Ethernet interface and the 433MHz radio link. It is a mediator in the data and commands transfer between SLAVE devices communicating with the MASTER by radio and the base station (PC computer usually located in laboratory and performing data processing). The



All test communicates must be positive for the correct operation of the MIDL data logger. The window contains also network configuration parameters that are necessary to know for establishing connection with the system.

### 11.5. Configuration of basic parameters of the MIDL system

The correct operation of the system needs initial configuration of the Internet link. The configuration parameters are included in a system file "server.ini" located on the MMC memory card. This file may be placed in the MIDL data logger in three ways:

- writing on the MMC card by means of an universal read/write device dedicated for MMC memory cards, connected to a PC computer, inserting the card into the slot in the MIDL device (MASTER or SLAVE) and switching on the power supply,
- accessing the cart in the device slot by WWW site,
- accessing the cart by means of FTP protocol to send the "server.ini" file by Internet.

Before accessing the card by WWW browser or FTP client the device must be connected to the computer by means of IP network.

### 11.6. System files

There is a number of file types in the MMC memory card. From a WWW site it is possible to access script files ("\*.scr" file extension) and output data files ("\*.txt" file extension). All files on the MMC memory card are accessible by FTP client or by reading the card in the universal card reader read/write device:

- files with „\*.htm”, „\*.css”, „\*.js” extensions – files of graphical user interface used by a WWW browser,
- files with „\*.scr” extensions – device executable script files,
- files with “\*.txt” extension - output data files generated by executable scripts,
- files with “\*.ini” – system files with the device configuration parameters.

The format and command of the executable script files are presented below.

### 11.7. Executable script files

Files with „\*.scr” extension treated by the device as executable script files.

**Table 17** below presents an example script file with commands that: fix the SLAVE RS232C serial port transmission speed to 9600 baud, give a name to the output data file where the data from the addressed sensor will be stored, send a command to the serial RS485 interface with the address activating the individual

sensor, format the data received from the sensor and setting the SLAVE device into the sleep mode for a given period of time. The beginning of the script is marked by [beg] and the end by [end] directives.

**Table 17.** An example of the executable script file with the sequence of commands controlling the MIDL data logger

---

```
[beg]
port(9600)
filename("RS485t.txt")
outp(RS485,"Command sent to the work interface RS485 \n\r")
fprintf("Result of the measurement received by RS485: ")
inp(RS485,14,4000)
sleep(120)
[end]
```

---

When the defined period of time, when the device is in the sleep mode, terminates, the script file executes from the beginning.

The script commands for autonomic, cyclic control measurements by the SLAVE device are presented in **Table 18**.

Each sensor connected to the SLAVE module should “understand” the script commands. This requires that each sensor is provided with an appropriate hardware and software interface. Therefore the term “sensor” means a device converting the analysed signal (*ex* temperature, pressure, electrical conductivity, etc.) into the corresponding electrical signal.

**Table 18.** Script file commands for MIDL data logger control

Command	Description
<code>port(baudrate, databits, stopbits, paritychecking);</code>	Setting parameters of the serial port
<code>outp(port, "data");</code>	Sending data by the working interface
<code>inp(port, length, wait);</code>	Receiving data from the working interface
<code>filename("name");</code>	Setting the file name where the data received from working interfaces will be stored
<code>sleep(sec);</code>	Bringing the MIDL into the sleep mode for defined number of seconds
<code>fprintf("format");</code>	Introduction of additional formatted data into the output file

Such a sensor integrated with a decision-making element, computation and communication facilities forms a smart sensor (Skierucha *et al.* [83], Wiczer [103]. Smart sensors must be also identified and have means for storing individual calibration data.

The presented data logger system for collecting physical and chemical parameters of soil environment represents modern trends in the development of measurement systems that is manifested by low power consumption, high capacity of storage memory and possibility to control the measurement process from any place in the world using Internet connection or application of wireless radio connection in the case when the access to the monitored object is limited. Traditional sensors and measurement devices, such as soil thermometers, reflectometric soil water content meters, soil tensiometers for water potential measurement, rain-gauges and others may be easily equipped with not expensive, intelligent communication interfaces enabling identification, addressing as well as hardware and software compatibility with the presented MIDL data logger. The system was designed in modular way for future modifications following the progress in the metrology of non-electrical quantities and the general technological development.

## 12. SOIL WATER STATUS MONITORING DEVICES

The Institute of Agrophysics introduces field and laboratory meters for the determination of:

- water content by means of Time-Domain Reflectometry (TDR) method,
- salinity (bulk electrical conductivity) of soils by means of TDR,
- temperature of the soil,
- soil water capillary pressure (suction force).

There are three types of meters available:

- Field Operated Meter (FOM),
- field operated Data LOGger (D-LOG) and
- Laboratory Operated Meter (LOM).

Also adequate kinds of probes are offered:

- Field Probe (FP) and
- Laboratory Probe (LP) respectively.

FOM is a portable, battery operated, microprocessor-controlled device designed for *in situ* field measurements of soil water content, temperature and salinity. It is particularly suitable for periodic measurements at random and/or fixed locations, where water content, temperature and salinity distribution is to be determined by readings taken at various levels of the soil profile. FOM provides a Mineral/Organic option switch for soils originated from mineral or organic parent material, thus no user calibration is needed to read the soil water content directly.

FP is a probe for momentary or for semi-permanent installation. Through a pre-augered pilot hole it can reach any depth down to 4 m without destroying either the soil structure or disturbing heat and mass transport in the soil. It can be left then intact for as long period of time as needed.

A single, mobile probe may also be used for momentary measurements in shallow layers of the soil profile by walking over the field and inserting the probe in chosen sites.

For semi-permanent installation, when deeper layers are to be monitored, several FPs can be inserted from the soil surface or horizontally through a sidewall of a soil pit. A probe installed once may be left intact in the soil for as long as necessary and then drawn out at the end of the experiment.

FOM and FP from the Institute of Agrophysics are offered in two versions:

- FOM/m, field operated meter for soil water content measurements,
- FOM/mts, field operated meter for simultaneous measurements of the soil water content, temperature and salinity (bulk electrical conductivity). FOM/m is equipped with a 3.5 digit LCD, whereas

FOM/mts is provided with a 256 by 64 dot matrix graphic LCD to display data and TDR trace simultaneously. Also adequate probes are offered:

- FP/m, field probe for measurements of soil water content,
- FP/mts, field probe for simultaneous measurements of soil water content, temperature and salinity.

LOM is an IBM PC compatible aided device working under control of special software. It has been designated mainly to control long term laboratory experiments which require monitoring of water, salt and heat transport by means of periodic recording of instantaneous soil water content, capillary tension, temperature and electrical conductivity profiles in chosen time intervals. To read water content a factory installed conversion equation for mineral or organic soils can be chosen and/or user determined calibration functions could be applied as well.

To switch between probes LOM is provided with a Single-Pole-f-Throw multiplexer (SPfT, where  $2 \leq f \leq 15$ ) for first level multiplexing and a special port to control second level multiplexers. Up to 15 of SPsT second level multiplexers can be incorporated, where  $2 \leq s \leq 8$ . This makes it possible to scan up to 120 LP/ms, 120 LP/t and 120 LP/p probes.

LOM works with the following probes:

- LP/ms, Laboratory miniProbe for recording instantaneous profiles of water content and salinity in soil columns or in undisturbed soil cores,
- UP/ms, User-made Probe for water content and salinity,
- LP/p, Laboratory Probe (minitensiometer) for measurements of soil water capillary pressure (suction force, matrix potential),
- LP/t, Laboratory Probe for temperature measurement.

Several LP-probes of a selected kind or of all types can be inserted through the wall of a soil column or a steel sampling cylinder, thus allowing vertical scanning of the instantaneous water content, capillary tension (matrix potential, suction force), temperature and electrical conductivity profiles. This makes it possible to collect a set of corresponding water content, water potential, electrical conductivity and temperature data from drying or wetting front transition, from which, after further processing, one can obtain a complete set of the unsaturated water flow characteristics of the soil *ie* water retention (PF) curve, unsaturated water conductivity (k-function), differential water capacity and unsaturated water diffusivity as well as the solute transport data. Also heat transport coefficients (as the thermal conductivity, thermal diffusivity, specific heat) can be determined if a heat flux meter is installed in the experimental column.

D-LOG/mpts is a moisture/pressure/temperature/salinity datalogger for field application that is able to switch between up to 120 probes type of FP/mts (or FP/m).

The above-mentioned TDR-based devices are worldwide patented and produced in the Institute of Agrophysics, Polish Ac. of Sciences in Lublin.

### 12.1. FOM/mts - Field Operated Meter for determination of moisture, temperature and salinity of soils

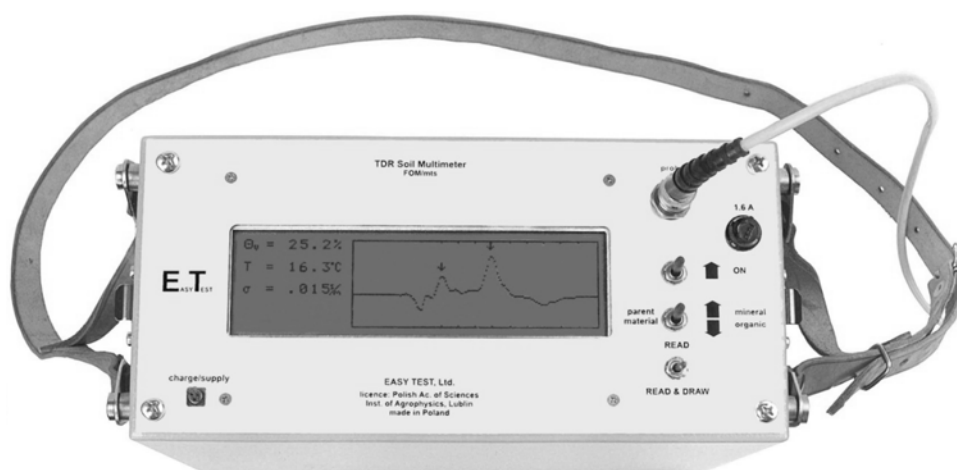


**Fig. 57.** Portable TDR meter, FOM/mts, for the measurement of soil water content using TDR technique as well as soil apparent electrical conductivity and temperature

FOM/mts (**Fig. 57**) is a TDR (Time-Domain Reflectometry) based, portable, battery operated, microprocessor-controlled device designed for *in situ* field measurements of soil water content, temperature and salinity (bulk electrical conductivity) from the same probe. It is designated for periodic measurements at random and/or fixed locations where water content, salinity and temperature distribution is to be determined by readings taken at various levels of the soil profile. It utilizes the FP/mts-type probe. FOM/mts is equipped with a 256 by 64 dot matrix graphic LCD to display data and TDR trace simultaneously. The TDR trace is a voltage-versus-time record of the voltage pulse round-trip along the probe. It is helpful to check the probe status during (break, short) and after its installation (excessive attenuation of the pulse). FOM/mts provides a Mineral/Organic option switch for soils originated from mineral or organic parent

material, thus no user calibration is needed to read the soil water content directly. Also FOM/mts-RS equipped with the RS232C serial port is offered. This makes it possible to operate the meter under control of any IBM compatible PC.

- Features:of FOM/mts
- Pulse: sin -like needle pulse having 200 ps rise-time :
- Range of readings:
  - volumetric water content: 0 ÷ 100 %
  - temperature: -20 ÷ +50 °C
  - electrical conductivity: 0.000 ÷ 1 S/m
- Accuracy:
  - water content absolute error: displayed water content ±2 %
  - temperature absolute error: ±0.8 °C or less if read from individually calibrated probe
  - el. conductivity relative error: ±10 % for 0 ÷ 1 S/m or less if read from individually calibrated probe
- Resolution of readings:
- volumetric water content: 0.1 %
- temperature: 0.1 °C
- el. conductivity: 0.001 S/m
- Time of test: less than 20 s
- Display: 256 x 64 dot matrix LCD
- Ambient temperature: 0 ÷ +50 °C
- Dimensions: 26 x18 x 13 cm
- Weight: 3.75 kg with battery
- Capacity: 150 readings in continuous mode
- Supply unit: 12 V, 2200 mAh maintenance-free lead-acid rechargeable battery
- Battery charger: automatic, overcharge-safe, wall charger
- Maintenance: The meter is not user serviceable. No special maintenance means are required. If the apparatus is to be stored, recharge the battery each three - four months. Temperature of storage: -10 ÷ +50°C.

## 12.2. New prototype version of FOM/mts soil water content, salinity and temperature measurements

The device presented in **Fig. 58** is the new generation of TDR soil water content, salinity and temperature meter constructed in the Institute of Agrophysics.

For compatibility reasons it uses the same probes as the ones developed some years ago and used in many research laboratories all over the world [29]. The meter has memory capable to store about 1000 data points that can be labelled for identification. The operation of the meter is by a five-pushbutton keypad that controls the display by means of user-friendly software. A small lithium-polymer rechargeable battery commonly used in mobile telephones supplies the device. It can be optionally equipped with the Global Positioning System (GPS) for giving longitude and latitude coordinates of the meter for localization. This feature is fundamental in application in precision agriculture



**Fig. 58.** Prototype of a handheld soil water content, salinity and temperature meter constructed with the application of modern components

New version has the following features:

- accuracy and resolution not worse than FOM/mts from Easy Test,light handheld enclosure,
- ability to register and store up to 1000 labelled readings,
- real time clock,
- operates with Easy Test TDR probes with different cable lengths (from 1.5 to 9.5 m),
- keyboard and LCD display (160x128 dots) with user friendly operating software,
- optionally equipped with GPS module for localization,
- connection by USB interface with PC compatible computer for data transfer,
- lithium-polymer (without memory effect enabling charging at any time) battery supply.

### 12.3. TDR Data LOGger for soil water content, temperature and salinity measurements



**Fig. 59.** An example of the D-LOG/10/mts-controlled stand incorporating six D-MUX/10/mts 2-nd level multiplexers. Maximum amount of the controlled FP/mts (or FP/m) probes is 60. For clarity only a single D-MUX was linked with the D-LOG and a single probe was connected to each D-MUX when taking the picture

D-LOG/mts (**Fig. 59**) is a TDR (Time-Domain Reflectometry) technology based, computer aided instrument, designed for periodic recording of instantaneous profiles of soil water content, temperature and salinity (bulk electrical conductivity) in chosen time intervals. It is suitable for long-term lysimeter-based investigations and also for field experiments, when monitoring of water, solute and heat transport is required.

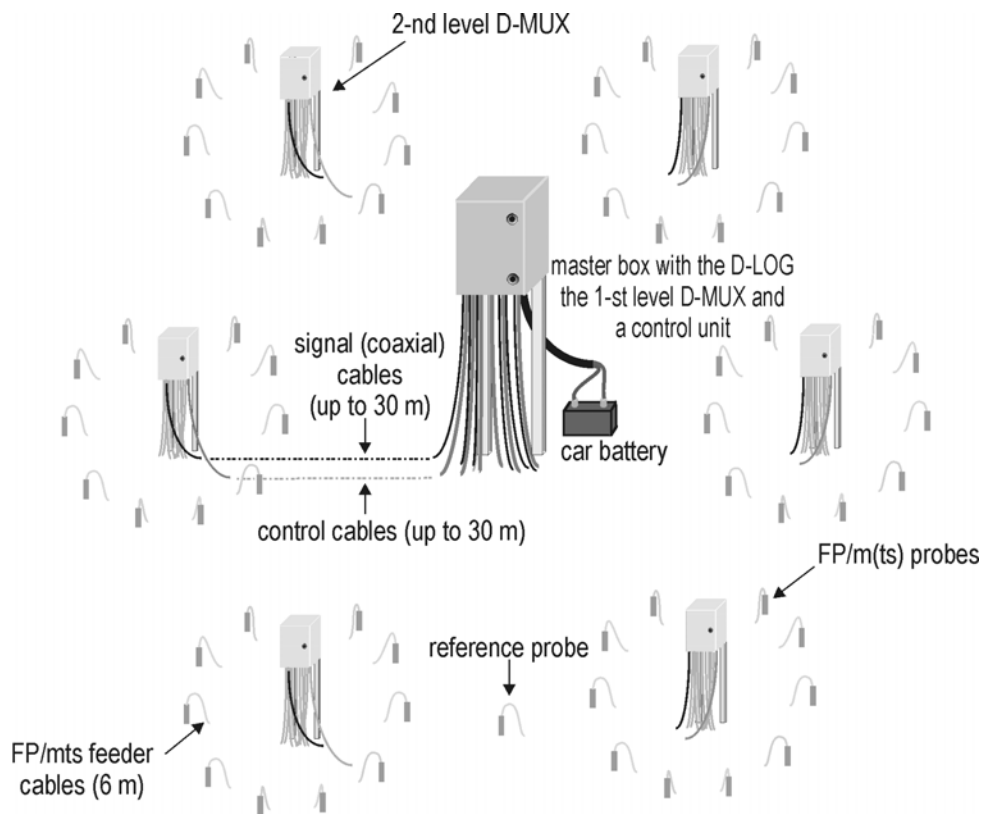


**Fig. 60.** Example of an arrangement of the D-LOG/mts system able to scan 60 FP/m(ts) probes. All cables are laid about 30 cm beneath the soil surface to protect them against static electricity, UV radiation and rodents as well. FP/mts feeder cables (6 m)

The example of an arrangement of the D-LOG/mts system able to scan 60 FP/m(ts) probes is presented in **Fig. 60**.

D-LOG is equipped with a built-in local computer having an RS232C serial port. It serves for:

- controlling pulse circuitry action

- recording voltage-versus-time traces
- calculating pulse attenuation and velocity of propagation
- calculating the soil dielectric constant, water content and electrical conductivity
- communicating with a master PC via the RS232C serial port

D-LOG uses probes type of FP/mts for water content, temperature and bulk electrical conductivity. Also FP/m probes can be applied if only water content is of concern. To calculate water content a factory-installed conversion equation can be used and/or a user-determined calibration function can be applied as well.

To switch between FP/mts or FP/m probes D-LOG is provided with an inherent 1-st level switch and optional amount of standing alone 2-nd level switches (D-MUX/n/...), as shown in figures. Each 2-nd level switch contains a water content, temperature and salinity control circuitry and also a single-pole-n-throw microwave switch, where  $2 < n < 16$ .

To protect against rainfall the D-LOG as well as D-MUXes are kept in metal, rain-proof enclosure.

**Hardware requirements (minimum):** IBM compatible PC equipped with:

- single disk station, minimum 360 KB,
- RS232C serial port configured as COM1,
- VGA card,
- real time clock.

**Software requirements:**

- MS DOS vers. 5 or newer. For older version of DOS there is also a text editor needed

The resolution and accuracy of the measurement of soil water content, electrical conductivity and temperature are the same as for FOM/mts. Time of test for water content, temperature, salinity integrated reading – 35 s, only for water content reading – 25 s.

D-LOG can switch between the maximum number of 15 D-MUX, each of the can switch up to 8 TDR probes. The whole system can work at ambient temperature range from 0 °C to 40 °C and it is supplied by a car battery. For power saving it can be introduced into a sleep mode with low power consumption of 3 mA, and after wake-up it consumes 600 mA in a run mode. The control unit of the system is a palmtop computer equipped with 15 MB flash memory card for data storage.

#### 12.4. FP/m, FP/mts - Field Probe for soil moisture, temperature and salinity measurement

FP is a Time-Domain Reflectometry (TDR) probe for momentary or semi-permanent installation (Fig. 61).



Fig. 61. FP/m, FP/mts - Field Probe for water content, temperature and salinity of soil developed in the IAPAS, Lublin

Thin-wall PVC body of the probe provides ultimate low heat conductivity, thus allowing avoiding the parasite "thermal bridge" effects on distribution of soil water content in the probe's sensor vicinity.

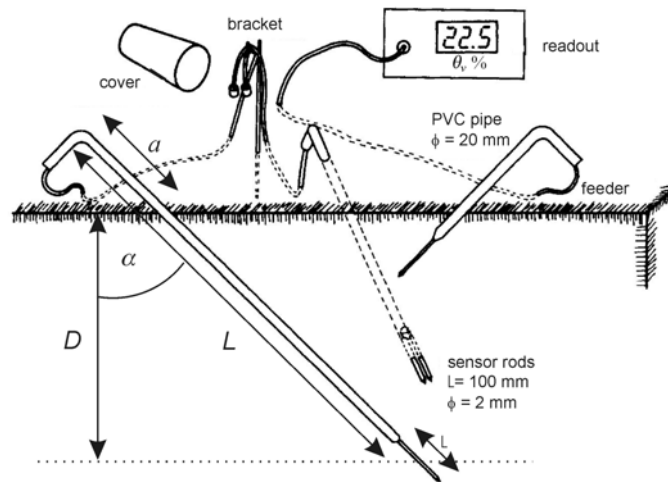


Fig. 62. The principle of installation of the FP-type probes. In order to minimize disturbances in the soil structure the probes are inserted into the soil via pilot holes, circularly distributed over the soil surface. The holes run slantwise and converge along a chosen vertical line. The cables are buried below the soil surface to protect them against the UV sun radiation as well as against rodents.

Through a preaugered pilot hole it can reach any depth (**Fig. 62**) without destroying either the soil structure or disturbing the heat and mass transport in the soil. For semi-permanent installation the probe can be inserted horizontally through a sidewall of a soil pit or slantwise, from the soil surface. The probe installed once may be left intact in the soil for as long as necessary, then drawn out at the end of the experiment.

FP/m is a probe for *in situ* field measurement of the soil water content, whereas FP/mts is its version for simultaneous measurement of water content, temperature and salinity (electrical conductivity) of the soil from the same sampling volume.

Both probes are suitable for periodic measurements at random and/or fixed locations, where instantaneous profiles of water content, temperature and salinity are to be determined by readings taken at various levels of the soil profile. Each of them may also be applied as a mobile probe (FP/m/m or FP/mts/m) for momentary measurements in surface layer of the soil, by walking over the field and inserting the probe in the soil surface layer at chosen sites.

The shortest available probe is 15 cm long. Its support pipe has not any bending. To place the probe at 5 – 15 cm depth it can be inserted horizontally through a sidewall of a shallow soil pit. The longest possible probe is 400 cm long (probes longer than 150 cm are delivered as a kit to be assembled by the user). In order to install FP in the soil, a pilot hole has to be preaugered from the soil surface, deviated out of vertical of an appropriate angle,  $\alpha$ . The probe length,  $L$ , and the depth,  $D$ , the sensor rods are meant to reach in the soil profile (the installation depth) are related as follows:

$$L = \frac{D}{\cos \alpha} - 5 + a \quad (89)$$

where:  $L$ ,  $D$  and  $a$  in cm and  $\alpha$  is the out of vertical deviation angle. The length,  $L$ , is distance between the base of the sensor rods and the bending point of the plastic support pipe and  $a$  is length of the part of the probe body sticking out the soil surface. Different combinations of  $L$ ,  $a$  and  $\alpha$  allow to reach the intended depth,  $D$ . Suggested magnitude for  $a$  is  $30^\circ$ .

For the regular FP/mts the temperature sensor is fixed inside the PVC body, at the base of the rods. If the probe is to be applied as the near surface (FP/mts/ns presented in **Fig. 63**) or as the mobile, vertically inserted one (FP/mts/m), then this base is located at the body-soil interface, where distortion of temperature distribution is maximal. In order to avoid the problem the sensor is enclosed

inside of a separate polyethylene body and connected to the FP/mts feeder cable from outside.

The FP/mts/m mobile probe has been thought to provide with the ground-truth reference data for calibration and/or verification of the multispectral satellite images in terms of water content of the soil surface layer.

Concerning the FP/mts/m mobile probe the thermometer, if not needed, can be detached. Length of the mobile probe body,  $L$ , is up to the user convenience.  $L = 70$  cm is suggested.



**Fig. 63.** A near-surface probe FP/mts/ns

The approximate region of influence of the FP probe, defined as a solid beyond of that changes in water content do not markedly affect readings of water content is presented in **Fig. 64**.

Features of the FP probes for soil water content, salinity and temperature measurement developed in IAPAS, Lublin:

- Sensor: a section of a transmission line made of two, 100 mm long parallel stainless steel rods having 2 mm diameter and separated by 16 mm
- Sensor support: a section of a PVC tube having 2 cm outer diameter and optional length (15 cm - 150 cm or longer) dependent on the intended depth of the sensor installation
- Cable length: 6 m from the sensor to the BNC terminating connector
- Region of influence: a cylinder having approximated diameter of 5 cm and height of 11 cm, circumferenced around the sensor rods.

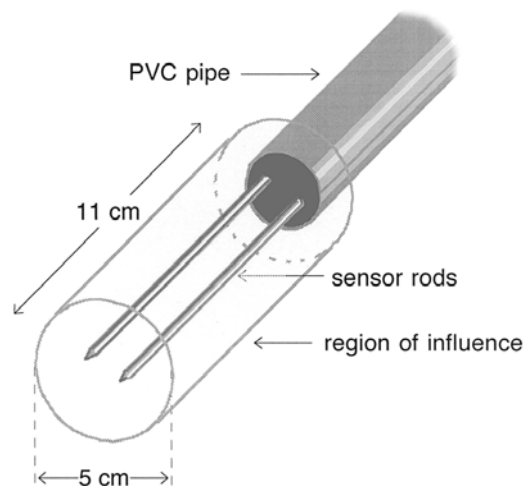


**Fig. 64.** Approximate region of influence of the FP probe, defined as a solid beyond of that changes in water content do not markedly affect readings of water content

### 12.5. LOM/mpts - Laboratory Operated Meter for recording soil moisture, matrix potential, temperature and salinity

LOM is a TDR (Time-Domain Reflectometry) technology based, computer aided instrument, designed to record mass and heat transport data. It is suitable for controlling long-term laboratory experiments on soil columns, which require monitoring of water, heat and salt transport (**Fig. 65**).

This is achieved by means of periodic recording of instantaneous profiles of water content, matrix potential (capillary water pressure, "suction force"), temperature and electrical conductivity in chosen time intervals. To record water content,  $\theta$ , a factory installed conversion equation  $\theta(\varepsilon)$  for mineral soils is implemented. A calibration function for organic soils as well as a user determined conversion equation could be also applied. A record of the pulse voltage against time, *ie* the TDR trace, can be stored for independent interpretation. Supplied software includes executable files and source codes as well. Several LP type miniprobes of selected type (or of all types) can be inserted through the side wall of a soil column or a steel sampling cylinder, thus allowing for vertical scanning of instantaneous profiles of water content, capillary pressure (matrix potential, suction force), temperature and salinity (bulk electrical conductivity).

This makes it possible to collect a set of corresponding data from transition of the soil solute (and temperature) front. From this, after processing, one can obtain a complete set of unsaturated water flow characteristics of the soil such as the water retention (PF) curve, the unsaturated water conductivity (k-function), the

differential water capacity and the unsaturated water diffusivity as well as the solute transport data. Also the heat flow parameters (thermal conductivity, thermal diffusivity, specific heat) can be determined if a temperature gradient is applied and a heat flux meter is installed in the soil column.

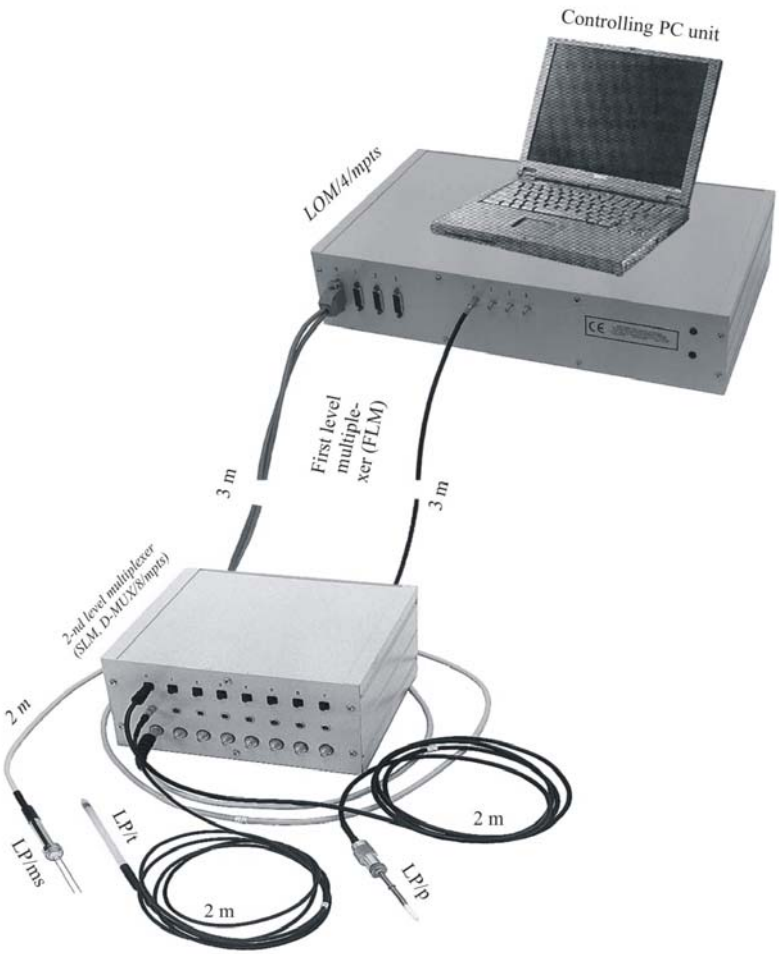


**Fig. 65.** Example of structure of a LOM/4/mpts based stand for recording instantaneous profiles of soil water content, capillary pressure of soil water, temperature and salinity (apparent electrical conductivity) from soil column(s), with application of a single MUX/8/mpts.

Probes are switched in two levels. For instance the LOM above is provided with a 3-pole-4-throw first level multiplexer (FLM) to switch between 1 to 4

second level multiplexers (SLMs). To switch between the probes 3-pole-8-throw multiplexers can be applied as the SLMs, as shown in the picture. For such configuration up to 32 LP/ms, 32 LP/t and 32 LP/p probes can be switched. Other options are also possible. The TDR LP/ms probes for water content and salinity use special microwave switches. Remaining probes (LP/p, LP/t) are switched using common solid-state switches and/or reed relays.

Characteristics of LOM/mpts meter:

- Pulse: sin -like needle pulse having rise-time of about 250 ps.
- Range:
  - apparent electrical conductivity,  $EC_a$ :  $0.000 \leq EC_a \leq 1$  S/m
  - dielectric constant,  $\varepsilon$ :  $2 \leq \varepsilon \leq 90$  (at  $EC_a < 0.3$  S/m)
  - volumetric water content,  $\theta$ :  $0 \leq \theta \leq 100$  % (at  $EC_a < 0.3$  S/m)
  - matrix potential,  $\psi$ :  $0 \leq \psi \leq 950$  mbar
  - temperature,  $T$ :  $-20 \leq T \leq +60$  °C
- Accuracy:
  - dielectric constant absolute error: displayed value  $\pm 2$
  - water content absolute error: displayed water content  $\pm 2$  % or less if contribution of solid matter is accounted for
  - el. conductivity relative error:  $\pm 5$  % of displayed value
  - matrix potential absolute error: displayed value  $\pm 8$  mbar
  - temperature absolute error:  $\pm 0.2$  °C
- Resolution:
  - dielectric constant: 0.1
  - water content: 0.1
  - el. conductivity: 0.001 S/m
  - matrix potential: 1 mbar
  - temperature: 0.01 °C
- Time of test:
  - dielectric constant: 6 s for first reading then about 3 s for each next single reading
  - water content: 6 s for first reading then about 3 s for each next single reading
  - electrical conductivity: 8 s for each single reading
  - matrix potential: 1.5 s for each single reading
  - temperature: 3 s for each single reading
- LOM switching capability:
  - maximum number of SLMs to control: 15
- SLM switching capability:
  - maximum number of LP/ms probes to switch: 8

- maximum number of LP/p probes to switch: 8
- maximum number of LP/t probes to switch: 8
- Total switching capability:
  - maximum number of LP/ms probes to switch: 120
  - maximum number of LP/p probes to switch: 120
  - maximum number of LP/t probes to switch: 120
- Ambient temperature,  $T_a$ :  $15\text{ }^\circ\text{C} < T_a < 25\text{ }^\circ\text{C}$
- Supply:  $\sim 220\text{ V}/110\text{ V}$ , 10 W
- Dimensions: width 330 mm, depth 340 mm, height 74 mm
- Weight: 3.5 kg
- Maintenance: the instrument is maintenance free
- Temperature of storage,  $T_s$ :  $-20\text{ }^\circ\text{C} < T_s < +70\text{ }^\circ\text{C}$ .

#### 12.6. LP/ms - Laboratory miniProbe for soil water content and salinity measurement

LP/ms (**Fig. 66**) - is a laboratory miniprobe designed for monitoring changes in water and salt distribution in soil columns or in soil cores sampled with standard sampling instrumentation. Several LP/ms can be inserted through the sidewall of a soil column or a steel sampling cylinder (**Fig. 67**), thus allowing for vertical scanning of the instantaneous moisture and electrical conductivity profiles.



**Fig. 66.** LP/ms - Laboratory miniProbe for soil water content and salinity measurement

Such an array, when combined with similarly installed minitensiometers (LP/p), makes it possible to collect a set of corresponding water content and matrix potential gradient data from drying or wetting front transition. From this one can obtain a complete set of the soil unsaturated water flow characteristics, *ie*

water retention (PF-curve), water conductivity (k-function), differential water capacity and unsaturated water diffusivity.

Features of LP/ms:

- Installation hole:
  - metric thread diameter of 8mm, height of 3.3 mm
- Sensor:
  - a section of a transmission line made of two, 53 mm long parallel stainless steel rods diameter of 0.8, separated by 5 mm
- Cable length:
  - 2 m from the sensor to the terminating connector (or multiplexer)
- Sphere of influence:
  - a cylinder having diameter of about 5 mm and height of about 60 mm, circumferenced around the sensor rods.

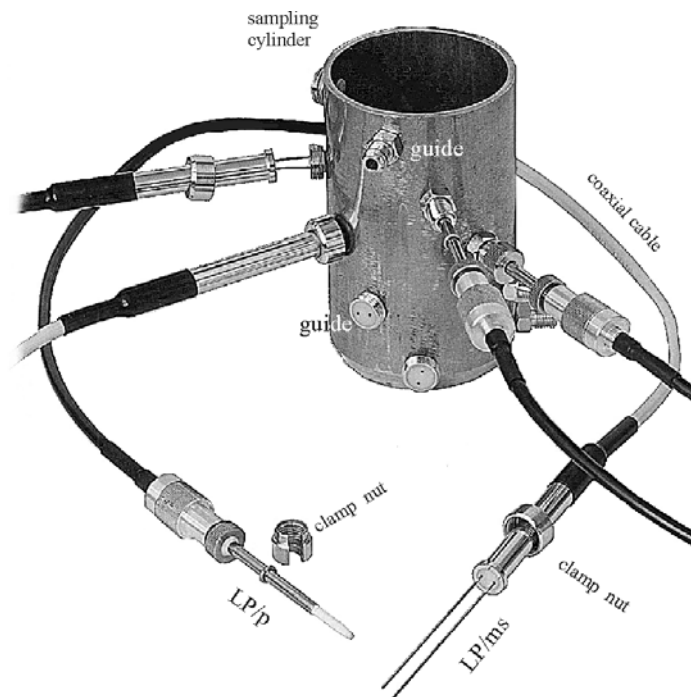


**Fig. 67.** A set of LP/ms and LP/p LOM controlled mini-probes inserted through a 2.75 mm thick wall of a sampling steel cylinder, having height of 100 mm and 55 mm inner diameter. The wall of the cylinder is provided with tapped holes equally distributed along the cylinder height in order to monitor independent layers of the soil. The holes are aligned spirally to minimize mutual shadowing in the vertical.

### 12.7. LP/t - Laboratory Probe for soil temperature

LP/t is a laboratory probe for monitoring instantaneous profiles of soil temperature in soil columns or in undisturbed soil cores (**Fig. 68**). Thin-wall half-rigid polyethylene body of the probe provides ultimate low heat conductivity, thus allowing avoiding the parasite “thermal bridge” effects. Several LP/t probes can be inserted through the wall of the soil column or the sampling cylinder, thus allowing for vertical recording of the instantaneous profiles of temperature. Such an array, when combined with miniprobes for soil moisture/salinity and also probes for matrix potential, makes it possible to collect a set of corresponding temperature data from non-isothermal transition of drying or wetting front, from which readings of bulk electric conductivity as well as matrix potential can be temperature corrected. Also heat transport coefficients (thermal conductivity, thermal diffusivity, specific heat) can be determined if a heat flux meter is installed in the column under investigation.

The wall of the cylinder containing a soil core is provided with tapped holes (8 mm diameter). A guide is screwed into the hole prior to the probe installation. This guide helps to avoid air gap around the probe, which otherwise might result while installing. LP/t is pushed into the soil core and fixed with a screwed gland.

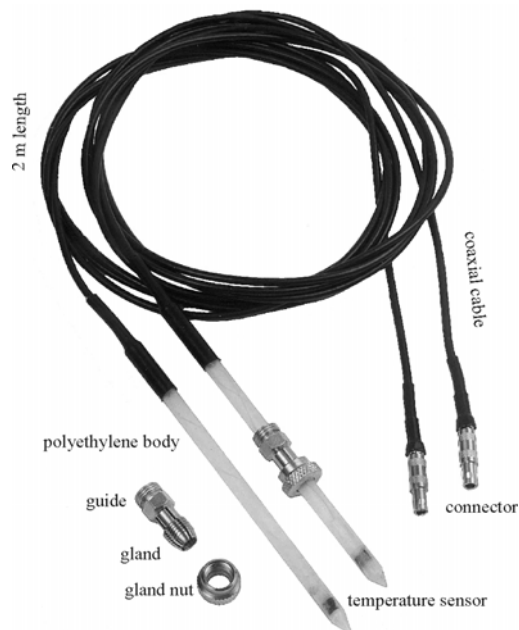


**Fig. 68.** LP/t - Laboratory Probe for soil temperature measurement

## 12.8. LP/p - Laboratory miniProbe for soil water capillary pressure

LP/p (Fig. 69) is a laboratory miniprobe designed for monitoring instantaneous profiles of soil water capillary pressure (matrix potential, suction force) in soil columns or in undisturbed soil cores sampled with standard sampling equipment.

The wall of a cylinder containing the soil core is provided with tapped holes (8 mm diameter). A guide is screwed into the hole prior to the probe installation. This guide helps to avoid air gaps between the ceramic suction cup and the soil, which otherwise might result while inserting the probe into the soil.

LP/p is pushed into the soil core and fixed with a clamp nut. Several LP/p can be inserted through the wall of a soil column or a steel sampling cylinder, thus allowing for vertical scanning of the instantaneous water potential profiles. Such an array, when combined with similarly installed miniprobes for soil moisture (see 12.6), makes it possible to collect a set of corresponding water content and matrix potential data from drying or wetting front transition (Fig. 70).

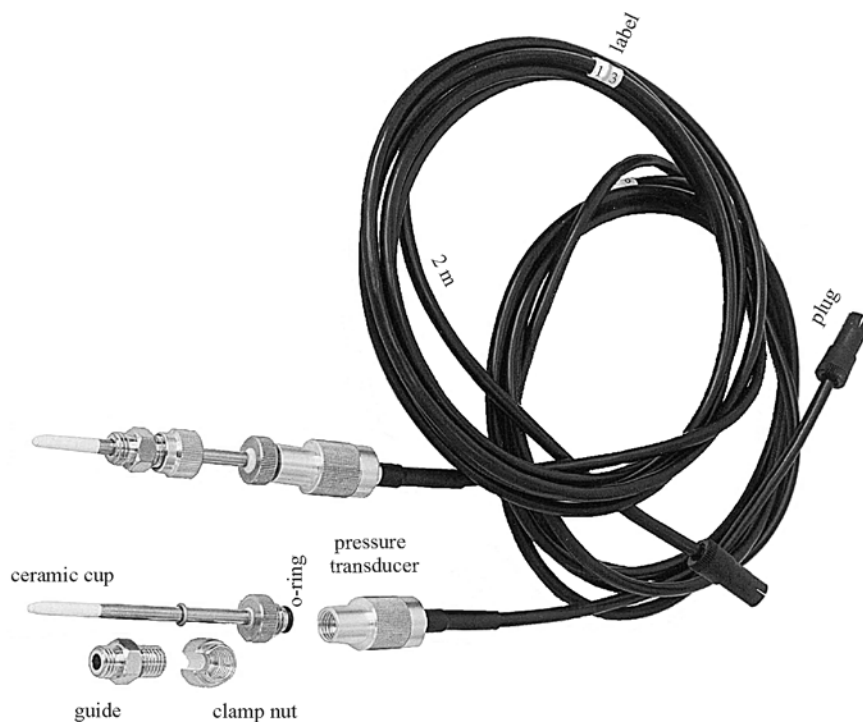
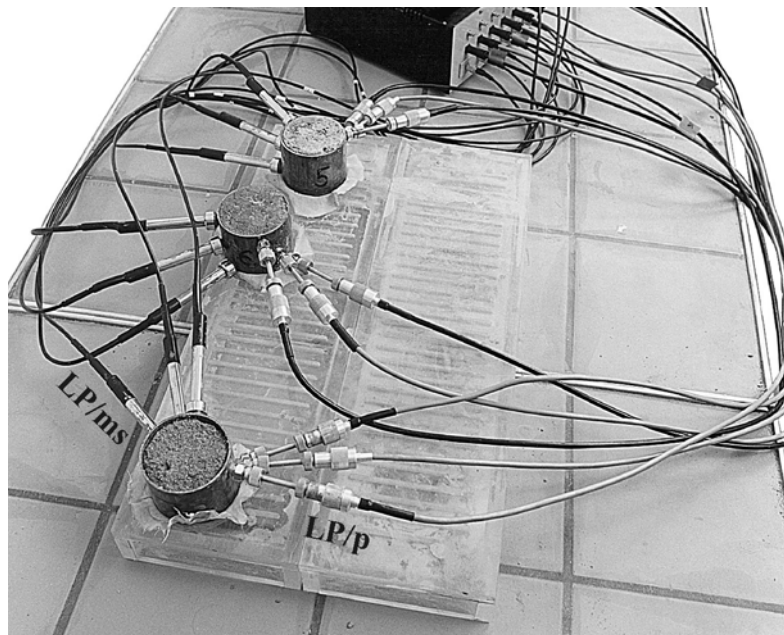


Fig. 69. LP/p - Laboratory miniProbe for soil water capillary pressure

From the collected data set, after further processing, one can obtain a complete set of the unsaturated water flow characteristics of the soil, that is: water retention (PF-curve), unsaturated water conductivity (k-function), differential water capacity and unsaturated water diffusivity.

Features of LP/p:

- Sensor:
  - pressure diaphragm: a 15 mm long ceramic
  - cup, 3 mm in diameter
  - pressure transducer: an integrated, fully active Wheatstone bridge with four piezoresistive strain gauge resistors diffused into a silicon diaphragm
  - air entry pressure: about 900 mbar
- Offset drift:  $\pm 20$  mbar/month
- Relative error:  $\pm 15$  %
- Resolution: 1 mbar
- Delay: 0 to 800 mbar in about 120 s, 800 to 0 mbar in about 3 s
- Cable length: 2 m
- Installation hole: 8 mm diameter tapped with 8x1 mm thread.



**Fig. 70.** Reading instantaneous profiles of soil water capillary pressure, water content and salinity from arrays of the LP/p and LP/ms miniprobes

### 13. REFERENCES

1. **Agilent Application Note 922:** Applications of PIN Diodes. 1999.
2. **Agilent Application Note 1304-2:** Time Domain Reflectometry Theory. 2002.
3. **Alharthi A., Lange J.:** Soil water saturation: dielectric determination. *Water Resour. Res.* 23(4), 591-595. 1987.
4. **Analog Devices:** AD7705/AD7706 2/3 Channel 16-Bit Sigma-Delta ADC. 1998.
5. **Annan A.P.:** Report of activities, Part B, *Geol. Surv. Can. Paper 77-1B*. 1979.
6. **Arble W.C., Shaw M.D.:** Bibliography on the methods for determining soil moisture. *Eng. Res. Bull. B-78, Coll. Of Eng. End. Arch., Univ. Park, Penn.*, 1959.
7. **Baker J.M., Allmaras R.W.:** System for automating and multiplexing soil moisture measurement by time-domain reflectometry. *Soil Sci. Soc. Am. J.* 54: 1-6. 1990.
8. **Baranowski J., Rusek A., Ramotowski M., Misiaszek S., Nowakowski W.:** Wide bandwidth stroboscope synchrosopes (in Polish). WNT, Warsaw, 1972.
9. **Birchak J.R., Gardner C.G., Hipp J.E., Victor J.M.:** High dielectric constant microwave probes for sensing soil moisture. *Proc. of the IEEE.* 62:(1):93-98. 1974.
10. **Blackham D.V., Pollard R.D.:** 1997. An Improved Technique for Permittivity Measurements Using a Coaxial Probe. *IEEE Trans. Instr. Meas.*, 46(5), 1093-1099.
11. **Bohl, H., Roth K.:** Evaluation of dielectric mixing models to describe the  $\theta(\epsilon)$  relation. Symposium in Evanston. Sept. 8-9, 1994.
12. **Boyarskii D.A., Tikhonov V.V., Komarova N.Yu.:** Model of dielectric constant of bound water in soil for applications of microwave remote sensing. *Progress In Electromagnetic Research*, 35:251-269, 2002.
13. **Campbell G.S., Gee G.W.:** Water potential miscellaneous methods. *Agronomy* 9, Part 1, 2-nd Ed, 619-633, 1986.
14. **Chelkowski A.** Physics of dielectrics (in Polish). PIW, Warsaw. 1972.
15. Chipcon Smart RF CC1000 - Single Chip Very Low Power RF Transceiver ([http://www.chipcon.com/files/CC1000\\_Data\\_Sheet\\_2\\_2.pdf](http://www.chipcon.com/files/CC1000_Data_Sheet_2_2.pdf)), 2004.
16. **COTO Technology:** Technical and Application Information (Relays), Coto Technology Website: [www.cotorelay.com](http://www.cotorelay.com)
17. **CRC handbook of chemistry and physics** (ed. R.C. Weast). CRC Press Inc. Boca Raton. Florida. USA. 1979.
18. **DS18B20:** Programmable Resolution 1-Wire Digital Thermometer Data Sheet, Dallas Semiconductors – Maxim.
19. **Dalton F.N., Herkelrath W.N., Rawlins D.S., Rhoades J.D.:** Time-domain reflectometry simultaneous measurement of soil water content and electrical conductivity with a single probe. *Science.* 224:989-990. 1984.
20. **Dalton, F. N., van Genuchten M. Th.:** The time-domain reflectometry method for measuring soil water content and salinity. *Geoderma.* 38:237-250. 1986.
21. **Dasberg S., Dalton F.N.:** Time Domain Reflectometry field measurements of soil water content and electrical conductivity. *Soil Sci. Soc. Am. J.*, Vol. 49, 293-297, 1985.
22. **Davis, J.L., Annan A.P.:** Electromagnetic detection of soil moisture: progress report I. *Canadian Journal of Remote Sensing.* 3:76-86. 1977.
23. **Davis J. L., W. J. Chudobiak:** In situ meter for measuring relative permittivity of soils, *Geol. Surv. Can., Paper 75-1, Part A*, 1985.
24. **Debye P.:** *Polar Molecules.* Dover. Mineola. N.Y., 1929.

25. **de Loor G.P.:** Dielectric properties of heterogeneous mixtures. *Appl. Sci. Res. B3:* 479-482. 1964.
26. **de Loor G.P.:** Dielectric properties of heterogeneous mixtures. BCRS (Nederland Remote Sensing Board) rep. No. 90-13. TNO Physics and Electronics Lab., The Hague. 1990.
27. **Dirksen C., Dasberg S.:** Improved calibration of Time Domain Reflectometry soil water content measurements. *Soil Sci. Soc. Am. J.* 57:660-667. 1993.
28. **Dobson M.C., Ulaby F.T., Hallikainen M.T., El-Rayes M.A.:** Microwave dielectric behavior of wet soil - Part II: Dielectric mixing models. *IEEE Transactions on Geoscience and Remote Sensing.* GE-23:35-46. 1985.
29. **Easy Test:** Soil water status monitoring devices. Instytut Agrofizyki PAN, Lublin. 2004.
30. **Fellner-Feldegg H.:** The measurement of dielectrics in Time Domain. *The Journal of Physical Chemistry.* 73: 616-623. 1969.
31. **Friedman S.P, Robinson D.:** Particle shape characterization using angle of repose measurements for predicting the effective permittivity and electrical conductivity of saturated granular media. 38(11), 1-11. 2002.
32. **Gardner C.M.K, Bell J.P., Cooper D., Dean T.J., Hodnett M.G.:** Soil Water Content. *Soil Analysis – Physical Methods* (edited by Smith K.A., Mullins C.E.). Marcel Dekker, Inc. New York. 1-73. 1991.
33. **Giese K., Tiemann R.:** Determination of the complex permittivity from thin-sample time domain reflectometry: Improved analysis of the step response wave form. *Adv. Mol. Relax. Processes.* 7: 45-59. 1975.
34. **Gliński J.:** Agrophysics in modern agriculture. *International Agrophysics*, vol. 6, No 1/2, 1-7, 1992.
35. **Gupta S.C, Hanks R.J.:** Influence of water content in electrical conductivity of the soils. *Soil Science Society of America Proceedings.* 36:855-857. 1972.
36. **Halbertsma J., van den Elsen E., Bohl H., Skierucha W.:** Temperature effects on TDR determined soil water content. *Proceedings of the Symposium: Time Domain Reflectometry Applications in Soil Science.* Research Center Foulum, Sept. 16, 1995. SP Report 11:35-37, Danish Institute of Plant and Soil Sci., Lyngby, Denmark, 1995.
37. **Hasted J.B.:** *Aqueous dielectrics.* Chapman and Hall, London, 1973.
38. **Heimovaara T.J.:** Design of triple-wire Time Domain Reflectometry probes in practice and theory. *Soil. Sci. Soc. Am. J.* 57: 1410-1417. 1993.
39. **Heimovaara T.J.:** Frequency domain analysis of time domain reflectometry waveforms, 1- Measurements of complex dielectric permittivity of soils. *Water. Res. Res.*, 30:189-199. 1994.
40. **HP54121T:** *Digitizing Oscilloscope Programming Manual*, Hewlett-Packard, Publication 54121-90907, 1989.
41. **Hilhorst M.A., Dirksen C.:** Dielectric water content sensors: time domain versus frequency domain. *Symposium and Workshop on Time Domain Reflectometry in Environmental, Infrastructure and Mining Applications*, Northwestern University, Evanston, Illinois. SP19-94: 23-33. 1994.
42. **Hittite Microwave Corporation:** *DC – 42 GHz RFIC/MMIC Components and Modules. Designers Guid.* 2003.
43. **HP AN 1217-1:** Basics of measuring the dielectric properties of materials.

44. **ISO 16586:** Soil quality. Determination of soil water content as a volume fraction on the basis of known dry bulk density. Gravimetric method. 2003.
45. **James D.W., Hanks R.J., Jurinak J.J.:** Modern Irrigated Soils. A Willey-Interscience Publication. John Wiley & Sons, Inc. 140-149. 1982
46. **Kirkham D., Taylor G.S.:** Some tests of a four-electrode probe for soil moisture measurements. Soil. Sci. Am. Proc. Vol. 14, 42-46. 1949.
47. **Kraszewski A.:** Microwave aquametry: An Effective Tool for Non-destructive Moisture Sensing. Subsurface Sensing Technologies and Applications, vol. 2(4), 347-362. 2001.
48. **Kraszewski A, Kulinski S, Matuszewski W:** Dielectric properties and a model of biphasic water suspension at 9.4 GHz. Journal of Applied physics. Vol. 47, No. 4: 1275-1277. 1976.
49. **Ledieu, J., P. De Ridder, P. De Clerck, Dautrebanede S.:** A method of measuring soil moisture by time-domain reflectometry. J. Hydrol. 88:319-328. 1986.
50. **Litwin R.:** Teoria pola elektromagnetycznego. Podręczniki Akademickie. Elektronika. WNT. 1968.
51. **Malicki M.A.:** A capacity meter for the investigation of soil moisture dynamics. Zeszyty Problemowe Postępów Nauk Rolniczych, 220, 201-214, 1983.
52. **Malicki M.A.:** The influence of physical soil properties on the electrode|soil parameters in the aspect of the measurement of soil moisture and salinity. Habilitation Thesis, Acta Agrophysica, Institute of Agrophysics Polish Academy of Sciences, Lublin (in Polish). 1993.
53. **Malicki M.A.:** Electric measurement of soil moisture and salinity using time domain reflectometry method (in Polish). Zesz. Probl. Post. Nauk Roln., 429, 215-221, 1996.
54. **Malicki M.A.:** Methodical aspects of water status monitoring in selected biological materials (in Polish). Acta Agrophysica, 19, Lublin 1999.
55. **Malicki M.A., Bieganowski A.:** Chronovoltammetric determination of oxygen flux density in the soil. International Agrophysics, 13(3), 237-281. 1999.
56. **Malicki M.A., Kotliński J.:** Dielectric determination of moisture of cereals grain using time domain reflectometry. International Agrophysics, Vol. 12, No. 3, 209-215. 1998.
57. **Malicki M.A., Kotliński J.:** Dielectric determination of moisture of wood using time domain reflectometry. International Agrophysics, Vol. 12, No. 3, 217-220. 1998.
58. **Malicki, M., Plagge A.R., Roth C.H.:** Reduction of soil matrix effect on TDR dielectric moisture determination by accounting for bulk density or porosity. European Journal of Soil Science, Vol. 47, No. 3, 357-366. 1996.
59. **Malicki M.A., Skierucha W.:** A manually controlled TDR soil moisture meter operating with 300 ps rise-time needle pulse. Irrigation Science. 10:153-163. 1989.
60. **Malicki M.A., Skierucha W.:** The problem of electromagnetic field frequency selection in the measurement of water content in saline soils (in Polish). Acta Agrophysica, 53:109-115. 2001.
61. **Malicki M.A., Walczak R.T.:** 1999. Evaluating soil salinity status from bulk electrical conductivity and permittivity. European Journal of Soil Science, 505-514.
62. **Malicki M.A., Walczak R.T., Koch S., Fluhler H.:** Determining soil salinity from simultaneous readings of its dielectric constant and electrical conductivity using

- TDR. Symposium on Time Domain Reflectometry in Environmental, Infrastructure, and Mining Applications Proceedings. September 7 - 9, Evanston, IL, USA 1994.
63. **Marshall, T.J., Holmes J.W.:** Soil physics (eds.). Cambridge University Press. Cambridge. 1979.
  64. **Measurement Computing:** GPIB Hardware Manual, Rev. 5, March 2002.
  65. **Microchip Data Sheet:** PIC16F87X 28/40-Pin 8-bit CMOS FLASH Microcontrollers, DS30292C, 2001.
  66. **MIDL:** Data logger for field monitoring of soil and ground physical and chemical parameters. Operation Manual (in Polish). Institute of Agrophysics Polish Academy of Sciences, Lublin, 2004.
  67. **MIDL:** Data logger for field monitoring of soil and ground physical and chemical parameters. Technical Manual (in Polish). Institute of Agrophysics Polish Academy of Sciences, Lublin, 2004.
  68. **MIDL:** Data logger for field monitoring of soil and ground physical and chemical parameters. Start-up Manual (in Polish). Institute of Agrophysics Polish Academy of Sciences, Lublin, 2004.
  69. **Mullins C.E.:** Matrix Potential. In Soil Analysis: Physical Methods (eds C.E. Mullins & K.A. Smith): 75-09, Marcel Dekker, New York, 1991.
  70. **Nadler A.:** Field application of the four-electrode technique for determining soil solution conductivity. Soil Sci. Soc. Am. J. 45:30-34. 1981.
  71. **O'Connor K.M., Dowding C.H.:** Geomeasurements by pulsing TDR cables and probes. CRC Press. 1999.
  72. **Or D., Wraith J.M.:** Temperature effects on soil bulk dielectric permittivity measured by time domain reflectometry: A physical model. Water Res. Res., 35, No.2: 371-383. 1999.
  73. **Oscik J.:** Adsorption (in Polish). PWN. Warszawa. 1983.
  74. **Pepin S, Livingston N.J., Hook W.R.:** Temperature-dependent measurement errors in time domain reflectometry determinations of soil water. Soil Sci. Soc. Am. J. 59:38-43, 1995.
  75. **Rhoades J.D., Ingvalson R.D.:** Determining salinity in field soils with soil resistance measurements. Soil Sci. Soc. Am. Proc. 35:54-60. 1971.
  76. **Rhoades J.D., Raats P.A., Prater R.J.:** Effects of liquid-phase electrical conductivity, water content and surface conductivity on bulk soil electrical conductivity. Soil Science Society of America Journal. 40:651-655. 1976.
  77. **Roth, K., R. Schulin, H. Flübler, Attinger W.:** Calibration of Time Domain Reflectometry for water content measurement using a composite dielectric approach. Water Resources Research. 26:2267-2273. 1990.
  78. **Skierucha W.:** The dependence of the propagation velocity of electromagnetic wave in the soil on the soil selected properties. PhD Thesis. Instytut of Agrophysics Polish Academy of Sciences, Lublin (in Polish). 1996.
  79. **Skierucha W.:** The influence of temperature on soil dielectric permittivity and the TDR determined soil moisture (in Polish). Acta Agrophysica, 22: 163-172. 1999.
  80. **Skierucha W.:** Microwave switches applied in reflectometric systems for soil moisture measurements (in Polish). Proceedings from XXXII Conference of Metrology - MKM2000. Rzeszów-Jawor, Poland. 2000.

81. **Skierucha W.:** Temperature effect on soil dielectric permittivity: description of laboratory setup and applied software (in Polish). *Acta Agrophysica*. 72:125-133. 2002.
82. **Skierucha W., Malicki M.A.:** Dielectric mixing models: validation in mineral soils. Poster Presentation. 17<sup>th</sup> World Congress of Soil Science. 14-21 August 2002, Bangkok. Thailand.
83. **Skierucha W., Wilczek A.M, Walczak R.T.:** Application of smart sensors in the measurement of soil physical parameters. *Research in Agricultural Engineering*, Vol. 50, (3), 96-102, 2004.
84. **Spósito, G., Prost R.:** Structure of water adsorbed on smectites. *Chem. Rev.*, 82, 553-572. 1982.
85. **Stanford Microdevices:** SSW-308 DC-3 GHz Low Cost GaAs MMIC SPDT Switch, [www.stanfordmicro.com](http://www.stanfordmicro.com).
86. **Steru, M.:** Electrical control of water content of materials (in French). *Measures & Contrôle Industriel*. 24:33-38. 1959.
87. **Strickland J.A.:** Time-Domain Reflectometry measurements. Tektronix Inc. Beaverton, Oregon 97005. 1970.
88. **Stogryn A.P.:** The microwave dielectric properties of sea and fresh water. Internet publication, [http://www.universityphysics.com/UniversityPhysics/Sti\\_rd/research/properties\\_of\\_seawater/index.htm](http://www.universityphysics.com/UniversityPhysics/Sti_rd/research/properties_of_seawater/index.htm).
89. **Stuchly M.A., Stuchly S.S.:** Coaxial Line Reflection Method for Measuring Dielectric Properties of Biological Substances at Radio and Microwave Frequencies - A Review. *IEEE Trans. Instr. Meas.*, IM-29(3), 176-183. 1980.
90. **Topp G.C., Davis J.L., Annan A.P.:** Electromagnetic determination of soil water content: measurements in coaxial transmission lines. *Water Resources Research*. 16:574-582. 1980.
91. **Topp G.C., Yanuka M., Zebchuk W.D., Zegelin S.:** Determination of electrical conductivity using Time Domain Reflectometry: soil and water experiments in coaxial lines. *Water Resources Research* 24, 945-952, 1988.
92. **Topp G.C., Zegelin S., White I.:** Impacts of the real and imaginary components of relative permittivity on time domain reflectometry measurements in soils. *Soil Sci. Soc. Am. J.* 64:1244-1252. 2000.
93. **Turski R. (ed.):** Pedology. Exercises for students of agriculture (in Polish). University of Agriculture in Lublin. 1993.
94. **US Salinity Laboratory:** (ed. Richards, L.A.) Diagnosis and Improvement of Saline and Alkali Soils. US Dept. Of Agriculture Handbook No. 60. 1954.
95. **Van den Elsen H.G.M., Kokot J., Skierucha W., Halbertsma J.M.:** An automatic time domain reflectometry device to measure and store soil moisture contents for stand-alone field use, *International Agrophysics*, 9, 235-241, 1995.
96. **von Hippel, A. R.:** Dielektryki i fale. PWN. Warszawa. 1963.
97. **Walczak R.T., Sławiński C.:** Study and modelling the mass and energy transfer in agrophysics (in Polish). *Eksploracja i Niezawodność*. 4, 6-15. 2000.
98. **Walczak R.T., Sławiński C.:** Thermodynamics of soil processes (in Polish). *Acta Agrophysica*, 48, 133-139, 2001.
99. **Wang J.R., Schumge T.J.:** An empirical model for the complex dielectric constant of soils as a function of water content. *IEEE Trans. Geosci. Remote Sensing*. GE-18:288-295. 1980.

100. **Whalley W.R.:** Considerations on the use of time-domain reflectometry (TDR) for measuring soil water content. *Journal of Soil Science*. 44:1-9. 1993.
101. **White, I., Zegelin S.J., Topp G.C., Fish A.:** Effect of bulk electrical conductivity on TDR measurement of water content in porous media. Special Publication SP 19-94. Symposium and Workshop on TDR in Environmental, Infrastructure, and Mining Applications. Northwestern University, Evanston, USA. 1994.
102. **Whitney M., Gardner F., Briggs L.J.:** An electrical method of determining the moisture content of arable soils. U.S. Dept. Agr., Div. Soils, Bull. 6. 1897.
103. **Wiczer J.:** Connectivity: smart sensors or smart interfaces. ISA 2001 Emerging Technologies Conference, Huston, TX, Sept. 10-13, 2001.
104. **Wilczek A., Mazurek W., Skierucha M.:** Application of wireless communication in automatic monitoring of temperature in soil profile (in Polish). *Acta Agrophysica* 93:123-133, 2003.
105. **Wright J.M., Or D:** Temperature effects on soil bulk dielectric permittivity measured by time domain Reflectometry: Experimental evidence and hypothesis development. *Water Res. Res.*, 35, No.2: 361-369. 1999.
106. **Zegelin S.J., White I., Jenkins D.R.:** Improved field probes for soil water content and electrical conductivity measurement using Time Domain Reflectometry. *Water Res. Res.*, 25, No.11: 2367-2376. 1989.

#### 14. INDEX OF FIGURES

<b>Fig. 1.</b>	Hardware setup for simultaneous measurement of soil water content and electrical conductivity using Time Domain Reflectometry method .....	16
<b>Fig. 2.</b>	Relation between the soil refractive index, $n$ , and its water content, $\theta$ , for mineral and organic soil samples as well as their mixtures. A - experimental data, B - regression $n(\theta)$ . .....	18
<b>Fig. 3.</b>	Relations between the refractive index, $n = \sqrt{\varepsilon}$ , and volumetric water content, $\theta$ , and related regression lines .....	20
<b>Fig. 4.</b>	Relative refractive index, $n = \sqrt{\varepsilon}$ , as the function of water content for selected wood types .....	21
<b>Fig. 5.</b>	Bulk electrical conductivity, $EC_{a-TDR}$ , of the investigated soil samples obtained using TDR pulse attenuation method accordingly to Eq. (3), versus reference data, $EC_{a-4p}$ , determined using four-electrode reference method.....	23
<b>Fig. 6.</b>	Comparison of the bulk electrical conductivity of the investigated soils, $EC_{a-TDR}$ , with the reference data, $EC_{a-4p}$ , after correction accordingly do the polynomial of <b>Fig. 5</b> .....	24
<b>Fig. 7.</b>	Frequency dispersion of the real part, $\varepsilon'$ , and module, $k$ , of the complex dielectric constant of the electrolyte for different conductivities.....	27
<b>Fig. 8.</b>	Frequency dispersion of the real part, $\varepsilon'$ , of the complex dielectric constant and the loss angle, $\delta$ , for the electrolyte for its various electrical conductivities, $EC_w$ .....	29
<b>Fig. 9.</b>	The relation $n(\theta)$ for soil samples moistened by KCl solutions of different electrical conductivities, $EC_w$ .....	32
<b>Fig. 10.</b>	TDR interpretation of soil as a tree phases medium in dielectric mixing model $\alpha$ .....	33
<b>Fig. 11.</b>	Determination of the dielectric constant of soil solid phase using extrapolation and three-phase soil dielectric mixing model $\alpha$ . .....	37
<b>Fig. 12.</b>	Relation between the soil relative dielectric constant, $\varepsilon$ , and soil volumetric water content, $\theta$ , for the investigated mineral soils. The solid line represents the empirical model (31) calculated for the average bulk density of the soil samples $1.42 \text{ [gcm}^{-3}\text{]}$ .....	38
<b>Fig. 13.</b>	Comparison of soil relative dielectric constants of the investigated soil samples measured by TDR method (horizontal axis) and	

	calculated from 3-phase model $\alpha$ (27) for different values of $\alpha$ parameter. ....	38
<b>Fig. 14.</b>	Comparison of the soil dielectric constants measured by TDR method (horizontal axis) and calculated by the empirical model (31) accounting for soil bulk density. ....	39
<b>Fig. 15.</b>	Values of dielectric constant of bound water, $\varepsilon_{bw}$ , related to the distance, $x$ , from the phases interface. ....	40
<b>Fig. 16.</b>	Effects of the 4-phase models for the investigated clay soils (Table 6, no. 10 and 11): A – for model $\alpha$ , B - for <i>de Loor</i> model and C – effect of regression model (31) accounting for soil bulk densities, the solid line represents model (31) for $\rho = 1,42$ [gcm <sup>-3</sup> ] ....	40
<b>Fig. 17.</b>	Comparison of the analysed soil dielectric constant measured by TDR method (horizontal axis) and calculated from the 4-phase model $\alpha$ ....	41
<b>Fig. 18.</b>	The experimental setup for the determination of temperature effect on soil dielectric permittivity determined by TDR method. ....	44
<b>Fig. 19.</b>	Block diagram of the laboratory setup for the determination of temperature effect on soil dielectric permittivity. ....	45
<b>Fig. 20.</b>	Block diagram of the TDR probe with the electronics for soil electrical conductivity and temperature measurements. ....	46
<b>Fig. 21.</b>	Application window presenting the state of the conducted experiment. ....	47
<b>Fig. 22.</b>	Set of reflectograms registered by the presented setup for the same soil sample in different temperatures. ....	48
<b>Fig. 23.</b>	The effect of the applied temperature corrections for TDR measurement in water: (43) – for the measured refractive index, $n$ (part A), and (46) – for the calculated volumetric water content, $\theta_{TDR}$ (part B). ....	58
<b>Fig. 24.</b>	Influence of temperature on the refractive index, $n$ , for peat soil and the results of applied corrections. ....	59
<b>Fig. 25.</b>	The temperature effect on the soil refractive index, $n$ , and the soil volumetric water content, $\theta_{TDR}$ , determined by TDR method for three mineral soils: sand, silt and clay and the results of the applied corrections according to Eq. (43) and Eq. (46). On the right side there are values of water content, $\theta$ , determined by thermo-gravimetric method. • - TDR determined values, line – correction on $n$ and $\theta$ . ....	61

<b>Fig. 26.</b>	Relaxation frequency of water molecules in relation to the distance from the solid surface and temperature according to (52) on the base of Debye model [24].....	63
<b>Fig. 27.</b>	Frequency dependence of real, $\epsilon'$ , and imaginary, $\epsilon''$ , parts of complex dielectric permittivity of salt-water mixtures for two values of electrical conductivity of the solution: $EC_a = 0.01$ and $0.5$ [ $\text{Sm}^{-1}$ ], at two temperatures: $T = 5$ and $55^\circ\text{C}$ of the solution.....	67
<b>Fig. 28.</b>	Relation between the soil refractive index, $n$ , and its water content, $\theta$ , for mineral and organic soil samples as well as their mixtures. <b>A</b> - experimental data, <b>B</b> - regression $n(\theta)$ . ....	72
<b>Fig. 29.</b>	Comparison of model values of the EM refractive index of the soil with the use of <b>A</b> – model I, <b>B</b> – model II, <b>C</b> – model III and <b>D</b> – model IV, with the values measured with TDR device (horizontal axis).....	76
<b>Fig. 30.</b>	Comparison of the values of soil water content, $\theta_{TDR}$ , calculated from the measured values of soil refractive index, $n$ , for <b>model I</b> – <b>A</b> and <b>model III</b> – <b>B</b> with the reference values determined by the thermogravimetric method .....	78
<b>Fig. 31.</b>	The absolute error, $\Delta\theta_{TDR}$ , of the reflectometric soil water content measurement in relation of its real value, $\theta$ , and the histograms of this error referring to the <b>model I</b> : <b>A</b> and the <b>model III</b> : <b>B</b> .....	79
<b>Fig. 32.</b>	The relative error, $\Delta\theta_{rel}$ , of the TDR soil water content results as related to the real values of its water content, $\theta$ , and the histogram of $\Delta\theta_{rel}$ for soil water content values calculated for the <b>model I</b> : <b>A</b> and the <b>model III</b> : <b>B</b> .....	80
<b>Fig. 33.</b>	Sensitivity of <b>model III</b> on the soil density, $\rho$ , in relation to the soil, $\theta$ .....	81
<b>Fig. 34.</b>	Frequency response of dielectric mechanisms: MW, IR, V and UV are respectively microwave, infrared, visible and ultraviolet spectrum .....	85
<b>Fig. 35.</b>	Basic elements of the time domain reflectometer for determination of velocity of propagation of electromagnetic waves in porous media .....	86
<b>Fig. 36.</b>	Basic elements of the frequency domain reflectometer for determination of complex dielectric permittivity of porous media .....	88
<b>Fig. 37.</b>	<b>A</b> - Open-ended coaxial probe in the form of coaxial line open to the space with material of unknown dielectric permittivity $\epsilon^*$ , <b>B</b> - modeling the discontinuity of electromagnetic field by lumped capacitances $C_f$ and $C_0$ .....	89

<b>Fig. 38.</b>	The three-rod TDR probe – <b>A</b> , and an Open-Ended Coax probe – <b>B</b> , used in the measurement of dielectric permittivity of soils. ....	91
<b>Fig. 39.</b>	Frequency change of real and imaginary parts of the complex dielectric permittivity of methanol for Cole-Cole modelled data and measured using open-ended coaxial probe .....	92
<b>Fig. 40.</b>	Comparison of real, $\epsilon'$ , and imaginary, $\epsilon''$ , parts of the complex dielectric permittivity for the selected soils, calculated from the TDR and Open-Ended Coax probe measurements. $\epsilon_{b-TDR}$ is the bulk dielectric constant measured by TDR.....	93
<b>Fig. 41.</b>	TDR meter output – probe in air .....	97
<b>Fig. 42.</b>	Examples of electromagnetic microwave switches .....	99
<b>Fig. 43.</b>	Construction of SPDT switches build on PIN diodes: <b>A</b> – typical connections, <b>B</b> – serial connection of the diodes in a single channel increase isolation of the switch .....	100
<b>Fig. 44.</b>	Scheme of connections of the tested prototype SP16T switches.....	101
<b>Fig. 45.</b>	Insertion loss and isolation between channels related to frequency for the MMIC device HMC253QS24 implemented in the prototype TDR switch .....	102
<b>Fig. 46.</b>	Prototype one-to-eight microwave switch for the application in TDR soil water content meter.....	103
<b>Fig. 47.</b>	Input pulse and output pulses from the tested SP16T switches.....	104
<b>Fig. 48.</b>	The reflected signal attenuation introduced by the prototype reed relay and MMIC GaAs switches when the TDR probe was inserted into dry (left picture) and wet (right picture) sand.....	104
<b>Fig. 49.</b>	Reflections observed from the tested SP16T switches and TDR probe in wet sand.....	105
<b>Fig. 50.</b>	Reflectograms presenting reflections of the needle pulse from the TDR probe rods with the application of the prototype MMIC switch (right column) and without it (left column). Left axis represents voltage in mV, $\theta$ is the water content of the measured soil samples .....	106
<b>Fig. 51.</b>	Multi Interface Data Logger (in the middle between TDR soil water content, salinity and temperature meters)) in the configuration for the measurement of 16 TDR FP/mts probes.....	109
<b>Fig. 52.</b>	Example setup of devices for soil and ground physico-chemical parameter monitoring system using wireless communication.....	110
<b>Fig. 53.</b>	Direct connection of SLAVE modules to Internet network .....	112
<b>Fig. 54.</b>	Simplified functional diagram of the MIDL setup in SLAVE configuration .....	113

<b>Fig. 55.</b>	Simplified functional diagram of the MIDL setup in MASTER configuration .....	114
<b>Fig. 56.</b>	Serial RS232C port terminal window with the MIDL system initial tests.....	115
<b>Fig. 57.</b>	Portable TDR meter, FOM/mts, for the measurement of soil water content using TDR technique as well as soil apparent electrical conductivity and temperature .....	121
<b>Fig. 58.</b>	Prototype of a handheld soil water content, salinity and temperature meter constructed with the application of modern components.....	123
<b>Fig. 59.</b>	An example of the D-LOG/10/mts-controlled stand incorporating six D-MUX/10/mts 2-nd level multiplexers. Maximum amount of the controlled FP/mts (or FP/m) probes is 60. For clarity only a single D-MUX was linked with the D-LOG and a single probe was connected to each D-MUX when taking the picture .....	124
<b>Fig. 60.</b>	Example of an arrangement of the D-LOG/mts system able to scan 60 FP/m(ts) probes. All cables are laid about 30 cm beneath the soil surface to protect them against static electricity, UV radiation and rodents as well. FP/mts feeder cables (6 m) .....	125
<b>Fig. 61.</b>	FP/m, FP/mts - Field Probe for water content, temperature and salinity of soil developed in the IAPAS, Lublin.....	127
<b>Fig. 62.</b>	The principle of installation of the FP-type probes. In order to minimize disturbances in the soil structure the probes are inserted into the soil via pilot holes, circularly distributed over the soil surface. The holes run slantwise and converge along a chosen vertical line. The cables are buried below the soil surface to protect them against the UV sun radiation as well as against rodents. ....	127
<b>Fig. 63.</b>	A near-surface probe FP/mts/ns .....	129
<b>Fig. 64.</b>	Approximate region of influence of the FP probe, defined as a solid beyond of that changes in water content do not markedly affect readings of water content .....	130
<b>Fig. 65.</b>	Example of structure of a LOM/4/mpts based stand for recording instantaneous profiles of soil water content, capillary pressure of soil water, temperature and salinity (apparent electrical conductivity) from soil column(s), with application of a single MUX/8/mpts.....	131
<b>Fig. 66.</b>	LP/ms - Laboratory miniProbe for soil water content and salinity measurement.....	133

<b>Fig. 67.</b>	A set of LP/ms and LP/p LOM controlled miniprobcs inserted through a 2.75 mm thick wall of a sampling steel cylinder, having height of 100 mm and 55 mm inner diameter. The wall of the cylinder is provided with tapped holes equally distributed along the cylinder height in order to monitor independent layers of the soil. The holes are aligned spirally to minimize mutual shadowing in the vertical. ....	134
<b>Fig. 68.</b>	LP/t - Laboratory Probe for soil temperature measurement .....	135
<b>Fig. 69.</b>	LP/p - Laboratory miniProbe for soil water capillary pressure .....	136
<b>Fig. 70.</b>	Reading instantaneous profiles of soil water capillary pressure, water content and salinity from arrays of the LP/p and LP/ms miniprobcs .....	137

## 15. INDEX OF TABLES

<b>Table 1.</b>	Selected properties of the investigated grain .....	20
<b>Table 2.</b>	Chosen properties of the investigated woods and parameters of $n(\theta)$ relation .....	20
<b>Table 3.</b>	Salinity indices for various soils (after Malicki <i>et al.</i> [62]), $EC_s$ [dSm <sup>-1</sup> ] is the electrical conductivity of a solution used to moisten soil samples.....	24
<b>Table 4.</b>	The parameters of the soils used for the preparation of soil mixtures. ....	30
<b>Table 5.</b>	The results of multiple regression method (22) $S_{yx}$ is the standard error of estimate.....	31
<b>Table 6.</b>	Selected properties of the investigated mineral soils, where $\rho$ [gcm <sup>-3</sup> ] is the soil bulk density, $\rho_s$ [gcm <sup>-3</sup> ] is the soil particle density .....	36
<b>Table 7.</b>	Selected physical parameters of the tested soils.....	57
<b>Table 8.</b>	Corrected and non-corrected temperature errors of the measurement of the refractive index, $n$ , for water and the TDR measured values of its content, $\theta_{TDR}$ .....	59
<b>Table 9.</b>	Regression coefficients in the relation $n(T)=a_0+a_1T$ for the tested mineral soils without and after the application of correction (43).....	60
<b>Table 10.</b>	The squared values of the correlation coefficient, $R$ , between the selected parameters of the analyzed set of data, no of cases 663. ....	71
<b>Table 11.</b>	Regression parameters $n(\theta)$ for the tested soils ( $R^2$ – squared value of the correlation coefficient, $S_{yx}$ – standard error of estimation). ....	72
<b>Table 12.</b>	The results of multiple regression analysis for all analyzed soil samples (no of cases - 663) .....	73
<b>Table 13.</b>	The results of multiple regression analysis for individual groups of soil 74	
<b>Table 14.</b>	Statistical parameters of the absolute errors for the models under investigation .....	80
<b>Table 15.</b>	Statistical parameters of $\Delta\theta_{rel}$ for the set of data with all soil samples under test and the subset of data with soil samples of water contents $\theta > 0.1$ .....	81
<b>Table 16.</b>	Localization and selected physical parameters of tested soil samples .....	90

<b>Table 17.</b> An example of the executable script file with the sequence of commands controlling the MIDL data logger .....	117
<b>Table 18.</b> Script file commands for MIDL data logger control.....	117